

**A STUDY ON NUMBER THEORETIC  
CONSTRUCTION AND PREDICTION OF TWO  
DIMENSIONAL ACOUSTIC DIFFUSERS FOR  
ARCHITECTURAL APPLICATIONS**

**A Thesis Submitted to  
the Graduate School of Engineering and Sciences of  
İzmir Institute of Technology  
in Partial Fulfillment of the Requirements for the Degree of**

**DOCTOR OF PHILOSOPHY**

**in Architecture**

**by  
Ayçe DÖŞEMECİLER**

**March 2011  
İZMİR**

We approve the thesis of **Ayçe DÖŞEMECİLER**

---

**Assist. Prof. Dr. Fehmi DOĞAN**  
Supervisor

---

**Assist. Prof. Dr. Serdar ÖZEN**  
Co-Supervisor

---

**Prof. Dr. Murat GÜNAYDIN**  
Committee Member

---

**Assoc. Prof. Dr. Selim Sarp TUNÇOKU**  
Committee Member

---

**Assist. Prof. Dr. Hüseyin Sami SÖZÜER**  
Committee Member

---

**Assoc. Prof. Dr. Sadık Cengiz YESÜGEY**  
Committee Member

**07 March 2011**

---

**Assoc. Prof. Dr. Serdar KALE**  
Head of the Department of Architecture

---

**Prof. Dr. Durmuş Ali DEMİR**  
Dean of the Graduate School of  
Engineering and Sciences

## ACKNOWLEDGEMENTS

This thesis would not have been accomplished without the assistance of many people whose contributions I gratefully acknowledge.

I wish to thank, first and foremost, my thesis co-supervisor Assist. Prof. Dr. Serdar Özen for his invaluable guidance and support. He always encouraged me to go further in my studies, gave the idea of DSP Method which formed the basis of this whole research. In fact, without his encouragement and great patience, I wouldn't dare to learn the concepts which I was not familiar at all.

I would also like to express my deep appreciation and sincere gratitude to my thesis supervisor Assist. Prof. Dr. Fehmi Doğan for his continuous support and optimism throughout the process. He helped me to look things from a different perspective, and guided me to get over the difficult times I have faced.

I would also like to thank my thesis committee members Prof. Dr. Murat Günaydın and Assoc. Prof. Dr. Selim Sarp Tunçoku for their irreplaceable guidance and support. Prof. Dr. Murat Günaydın always asked me questions which made me realize I should go deeper in my research and thought me an important lesson about how to demonstrate and explain a complex phenomenon in simplicity. I believe he made me understand my research better. I also take this opportunity to express my special gratitude towards Assist. Prof. Dr. Zeynep Aktüre for helping me to write the abstract and the outline of the thesis. She patiently guided me and thought me the essentials of writing an abstract which I still find difficult.

I had an exceptional opportunity to study and collaborate with Prof. Umberto Iemma and Vincenzo Marchese from Roma Tre University Department of Mechanical and Industrial Engineering. They kindly shared their expertise with me and without their software support; this thesis would not be possible. Since the beginning of the prediction stage, Prof. Iemma supported me with his advice and unsurpassed knowledge of Boundary Element Method. I cannot find words to express my gratitude to Vincenzo Marchese. He helped me to build my study case, answered every question without losing patience, and I believe I have learned so much from him about the Boundary Element Method which I will use throughout my academic studies.

During the first research phase, I had an opportunity to discuss the method with Dr. Andrew Tirkel, who developed the DSP Method with his colleagues. He kindly

replied all my questions and gave me ideas about other methods which I will use in my future studies.

I would also like to thank Dr. Peter D'Antonio for sharing the data of diffusers he developed and offering me help in my future studies.

The thesis has been a long process. Since the beginning, I had the opportunity to take invaluable advice from Prof. Dr. Mehmet Çalışkan. He kindly shared his pioneering studies about the concert hall acoustics. His joy and devotion to his studies always encouraged me and he has been an excellent mentor to me.

I shared the initial proposal of this study with Late Assoc. Prof. Dr. Deniz Şengel years ago. Her courage always inspired me and she is missed.

I have been fortunate to have good friends, without whom life would be bleak. I would like to thank Yenal Akgün, Erdal Uzunoğlu, Özlem Taşkın, Birtan Yetkinoğlu, childhood friends Eylem Taugait, Teoman Ünal and Saygın Ersin for their support at tough times, and always being there when needed.

Finally, I would like to thank my parents for their constant support and encouragement in all my educational life. They taught me to follow my dreams no matter what and helped me to see the good in every situation. Special thanks are due to my brother, Özgün who always makes me laugh with his special sense of humor and makes my life easier (not always).

# ABSTRACT

## A STUDY ON NUMBER THEORETIC CONSTRUCTION AND PREDICTION OF TWO DIMENSIONAL ACOUSTIC DIFFUSERS FOR ARCHITECTURAL APPLICATIONS

Defined as the scattering of sound independent from angle, optimum diffusion is very important for the perception of musical sound. For this purpose, Schroeder used mathematical number sequences to propose 'reflection phase grating diffusers', of two main types: Single plane or one-dimensional (1D) diffusers that scatter sound into a hemi-disc, and two dimensional (2D) diffusers that scatter into a hemisphere to disperse strong specular reflections without removing sound energy from the space, which is the main advantage of these devices. Currently, two methods are used to design 2D diffusers: Product Array and Folding Array Methods. Both are based on number theory and used methodologically in the field of acoustics, producing results that offer limited diffusion characteristics and design solutions for a variety of architectural spaces ranging from concert halls to recording studios where Schroeder diffusers are widely used. This dissertation proposes Distinct Sums Property Method originally devised for watermarking digital images, to construct adoptable 2D diffusers through number theoretical construction and prediction. At first, quadratic residue sequence based on prime number 7 is selected according to its autocorrelation properties as the Fourier transform of good autocorrelation properties gives an even scattered energy distribution. Then Distinct Sums Property Method is applied to construct 2D arrays from this sequence from which well depths and widths are calculated. Third, the aimed scattering and diffusion properties of the modeled 2D diffuser are predicted by Boundary Element Method which gives approximate results in accordance with the measurements based on Audio Engineering Society Standards. Fourth, polar responses (i.e. the scattering diagrams for specific angles) in each octave band frequency are obtained. Finally, predicted diffusion coefficients for uniform scattering are calculated and compared to the reference flat surface's coefficients and previous studies' results.

# ÖZET

## MİMARİ UYGULAMALAR İÇİN İKİ BOYUTLU AKUSTİK SAÇICILARIN SAYI TEORİSEL KURULUMU VE ÖNGÖRÜLMESİ ÜZERİNE BİR ÇALIŞMA

Sesin açıdan farklı olarak dağılması olarak tanımlanan ideal saçıcılık, müzikal seslerin algısında çok önemlidir. Bu amaçla, Schroeder matematiksel sayı serilerini kullanarak, iki ana tipte olan ızgarasal fazlı yansıma saçıcılarını önermiştir: Sesi yarı dairesel olarak saçan bir boyutlu (1D) saçıcılar ve sesi yarı küresel olarak saçan iki boyutlu (2D) saçıcılar. Bu saçıcıların ana avantajı, direkt gelen ses ışınlarını, ortamdaki ses enerjisini azaltmadan saçmalarıdır. Halen 2D saçıcılar tasarlamak için iki metod kullanılmaktadır: Çarpım Dizisi Metodu ve Katlanan Dizi Metodu. İki metod da sayı teorisine dayanmakta ve günümüzde akustik alanında kullanılmaktadır. Ancak sundukları saçıcılık özellikleri ve konser salonlarından kayıt stüdyolarına değişen mimari mekanlar için tasarım çözümleri sınırlıdır. Bu tez, farklı seçimlerde 2D saçıcıların sayı teoriksel kurulumu ve öngörülmesinde dijital resimlerin filigranında kullanılan Ayrık Topamlar Özelliği Metodu önermektedir. İlk olarak, iyi otokorelasyon özelliklerine sahip olduğu bilinen, asal sayı 7'yi temel alan kuadratik kalan sayı serisi seçilmiştir. Çünkü bilindiği üzere ideal otokorelasyonun Fourier dönüşümü dengeli saçılan enerji dağılımı göstermektedir. Sonra, Ayrık Topamlar Özelliği Metodu kullanılarak 2D diziler oluşturulmuş ve hücre derinlikleri ve genişlikleri hesaplanmıştır. Üçüncü olarak modellenmiş 2D saçıcının sesi saçma özellikleri, Audio Engineering Society standartlarıyla uyumlu olduğu bilinen Sınır Eleman Yöntemi ile öngörülmüştür. Her oktav band frekanstaki kutupsal yansımalar elde edilmiştir. Son olarak öngörülmüş saçılım katsayıları hesaplanmış, referans düz yüzey katsayıları ve önceki çalışmaların sonuçlarıyla karşılaştırılmıştır.

*Dedicated to late Emeritus Professor Manfred Robert Schroeder  
(12 July 1926 – 28 December 2009)*

# TABLE OF CONTENTS

LIST OF FIGURES .....	x
LIST OF TABLES.....	xiv
CHAPTER 1. INTRODUCTION .....	1
1.1. Definition of the Problem .....	1
1.2. Aim and Scope of the Study .....	10
1.3. Limitations and Assumptions .....	10
1.4. Method .....	12
1.4.1. Construction.....	12
1.4.2. Prediction .....	13
CHAPTER 2. SCHROEDER DIFFUSERS .....	16
2.1. Diffusion from Schroeder Diffusers .....	16
2.2. One Dimensional Diffusers.....	22
2.2.1. Maximum Length Sequence Diffusers .....	22
2.2.2. Quadratic Residue Diffusers .....	24
2.2.3. Primitive Root Diffusers .....	29
2.3. Two Dimensional Diffusers.....	31
2.3.1. Product Array Method .....	31
2.3.2. Folding Array Method .....	37
CHAPTER 3. CONSTRUCTION OF TWO DIMENSIONAL QUADRATIC RESIDUE DIFFUSERS WITH DISTINCT SUMS PROPERTY METHOD.....	40
3.1. Distinct Sums Property Method.....	40
3.2. Application of Distinct Sums Property Method to Quadratic Residue Sequence for $N = 7$ and Autocorrelation Properties .....	41
3.3. Construction of Two Dimensional Quadratic Residue Diffusers .....	42



CHAPTER 4. PREDICTION OF SCATTERING FROM TWO DIMENSIONAL QUADRATIC RESIDUE DIFFUSERS WITH BOUNDARY ELEMENT METHOD .....	50
4.1. Theory and Formulation of Boundary Element Method.....	51
4.2. The Formation of the Prediction Setup for the Boundary Element Method Software .....	55
4.3. The Results.....	58
CHAPTER 5. CONCLUSIONS .....	70
5.1. Future Work.....	71
BIBLIOGRAPHY .....	72
APPENDICES .....	78
APPENDIX A. MATLAB SCRIPTS .....	78
APPENDIX B. LIST OF RECEIVER POINTS.....	87
APPENDIX C. INPUT AND OUTPUT FILES OF BEM SOFTWARE.....	89

# LIST OF FIGURES

<u>Figure</u>	<u>Page</u>
Figure 1.1. Lateral reflections added by Schroeder et al. to concert hall impulse responses. The result is improved subjective preference. . . . .	4
Figure 1.2. One dimensional quadratic residue diffuser . . . . .	6
Figure 1.3. Scattering patterns of one and two dimensional diffusers . . . . .	7
Figure 1.4. Folding Array Construction Method . . . . .	8
Figure 1.5. Omnifusor . . . . .	9
Figure 1.6. The Distinct Sums Property Array Method . . . . .	9
Figure 1.7. The Application of DSP Method for One Dimensional Quadratic Residue Sequence for $N = 7$ . . . . .	14
Figure 2.1. Cylindrical wave reflected from a flat surface computed with FDTD method . . . . .	17
Figure 2.2. Cylindrical wave reflected from a Schroeder diffuser computed with FDTD method . . . . .	18
Figure 2.3. Comparison of the spatial and temporal response of a flat surface and a Schroeder diffuser . . . . .	18
Figure 2.4. Comparison of the temporal and frequency response of a flat surface and a Schroeder diffuser . . . . .	19
Figure 2.5. Cross section of a one period of maximum length sequence for $N=7$ .	22
Figure 2.6. Cross section of a one period of an active maximum length sequence for $N=7$ . The central well has active controller . . . . .	24
Figure 2.7. The scattering from three surfaces at 500 Hz. and 1000 Hz: Thin line: plane surface, bold line: active MLS diffuser, dotted line: passive MLS diffuser . . . . .	24
Figure 2.8. One dimensional quadratic residue diffuser . . . . .	25
Figure 2.9. One dimensional quadratic residue diffusers made from different materials . . . . .	25
Figure 2.10. Scattering from a quadratic residue sequence and a flat surface . . .	26

Figure 2.11. Cross-section of one dimensional quadratic residue diffuser based on prime number 7 . . . . .	29
Figure 2.12. Scattering from PRD based on $N = 7$ , a plane surface, and PRD based on $N = 37$ and for normal incidence . . . . .	30
Figure 2.13. Two dimensional quadratic residue sequence for $N=7$ based on Product Array Method . . . . .	32
Figure 2.14. Scaled model of two dimensional quadratic residue sequence for $N=7$ based on Product Array Method . . . . .	33
Figure 2.15. Autocorrelation plot of two dimensional quadratic residue sequence for $N=7$ based on Product Array Method . . . . .	34
Figure 2.16. Power spectrum of two dimensional quadratic residue sequence for $N=7$ based on Product Array Method . . . . .	34
Figure 2.17. A sequence array for two dimensional quadratic residue diffuser for $N = 7$ . . . . .	35
Figure 2.18. Scattering from two dimensional quadratic residue diffuser for $N = 7, s_n = \{4, 1, 2, 0, 2, 1, 4\}$ (top), and a flat surface (below) at four times the design frequency . . . . .	35
Figure 2.19. Autocorrelation plot of two dimensional quadratic residue sequence for $N=7, s_n = \{4, 1, 2, 0, 2, 1, 4\}$ based on Product Array Method . . . . .	36
Figure 2.20. Power spectrum of two dimensional quadratic residue sequence for $N=7, s_n = \{4, 1, 2, 0, 2, 1, 4\}$ based on Product Array Method . . . . .	36
Figure 2.21. Folding Array Construction Method . . . . .	38
Figure 2.22. Scattering from 2D primitive root diffuser which is folded into a $6 \times 7$ array . . . . .	38
Figure 2.23. Skyline . . . . .	39
Figure 2.24. Scattering from registered trademark Skyline at $3/4, 1, 4, 8, 12$ times design frequency, $f_0$ . . . . .	39
Figure 3.1. The Distinct Sums Property Array Method . . . . .	41
Figure 3.2. The Application of DSP Method for One Dimensional Quadratic Residue Sequence for $N = 7$ . . . . .	43
Figure 3.3. Autocorrelation Plot of 2D Quadratic Residue Sequences for $N = 7$ based on DSP Method for $m = 1, 2, 3$ . . . . .	44

Figure 3.4. Autocorrelation Plot of 2D Quadratic Residue Sequences for $N = 7$ based on DSP Method for $m = 5, 6, 7$ . . . . .	45
Figure 3.5. Power Spectrum of 2D Quadratic Residue Sequences for $N = 7$ based on DSP Method for $m = 1, 2, 3$ . . . . .	46
Figure 3.6. Power Spectrum of 2D Quadratic Residue Sequences for $N = 7$ based on DSP Method for $m = 4, 5, 6$ . . . . .	47
Figure 3.7. The technical drawings of 2D quadratic residue sequences for $N = 7$ based on DSP Method for $m = 1$ A: Isometric View B:Top View C:Left View D: Front View . . . . .	49
Figure 4.1. The prediction of scattering from a surface in far-field: Cont. line: BEM, Dotted line: Fraunhofer . . . . .	51
Figure 4.2. The prediction of scattering from a surface in near-field: Cont. line: BEM, Dotted line: Fraunhofer . . . . .	51
Figure 4.3. Geometry used for prediction with BEM . . . . .	52
Figure 4.4. A meshed Schroeder diffuser . . . . .	54
Figure 4.5. The measurement procedure of AES . . . . .	56
Figure 4.6. The geometry of the prediction of 2D quadratic residue diffuser based on DSP Method . . . . .	56
Figure 4.7. Scattered sound pressure levels in dB for normal sound incident on 2D quadratic residue diffuser based on DSP Method for $m = 1$ modulation at x-coordinate . . . . .	62
Figure 4.8. Scattered sound pressure levels in dB for normal sound incident on 2D quadratic residue diffuser based on DSP Method for $m = 1$ modulation at y-coordinate . . . . .	65
Figure 4.9. Diffusion coefficients of 2D quadratic residue diffuser based on DSP Method for $m = 1$ and reference flat panel at octave band frequencies . . . . .	67
Figure 4.10. Normalized diffusion coefficients of 2D quadratic residue diffuser based on DSP Method for $m = 1$ at octave band frequencies . . . . .	67
Figure 4.11. Left: FRG, Omniffusor Right: Omniffusor . . . . .	68
Figure 4.12. Diffusion coefficients of 2D quadratic residue diffuser based on DSP Method for $m = 1$ and FRG Omniffusor at octave band frequencies . . . . .	68

Figure 4.13. Diffusion coefficients of 2D quadratic residue diffuser based on DSP

Method for  $m = 1$  and Omnifusor at octave band frequencies . . . . 69

# LIST OF TABLES

<u>Table</u>	<u>Page</u>
Table 3.1. Peak to Largest Sidelobe Ratios . . . . .	42
Table 3.2. The Calculation of Well Depths for 2D Quadratic Residue Sequence for $N = 7$ . . . . .	48
Table 4.1. Predicted Pressures $P_r$ in Pa. and Sound Pressure Levels in dB. from 2D Quadratic Residue Diffusers based on DSP Method for $m = 1$ at x-coordinate for 125 Hz., 250 Hz., and 500 Hz. . . . .	60
Table 4.2. Predicted Pressures $P_r$ in Pa. and Sound Pressure Levels in dB. from 2D Quadratic Residue Diffusers based on DSP Method for $m = 1$ at x-coordinate for 1000 Hz., 2000 Hz., and 4000 Hz. . . . .	61
Table 4.3. Predicted Pressures $P_r$ in Pa. and Sound Pressure Levels in dB. from 2D Quadratic Residue Diffusers based on DSP Method for $m = 1$ at y-coordinate for 125 Hz., 250 Hz., and 500 Hz. . . . .	63
Table 4.4. Predicted Pressures $P_r$ in Pa. and Sound Pressure Levels in dB. from 2D Quadratic Residue Diffusers based on DSP Method for $m = 1$ at y-coordinate for 1000 Hz., 2000 Hz., and 4000 Hz. . . . .	64

# CHAPTER 1

## INTRODUCTION

### 1.1. Definition of the Problem

The acoustics of music performance spaces play a major role in the perceived sound by the audience. Fine acoustic quality enriches the music while the poor weakens (Cox & D'Antonio 2003). Today acoustic diffusers have been widely used in music performance spaces to achieve that acoustic quality.

When a sound wave strikes on a surface, it is transmitted, absorbed, or reflected. We call the surface a diffuser when a reflected sound wave is dispersed both spatially and temporally from the surface, and the reflection becomes a diffuse reflection. This thesis concentrates on the phase grating diffusers introduced by Schroeder in 1975. Schroeder diffusers consist of a series of wells with same widths and different depths which are designed according to the mathematical sequences such as quadratic residue and primitive root sequences. These diffusers disperse sound into a hemi-disc. This study aims to construct “two dimensional quadratic residue diffusers”, which disperses sound into a hemisphere, with a new method in acoustics, the Distinct Sums Property Method.

In order to understand the theory behind the diffusers and the need for diffusing surfaces in music performance spaces, it is important to mention the brief history of music performance spaces and address the problems which lead to the invention of Schroeder diffusers. The history of music performance spaces goes back to Greek Period (650 BC) (Long 2006). Given today's classical acoustic repertoire in concert halls and the varying acoustic demands from one concert hall, we need to review the history of concert hall acoustics starting with Baroque Period (1600–1750), and then continue with Classical Period (1750–1820), Romantic Period (1820–1900) and Twentieth Century (1900–2000)(Beranek 2004; Long 2006). Each period has its own musical characteristics resulting in different acoustic requirements. In addition Beranek (2004) points that the composers usually wrote music for a specific church, a concert hall or an opera house which is highly different from today's circumstances. Therefore the music sounded

best when played at the aimed architectural space. For instance, the architecture, hence the acoustical properties of the spaces, shaped the Baroque music at the Baroque Period (Beranek 2004). Interestingly, there were two acoustically opposite performance spaces serving for secular music and sacred music. Secular music was composed for ballrooms of palaces or small theaters which had reflective hard surfaces. Therefore, these private spaces with low reverberation time (less than 1.5 s) were perfect for secular music, or Baroque orchestral music (Beranek 2004). On the contrary, Baroque sacred music was composed for variety of churches or cathedrals. Plainchants were listened in highly reverberant large eighteenth century churches while much Baroque music were composed for Lutheran churches which had dry acoustics.

At the Classical Period which started around 1750s, audiences enjoyed music which was composed in Classical style. The composers such as Haydn, Mozart and Beethoven were influenced by the increasing number of music publishers. The style was more independent compared to Baroque Period. In fact, the strict structure of Baroque music, such as interweaving of equal parts was changed to the idea of accompanied melody. Therefore, Classical music had a bigger sound with fullness and depth when compared to the clarity of the Baroque Period. During Classical Period, the biggest change was the public interest and expanding audience which required larger performance spaces. Therefore, the first concert halls designed specifically for concerts were built in the middle of nineteenth century. Full orchestra was required for the musical depth of classical music and so larger spaces were built for higher reverberation times. Today, the required reverberation time for classical music is ranged between 1.6 to 1.8 seconds.

From 1820 to 1900, audience enjoyed Romantic music. Romantic Period introduced the audience with more emotional, personal and poetic tones (Long 2006). However, Long (2006) states that the Classical and Romantic Period cannot be strictly departed from each other in terms of time periods for the reason of continuous progress in music. Therefore, although Beethoven lived in Classical Period, it is believed that some of his music such as Sixth and Ninth symphonies can be considered in Romantic Period. He influenced the famous composers such as Schubert, Brahms, Mendelssohn and Wagner (Long 2006). All of these composers and Debussy, Tchaikovsky increased the size and color of the orchestra, and they explored new melodies. Therefore, the clear definition of musical tones during Baroque and Classical Period was over with the introduction of



complex orchestral harmonies, and the music required spaces that provides high fullness of tone and less clarity. This is why the concert halls built at the end of the nineteenth century had longer reverberation times, about 1.9 to 2.1 seconds (Beranek 2004).

From the beginning of twentieth century, concerts have grown into a more cultural activity world-wide, as compared to having a more religious flavor in Baroque Period. Hence, today the concert halls have to meet the requirements of the music of earlier times, and the recent compositions which result in variety of acoustic conditions. The famous orchestras travel around the world's famous concert halls which have different acoustical properties. In addition, the public interest to music has resulted in larger concert halls that host larger audience.

On the other hand, since the beginning of the 1950s, the modern architecture shaped the design of the concert halls. The simple, modernist style of today's architecture and larger concert halls that host many people has resulted in problems at the acoustics of modern halls (Beranek 2004; Cox & D'Antonio 2003). At the eighteenth and nineteenth century, the spaces for concerts had ornaments, niches, and coffers which diffuse the sound and gave the music a non-glary tone (Beranek 2004; Haan & Fricke 1997; Hidaka & Beranek 2000). In addition, the energy produced by the orchestra was easily preserved at these smaller spaces when compared to today's larger halls. In fact, Beranek (2004), one of the well-known experts in acoustics, stated that the three halls which still rated highest by the famous conductors and music critics are built in 1870, 1888, and 1900. These concert halls are Grosser Musikvereinssaal in Vienna, Concertgebouw in Amsterdam, and Boston Symphony Hall in Boston. As a result, the flat walls of the modernist style of the twentieth century has brought acoustical problems such as glare, distortion of sound, and the non-preservation of the sound energy in larger spaces. Contrary to poor architectural acoustics, improvements in the science of acoustics offer significant insights. There are universally accepted subjective and objective criteria to measure and evaluate acoustic quality of the concert halls today.

Since 1960s, many acousticians have studied the relationship between subjective responses and objective acoustic measurements in concert halls to overcome the aforementioned problems. During the late 1960s and early 1970s, it has been proven that early lateral reflections are essential for subjective spatial impression; a sense of being enveloped by the sound (Barron 1971; Marshall 1967; Schroeder et al. 1974). Later, in

1981 Barron and Marshall proposed the objective measure of early lateral energy fraction (LF), which has found to be linearly related to subjective spatial impression (SI). Beranek describes spatial impression as “the difference between feeling inside the sound and feeling on the outside observing it, as through a window” (Beranek 1992, page:8).

Furthermore, in his comparative study of European concert halls in 1974, Schroeder et al. stated that halls that have lateral reflections from the sides have better sound performance than the halls with sound waves only coming from the front direction (see Figure 1.1). To provide lateral reflections to the listeners’ ears, Schroeder (1975; 1979) proposed “phase grating diffusers” based on mathematical sequences that reflect sound energy in all directions except specular direction, thus resulting in better diffusion. The proposed diffusers were also advantageous for the reason of not removing the sound energy from the space like absorbers (Cox & D’Antonio 2003; Schroeder 1979). Because in case of today’s large concert halls, every amount of energy produced by the orchestra should be conserved within the hall for reverberation and richness. In addition, these diffusers also met the requirements of modern architecture by their innovative design.

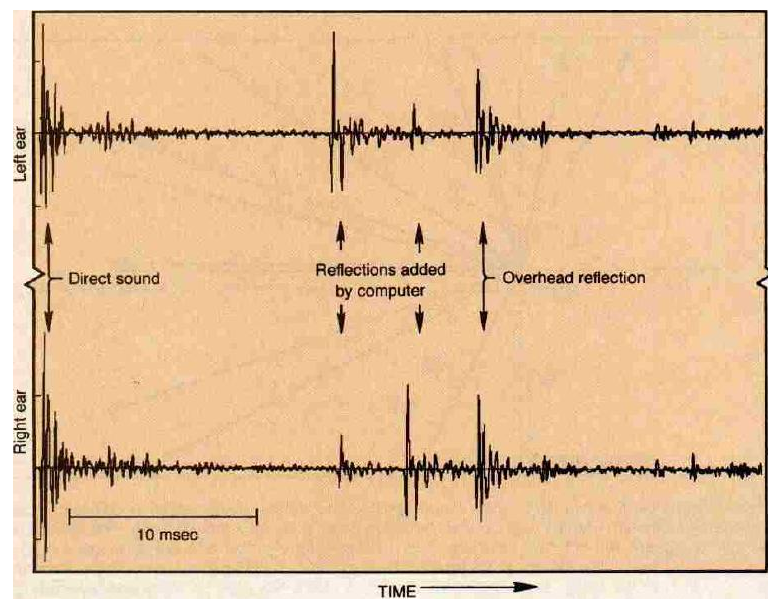


Figure 1.1. Lateral reflections added by Schroeder et al. to concert hall impulse responses. The result is improved subjective preference (Source: Schroeder 1980, page:28)

The subjective responses of the audience at the concert halls are described and judged by five elements (Beranek 1992):

1. Spatial Impression (SI): Spatial impression is related to the measured early

lateral reflections as mentioned before, and describes the communication between the audience and the orchestra (Beranek 1992; Barron & Marshal 1981).

2. Liveness: Beranek (1992) also describes the liveness as reverberance and the term is directly related to the measured reverberation times of the hall. The halls which has low reverberation times are called “dry” while longer reverberation times make the hall “live”.

3. Warmth: This element is described as the subjective response related to the bass component of music performed by the orchestra. The warmth increases if the music is rich in bass. Beranek (1992) states that if the measured reverberation times of large halls are less than 2.1 seconds, the warmth is linearly correlated with the reverberation times at low frequencies.

4. Loudness: This term is related to the reverberation time and size of the concert hall. The direct sound from the orchestra and the reverberant sound effects the loudness. Therefore, the ratio of reverberation times and the measured distances from the stage to the volume of the concert hall is related to the loudness (Beranek 1992).

5. Diffusion: The aforementioned study of Schroeder et al. (1974) clearly proves the importance of the diffusing surfaces on the subjective preference. Beranek (1992) also mentions that the hard reflective surfaces gives the performed music a harsh sound; and the concert halls should have diffusive surfaces in order to provide early lateral reflections in all directions to prevent focus of the sound at certain locations of the hall.

This study is focused on the first and fifth item of the list above to improve the subjective responses of the audience in terms of introducing two dimensional phase grating diffusers. Since their discovery in the 1970s by Manfred Schroeder, reflection phase grating diffusers, so-called ‘Schroeder diffusers’ have been widely used worldwide in many applications including concert halls, recording studios, churches, and listening rooms (Cox & D’Antonio 2000, 2004; Cox & Lam 1994; D’Antonio 1989; Järvinen et al. 1998). In concert halls, the major role of diffusing surfaces on acoustic quality has been widely accepted today (Haan & Fricke 1997; Hidaka & Beranek 2000; Jeon et al. 2004). In 1997, Haan and Fricke investigated the relationship between the diffusion of sound and the acoustical quality of fifty-three halls known world-wide. They proved that subjective surface diffusivity index correlates very highly with acoustic quality index. Not surprisingly, the best three halls mentioned above rated highest. Later in 2000, Hidaka

and Beranek conducted a study on objective and subjective evaluation of twenty-three opera houses in Europe, Japan, and the Americas. They stated that “every opera house and concert hall with ratings above ‘passable’ has architectural means for bringing about diffusion of the reverberant sound field” (Hidaka & Beranek 2000, p:379).

Schroeder diffusers can be classified into two main types: Single plane or one-dimensional (1D) diffusers and two-dimensional (2D) diffusers (Cox & D’Antonio 2000; 2004). One-dimensional diffusers consist of an array of wells that have equal widths and different depths based on number sequences. The wells are separated by thin fins. The most common investigated one-dimensional diffuser is based on Quadratic Residue sequence which has been introduced by Schroeder in 1979 and is shown in Figure 1.2. In fact, Schroeder proposed different mathematical sequences for the design of diffusers such as Primitive Root and Index sequences. In addition, numerous studies on the development and modification of one-dimensional diffusers have been carried out (Angus 1992; 1999; 2001; Cox 1995; Cox & D’Antonio 2000; Cox et al. 2006; D’Antonio 1990; 1992; Järvinen et al. 1998; 1999).



Figure 1.2. One dimensional quadratic residue diffuser (Source: Cox & D’Antonio 2000, page:121)

Concept of reflection phase grating diffusers based on different sequences will be theoretically and quantitatively analyzed in Chapter 2 in detail. In brief, Schroeder diffusers are designed by the following concept. Sound comes incident on the diffusers. Plane waves propagate within each well; then radiate from the wells into the space. Waves have different phase due to the phase change and therefore creates an interference pattern. Consequently, the relative phases of the waves can be modified by changing well depths. Therefore, scattering depends on the choice of well depths (Cox 1995; Cox & D’Antonio

2004).

One-dimensional diffusers scatter sound into a hemi-disc (D'Antonio & Cox 2000). But there is also a need for a diffuser that provides scattering into a hemisphere which would be successful at dispersing strong specular reflections as shown in Figure 1.3. And, this can only be achieved by two-dimensional diffusers (Cox & D'Antonio 2004; D'Antonio & Cox 2000; Schroeder 1979). Cox and D'Antonio (2009) have stated two known methods for designing two-dimensional diffusers. The key point is to preserve and transfer the one dimensional diffusion properties when forming two dimensional diffusers, and it is related to the autocorrelation properties of the number sequence which is described in Chapter 2 in detail. The first method is the Product Array Method, applying two number sequences at x and z directions in form of Equation 1.1:

$$A_{i,j} = P_i \times Q_j \quad (1.1)$$

where P and Q are two number sequences with length of  $p$  and  $q$ , and A is the array of size  $pq$  (Schyndel et al. 1999). Quadratic residue and primitive root sequences can be used to form such diffusers. In fact, in his pioneer work in 1979, Schroeder proposed two-dimensional quadratic residue diffusers based on Product Array Method.

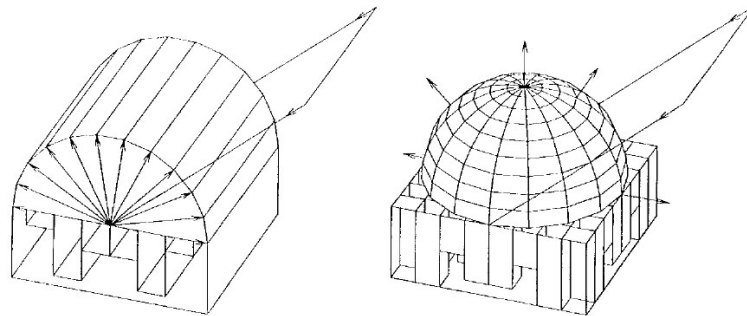


Figure 1.3. Scattering patterns of one and two dimensional diffusers (Source: Everest 2001, page:310)

The other method is called Folding Arrays Method and is based on Chinese Remainder Theorem which folds a 1D sequence into 2D array while preserving the autocorrelation properties of the 1D sequence (Cox & D'Antonio 2009; MacWilliams & Sloane 1976; Schyndel et al. 1999). Chinese Remainder Theorem is based on reconstructing certain range of integers from their residues modulo a set of coprime moduli. For instance, 15 integers from 0 to 15 can be reconstructed from their two residues modulo 3 and mod-

ulo 5 which are coprime factors of 15). If we say  $r_3 = 1$  and  $r_5 = 0$ , then the unknown number is 10 (Schroeder 1997). Figure 2.21 shows the principle of the method.

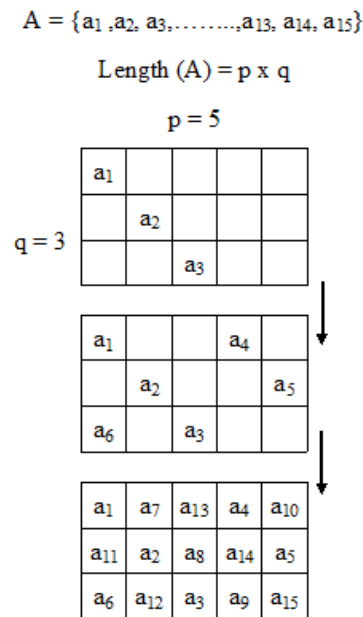


Figure 1.4. Folding Array Construction Method

This technique can be also applied to quadratic residue sequence for large moduli, primitive root sequence, and other sequences such as Chu sequence. In fact, D'Antonio and Konnert (1995) designed a two dimensional primitive root diffuser with Folding Arrays Method under the registered trademark Skyline. In addition, Cox and D'Antonio (2004) modified primitive root sequence based on prime number 43 folded into a  $6 \times 7$  array and found that the folding technique is successful. Other than these studies which are based on two known methods, D'Antonio and Konnert (1987) modified two-dimensional quadratic residue diffusers under the registered trademark Omniffusor and FRG Omniffusor with a well-depth optimization technique over the Product Array Method. Omniffusor is shown in Figure 1.5. Today, two-dimensional quadratic residue diffusers have been commercially exploited and developed.

However, contrary to one-dimensional diffusers, Cox and D'Antonio (2009) agreed that there is limited study on the measurement and prediction of multi-dimensional diffusers. Furthermore, research on the literature of multi-dimensional diffusers shows that the further studies after Schroeder (1979) are limited to the works of Cox and



Figure 1.5. Omniffusor (Source: RPG Diffusor Systems 2009)

D'Antonio (2009), D'Antonio and Konnert (1990; 1995), D'Antonio et al. (1990) and Angus and Simpson (1997). In fact, constructing multi dimensional arrays from one-dimensional sequences have been also studied in other fields such as digital watermarking (Schyndel et al. 1999; 2000; Tirkel et al. 1998a; 1998b), encoding devices used in physics, astronomy, television, medicine and radiation safety (Fedorov & Tereshchenko 1999), and coded aperture imaging and optical systems (Fan & Darnell 1996). The Distinct Sums Property (DSP) Method introduced and investigated by Tirkel et al. (1998a; 1998b) and Schyndel et al. (1999; 2000) is a method used in digital watermarking for forming two dimensional arrays from one dimensional sequences. The method which is shown in Figure 3.1 is based on using cyclic shifts of the seed sequence in the rows or columns of the array and offers different construction possibilities.

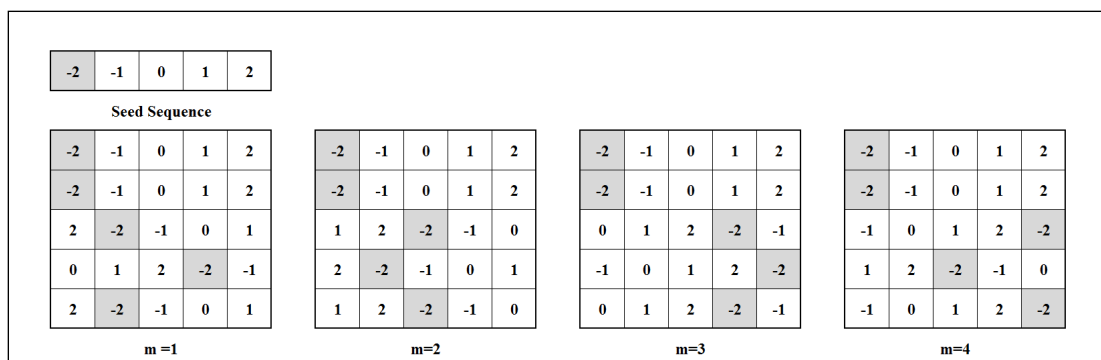


Figure 1.6. The Distinct Sums Property Array Method (Source: Schyndel et al. 1999, page: 359 )

In addition, the method preserves the autocorrelation properties of the seed sequence in two dimensional arrays. Therefore, applying The Distinct Sums Property Method used in digital watermarking to construct two dimensional acoustic diffusers enables new two dimensional acoustic diffusers with good diffusion properties. The research

shows that the two dimensional acoustic diffusers based on DSP Method have successful diffusion properties. Furthermore the previous studies of D'Antonio and Konnert (1990; 1995) and D'Antonio et al. (1990) resulted in diffusers with limited visual choices. Using the same diffuser in rows and columns, rotating them, or applying a binary sequence to determine the overall design in order to create a visual difference gives the architect limited choice. Therefore, there should be a variety of design options for the architect to choose from without giving up the acoustic requirements.

## **1.2. Aim and Scope of the Study**

This dissertation aims to design new two dimensional acoustic diffusers based on quadratic residue sequence with the Distinct Sums Property Method which is used in digital watermarking. As stated before, there is limited study on the construction and prediction of two dimensional diffusers. Although there are commercially available two dimensional diffusers like Omniffusor, FRG (Fiber Reinforced Gypsum) Omniffusor and Skyline, the prediction of scattering from two dimensional acoustic diffusers with Boundary Element Method (BEM) are not systematically stated in books related to the field of acoustics. Polar response data and related diffusion coefficients of new diffusers introduces new scientific data for future studies. In addition, construction and prediction of new two dimensional diffusers with BEM will contribute to the current literature on the subject.

Furthermore, current methods to construct two-dimensional diffusers from one-dimensional sequences limit the design and therefore possibilities of new diffuser structures. Hence, applying the Distinct Sums Property Method to construct two dimensional quadratic residue diffusers will enable multi-choice options for the architects and acousticians.

## **1.3. Limitations and Assumptions**

This dissertation proposes to develop two dimensional quadratic residue diffusers based on the Distinct Sums Property Method. The development and evaluation of acoustic



diffusers in the twentieth century was concentrated on concert hall applications. But today, acoustic diffusers cover a wide area of applications such as concert halls, music recording rooms, churches and music education facilities. Therefore, this thesis does not limit the application areas of the proposed diffusers.

One dimensional quadratic residue diffusers are chosen to construct two dimensional diffusers for the reason of optimum diffusion characteristics. Between the design frequency and the upper frequency limit, Cox and D'Antonio (2009) states that optimum diffusion can be achieved. However, primitive root diffusers work only at discrete frequencies and produce an even polar response only at large moduli (Cox & D'Antonio 2009).

In addition, the design of the quadratic residue diffusers are based on prime number 7 for the application purposes. Previous studies of D'Antonio and Konnert (1990; 1995), D'Antonio et al. (1990) shows that the dimensions of two dimensional acoustic diffusers should be around 60 centimeters x 60 centimeters with varying depths according to application requirements. Only the diffuser based on prime number 7 achieves a modular dimension. In addition, the proposed diffusers will cover the walls or ceilings of a music performance area with a required design pattern. In order to be compatible with other structures such as acoustic tiles and for construction advantages, the quadratic residue diffusers are based on prime number 7.

The material selection of proposed two dimensional diffusers is also limited to reflective hard materials such as wood, plexiglass and fiber reinforced gypsum. Schroeder diffusers based on quadratic residue sequence already shows sound absorption characteristics, which was first experimentally investigated by Commins et al. (1988). Then Fujiwara and Miyajima (1992), and Kuttruff (1994) studied the low-frequency absorption of Schroeder diffusers. However, later in 1995, Fujiwara and Miyajima found that the poor quality of the construction of Schroeder diffusers at the previous study was the reason of absorption. In order to avoid such results, the absorption properties should be minimized by optimization of well width, proper sealing of joints, and using rough construction materials (Cox & D'Antonio 2009). When it comes to the prediction of the scattering with BEM, Cox (1994; 1995) and Cox and Lam (1994) states that the diffusers should be assumed to have hard reflective surfaces which are non-absorbent. Therefore the proposed diffusers are assumed to have hard reflective surfaces and the sound absorp-

tion properties are beyond the scope of the thesis. In addition, possible precautions will be taken to minimize absorption in future architectural applications. However, it is crucial to state that studies covering hybrid surfaces providing partial absorption, partial reflection are vital and offers suitable solutions for spaces requiring both properties like studios. Therefore, the hybrid surfaces is thought to be investigated for future studies<sup>1</sup>.

## 1.4. Method

This study aims to develop two-dimensional quadratic residue diffusers with the Distinct Sums Property (DSP) Method. In order to characterize the diffuser's performance, the diffuser should be constructed upon the design equations for the given sequence. Then the diffuser should be exactly modeled with real geometry for the prediction process. This thesis consists of two major phases:

1. Construction
2. Prediction

### 1.4.1. Construction

Firstly, the quadratic residue sequence for prime number 7 is used as a seed sequence. In order to form two dimensional diffusers with the DSP Method, a grid consisting of 7 rows and 7 columns is created. The DSP Method offers  $N - 1$  designs where  $N$  is the prime number and the length of the sequence. Therefore, 6 arrays are constructed with different cyclic shifts from  $m = 1$  to  $m = 6$  which is shown in Figure 3.2. Distinct Sums Property Method is chosen for the reason of preserving good autocorrelation and Fourier properties. Cox and D'Antonio (2004) stated that one way of finding a proper sequence is to look for sequences with good autocorrelation properties. Autocorrelation is the correlation of a signal with itself (Manolakis 2005). The Fourier transform of an autocorrelation function gives the scattered energy distribution (Cox & D'Antonio 2009). Therefore, a good diffuser has even scattered energy distribution, and has good autocorrelation properties. Therefore, in order to proceed with the construction, two dimensional

---

<sup>1</sup>For the concept and design of hybrid surfaces see Angus (1995), Angus and D'Antonio (1999), Cox et al. (2006), Cox and D'Antonio (1999), D'Antonio (1998), and Wu et al. (2000; 2001).

autocorrelation function of each array is calculated and plotted with MATLAB. The results showed that the arrays has ideal two dimensional autocorrelation properties for the further progress.

For the array of  $m = 1$ , the well widths are set in accordance with the previous 2D diffusers which are also specified the upper frequency limit (D'Antonio .& Konnert 1990; 1995; D'Antonio et al. 1990). A design frequency is also set to provide diffusion for maximum possible bandwidth and well depths are calculated for each well for the given design frequency. The thicknesses of the fins separating each well are chosen realistically for future construction. At the end of the calculations, cross-check equations are applied for the probable design failures. Finally, all the data and dimensions are transferred into CAD program and modeled in 3D.

### **1.4.2. Prediction**

As the modeling method for diffusers, BEM is chosen because it is the most accurate and effective method which highly correlates with the measurement results (Cox 1992, Cox & D'Antonio 2009, Cox & Lam 1994; D'Antonio 1995). In addition, theoretic background of BEM at predicting the scattering from Schroeder diffusers and reflective surfaces has been verified with the studies of Cox (1994; 1995; 1998), Hargreaves and Cox (2005), Kawai and Terai (1990), and Lam (1999).

To optimize a diffuser, it is essential to predict the reflected pressure from the surface. Long computational times and storage limitations limit the prediction of scattering techniques which use whole space prediction algorithms. Therefore, predicting the scattering from the diffuser's surface isolated from other surfaces and with boundaries is considered. Boundary Element Method is a numerical computational method to solve partial differential equations which requires calculating only the boundary values. Consequently, for prediction, BEM is used throughout the prediction phase.

Boundary Element Method works by constructing a mesh of the modeled structure. A specialized meshing software is used to mesh the 3D modeled diffuser. There are different methods based on different integral equations varying in accuracy and computational time. Considering the mentioned studies, Standard Boundary Element Method

Seed Sequence  $s_n = \{0, 1, 4, 2, 2, 4, 1\}$

0	1	4	2	2	4	1
0	1	4	2	2	4	1
1	0	1	4	2	2	4
2	4	1	0	1	4	2
1	4	2	2	4	1	0
2	4	1	0	1	4	2
1	0	1	4	2	2	4

m=1

0	1	4	2	2	4	1
0	1	4	2	2	4	1
4	1	0	1	4	2	2
1	4	2	2	4	1	0
4	2	2	4	1	0	1
1	4	2	2	4	1	0
4	1	0	1	4	2	2

m=2

0	1	4	2	2	4	1
0	1	4	2	2	4	1
2	4	1	0	1	4	2
4	1	0	1	4	2	2
2	2	4	1	0	1	4
4	1	0	1	4	2	2
2	4	1	0	1	4	2

m=3

0	1	4	2	2	4	1
0	1	4	2	2	4	1
2	2	4	1	0	1	4
4	2	2	4	1	0	1
2	4	1	0	1	4	2
4	2	2	4	1	0	1
2	2	4	1	0	1	4

m=4

0	1	4	2	2	4	1
0	1	4	2	2	4	1
4	2	2	4	1	0	1
1	0	1	4	2	2	4
4	1	0	1	4	2	2
1	0	1	4	2	2	4
4	2	2	4	1	0	1

m=5

0	1	4	2	2	4	1
0	1	4	2	2	4	1
1	4	2	2	4	1	0
2	2	4	1	0	1	4
1	0	1	4	2	2	4
2	2	4	1	0	1	4
1	4	2	2	4	1	0

m=6

Figure 1.7. The Application of DSP Method for One Dimensional Quadratic Residue Sequence for  $N = 7$

based on Helmholtz-Kirchhoff integral equation is the most accurate but the slowest methods for the prediction of diffusers. However, the accuracy of the method is vital in case of applying a new method and predicting the results. Therefore, Standard Boundary Element Method is used to predict the scattering. In order to speed the computational time, some adjustments are made on the 3D model according to the previous studies by Cox and D'Antonio (2009), Hargreaves and Cox (2005). The geometry of the test setup in BEM software is modeled according to the Audio Engineering Society Standard AES-4id-2001(r2007):AES information document for room acoustics and sound reinforcement systems - Characterization and measurement of surface scattering uniformity and the studies of Cox and D'Antonio (2009).

The distribution of the scattered energy is described by polar responses in octave band frequencies for a given angle of incidence. Therefore, a successful diffuser produces a polar response in all angles in the reflected sound field (Cox & D'Antonio 2009). Consequently, to evaluate the quality of the scattering produced by the diffusers, scattered polar responses are obtained with BEM for each octave band frequency. Secondly, to evaluate the scattering by a single merit, the diffusion coefficient for each octave band frequency is calculated in accordance with AES-4id-2001(r2007). The obtained diffusion coefficients of the 2D DSP diffuser are plotted with the reference flat surface with same dimensions and normalized to see the actual performance. The diffusion coefficients of the new diffuser are compared with FRG Omniffusor and Omniffusor (D'Antonio et al. 1990) which are also based on quadratic residue sequence.

## CHAPTER 2

### SCHROEDER DIFFUSERS

#### 2.1. Diffusion from Schroeder Diffusers

Acoustics is the science of sound. Since we define sound as a wave, the behavior of sound waves play an important role when dealing with the acoustic problems. A sound wave hitting on a surface may behave in three ways: It is transmitted, absorbed or reflected. The acoustical properties of the surface effects the amount of the sound energy which goes into transmission, absorption or reflection (Long 2006). The room acoustics deal with the boundary of the surfaces, so we concentrate on the absorption and reflection.

The reflection can occur in two ways: It can be specularly reflected by a large flat surface or it can be scattered by a diffusing surface. Large flat panels reflect sound waves specularly, therefore creating a mirror reflecting light effect. The amount of the sound energy is preserved and reflected in the specular direction with equal incidence and reflection angles (Cox & D'Antonio 2003). In 2009, Cox and D'Antonio have studied the behavior of a flat surface with Finite Difference Time Domain (FDTD) method which is a simulation technique currently being used in electromagnetism. A cylindrical wave was sent to the flat surface and the response of the panel have been calculated. As seen in Figure 2.1 , the reflected wave has the same angle of the incident sound which was normal to the surface, so the reflected wave just changed direction.

The diffusers are generally defined as surfaces which has geometrical shapes or corrugates which scatters sound. However, scattering the sound in certain bandwidths not always results in desired sound environments. Cox and D'Antonio (2009) states that not all corrugated or geometrically shaped surfaces can be called a diffuser. The surface should disperse the incident sound wave both spatially and temporally. Spatial dispersion in all angles means that the surface scatters sound in all angles independent from the angle of the incident sound. In addition, to prevent coloration meaning that the scattered component is interfering with the incident sound, there should be temporal dispersion. Therefore, optimum diffusion occurs when surfaces diffuse sound both spatially and tem-

porally. Same study for plane surfaces was applied to Schroeder diffusers using the FDTD method (Cox & D'Antonio 2009). A cylindrical wave was sent to the surface of the diffuser. As seen in Figure 2.2, the reflected wavefront is dispersed in angles and temporal dispersion occurs due to the time the sound wave takes to travel in and out of the wells.

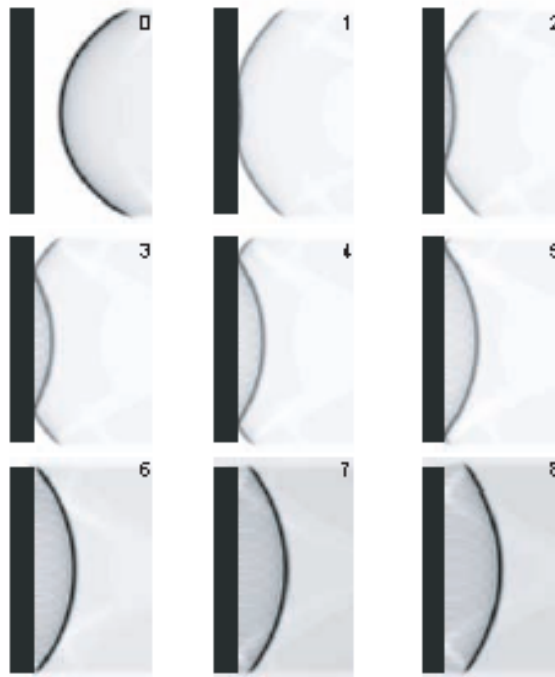


Figure 2.1. Cylindrical wave reflected from a flat surface computed with FDTD method (Source: Cox & D'Antonio 2009, page:35)

For better comparison, it is important to state the measured spatial and temporal responses. Figure 2.3 shows the temporal and spatial response of a flat surface and a Schroeder diffuser. The flat surface's time response indicate the similarity with the direct sound. As seen, the reflection occurs with the nearly same sound pressure level and lasts for a short time. Spatial response shows the direction change of the reflected sound which may lead to echo problems. The spatial response of the Schroeder diffusers indicates the dispersion occurring independent from the incident sound. For the temporal response, the reflections are altered and lasts for a longer time period.

Furthermore, in music, the surface's frequency responses play an important role. The original sound from the orchestra should be properly reflected in order to prevent coloration. It is not acceptable for the surface to emphasize some frequencies and deemphasize the others (Cox & D'Antonio 2003). This leads to hearing some of the instruments' frequency while not hearing others'. Figure 2.4 shows the temporal and frequency

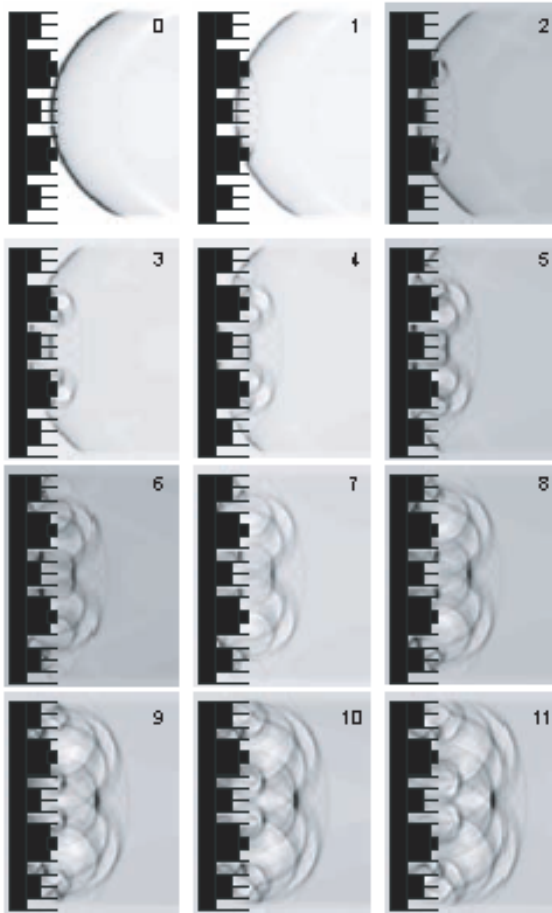


Figure 2.2. Cylindrical wave reflected from a Schroeder diffuser computed with FDTD method (Source: Cox & D'Antonio 2009, page:36)

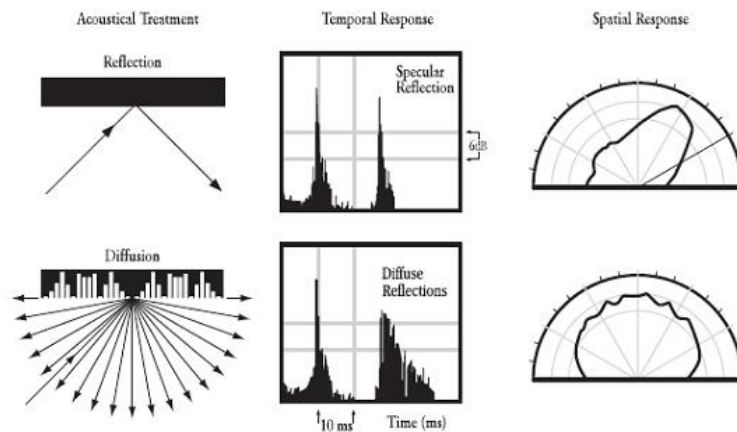


Figure 2.3. Comparison of the spatial and temporal response of a flat surface and a Schroeder diffuser (Source: Cox & D'Antonio 2003, page:120)



responses of a flat surface and a Schroeder diffuser. The flat reflector reflects high frequencies but attenuates the lower frequencies depending on the size and shape. However, Schroeder diffuser shows peaks and lows indicating a more successful reflection of the original sound in terms of frequency (Cox & D'Antonio 2009).

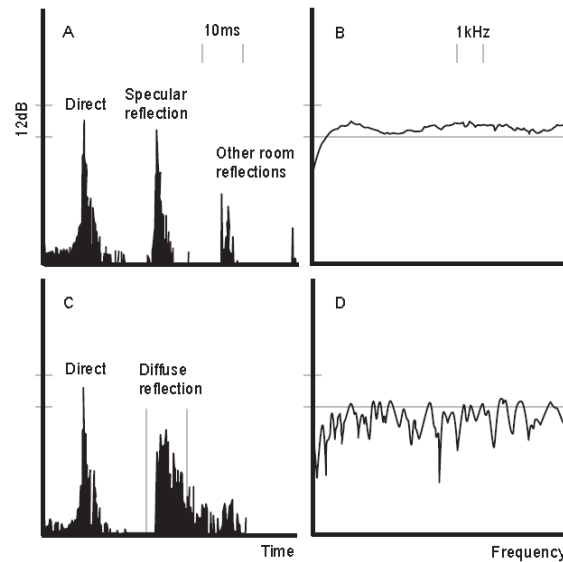


Figure 2.4. Comparison of the temporal and frequency response of a flat surface and a Schroeder diffuser (Source: Cox & D'Antonio 2009, page:37)

The optimum diffusion of Schroeder diffusers comes from the fundamentals of number theory. Schroeder diffusers consist of a series of wells separated by thin fins. In order to provide spatial and temporal dispersion while preserving the total reflection, well depths are determined upon a number sequence. The exponentiated number sequence gives the reflection coefficients of the surface. For instance, for quadratic residue sequence, the surface reflection coefficients ( $R(x)$ ) are given by Equation 2.1 (Schroeder 1979):

$$R(x) = e^{(2\pi \cdot j \cdot s_x / N)} \quad (2.1)$$

where  $s_x$  is the sequence number calculated for the  $x^{th}$  element of the sequence and  $N$  is the modulo of the sequence. In optics, Joseph von Fraunhofer found that the far-field scattering can be determined from the Fourier transform of the surface reflection coefficients (Cox & D'Antonio 2009; Brooker 2003). This method is also applied to acoustics but it is more limited in terms of low frequency predictions and oblique source and re-

ceiver points (Cox, Avis & Xiao 2006; Cox & D'Antonio 2009). However, Fraunhofer model is generally used at the design stage of new sequences for the reason of using simple equations (Cox & D'Antonio 2009). Therefore, scattering in terms of the pressure magnitude  $|p|$  from a surface according to Fraunhofer model is given by Equation 2.2 (Cox & D'Antonio 2004; Schroeder 1975):

$$|p(\theta, \psi)| \approx \left| A \int_s R(x) e^{jkx[\sin(\theta) + \sin(\psi)]} dx \right| \quad (2.2)$$

where  $R(x)$  is the reflection coefficients along a wall,  $\theta$  the angle of reflection with respect to the normal of the direction of the wall,  $\psi$  the angle of incidence with respect to the normal of the direction of the wall,  $x$  the distance along the surface, and  $k$  the wavenumber. The relationship between scattering angle  $\theta$  and the spatial frequency  $k$  is given by Equation 2.3:

$$k = 2\pi(\sin(\theta) - \sin(\psi))/\lambda \quad (2.3)$$

To obtain scattered energy for  $\theta_{max} = 90$  for normal incidence  $\psi = 0$ , the highest spatial frequency  $k$  should be equal to:

$$k_{max} = 2\pi/\lambda \quad (2.4)$$

The Fourier transform of the surface reflection factors  $R(x)$  nearly equals to the scattered energy distribution as stated in Equation 2.2. Wiener-Khinchine theorem states that power spectrum is the Fourier Transform of the autocorrelation function (Bracewell 2000). This theorem can be applied to number theoretic diffusers and makes it easier to investigate other number sequences. Consequently if the scattered energy distribution is constant, it shows that the diffuser has good scattering properties. If we apply Wiener-Khinchine theorem to diffusers, the Fourier Transform of the autocorrelation of the surface reflection coefficients gives the scattered energy distribution. Therefore, a good diffuser is one which has a Dirac delta function autocorrelation function for the reflection coefficients as it will result in an even scattered energy distribution (Cox & D'Antonio 2009; Schroeder 2006).

The autocorrelation is defined as the correlation of the signal with itself (Smith

1999). It is used to represent the degree of self-similarity over a given time series (Girod 2001). The signal and the lagged version of itself is calculated. The discrete autocorrelation of a sequence  $\hat{a}_n$  is given by Equation 2.5 (Fan & Darnell 1996):

$$R_a(\tau) = \sum_{n=0}^{N-1} \hat{a}_n \hat{a}_{n+\tau}^* \quad (2.5)$$

Giving the Fourier transform of a sequence  $\hat{a}_n$  in Equation 2.6, if we apply Wiener-Khinchine theorem and state the relationship between the autocorrelation function and its Fourier transform as in Equation 2.7 (Fan & Darnell 1996):

$$F(k) = \sum_{n=0}^{N-1} \hat{a}_n e^{-j \frac{2\pi n k}{N}} \quad (2.6)$$

$$\begin{aligned} R(\tau) &\leftrightarrow \sum_{\tau=0}^{N-1} R(\tau) e^{j \frac{2\pi \tau k}{N}} \quad (2.7) \\ &= \sum_{\tau=0}^{N-1} \left[ \sum_{n=0}^{N-1} \hat{a}_n \hat{a}_{n+\tau}^* \right] e^{j \frac{2\pi \tau k}{N}} \\ &= \sum_{n=0}^{N-1} \hat{a}_n^* e^{j \frac{2\pi n k}{N}} \sum_{m=n}^{N+n-1} \hat{a}_m e^{-j \frac{2\pi m k}{N}}, (m = \tau + n) \\ &= F^*(k) F(k) = |F(k)|^2 \end{aligned}$$

Autocorrelation of a sequence which has delta function will have a strong peak at  $\tau = 0$  and will be 0 for all other  $\tau$  given by Equation 2.8 (Fan & Darnel 1996):

$$R_a(\tau) = \begin{cases} E & \text{for } \tau = 0 \\ 0 & \text{for } \tau \neq 0 \end{cases} \quad (2.8)$$

These sequences are called perfect sequences and have an even scattered energy distribution, e.g. a flat power spectrum. Assuming that the sequence  $\hat{a}_n$  is perfect, Equation 2.7 becomes:

$$R(\tau) \leftrightarrow \sum_{\tau=0}^{N-1} R(\tau) e^{j \frac{2\pi \tau k}{N}} = R(0) e^{j \frac{2\pi k 0}{N}} = E \quad (2.9)$$

or we can write:

$$|F(k)| = \sqrt{R(0)} = \sqrt{E} \quad (2.10)$$

Therefore, if all the elements of the sequence  $\hat{a}_n = (a_1, a_2, \dots, a_n]$  has the same magnitude

of  $F(k) = \sqrt{R(0)} = \sqrt{E}$ , we can say that a diffuser based on a perfect sequence has even scattered energy based on the Fraunhofer or Fourier model. The sequence properties determines the general design parameters for the Schroeder diffusers. Consequently it will be proper to analyze each of them individually.

## 2.2. One Dimensional Diffusers

### 2.2.1. Maximum Length Sequence Diffusers

Maximum length sequences are good type of pseudo-random sequences which are very useful in applications such as system identification, synchronization, spread-spectrum communication, cryptography, and radar (Fan & Darnell 1996; MacWilliams & Sloane 1976). These sequences have a period length of  $N = 2^m - 1$ . Figure 2.5 shows the cross section of a one period of maximum length sequence for  $N = 7$  which is  $s_n = \{1, 1, 0, 1, 0, 0, 0\}$ .

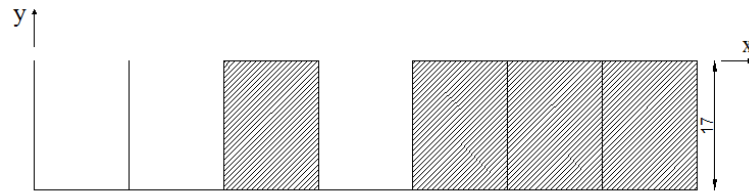


Figure 2.5. Cross section of a one period of maximum length sequence for  $N=7$  (Source: Cox, Avis & Xiao 2006, page:809)

Schroeder (1975) first investigated the maximum length sequence diffusers and gave the reflection coefficients as in Equation 2.11:

$$R(x) = \sum_{n=-\infty}^{\infty} s_n \text{rect} \left( \frac{x}{d} - n \right) \quad (2.11)$$

$$rect(x) = \square(x) \begin{cases} 0 & \text{if } x > \frac{1}{2} \\ \frac{1}{2} & \text{if } x = \frac{1}{2} \\ 1 & \text{if } x < \frac{1}{2} \end{cases} \quad (2.12)$$

where  $R(x)$  is the reflection coefficients along a wall,  $s_n$  is the corresponding sequence for the  $n^{th}$  element, and  $d$  is the well depth. Scattering in terms of the pressure magnitude  $|p|$  from a surface according to Fraunhofer model is given by Equation 2.2 (Cox & D'Antonio 2009). Normally, an incident wave is reflected from a hard surface with a reflection factor ( $R_n$ ) of +1. According to maximum length sequence for  $N = 7$ ,  $\{1, 1, 0, 1, 0, 0, 0\}$ , if we set back the wells like in Figure 2.5 by a quarter wavelength,  $\lambda/4$ , the wave will travel an additional  $\lambda/2$ . Therefore it is shifted by  $\pi$ , and so the complex amplitude is  $e^{i\pi}$  is equal to  $-1$  for the design frequency (Schroeder 1997). The pressure magnitude at the design frequency becomes (Cox & D'Antonio 2009):

$$|p_m| \approx \left| A \int_s R(x) e^{j\frac{2\pi x m}{Nd}} dx \right| = \left| A \sum_{n=1}^N R_n e^{j\frac{2\pi n m}{N}} \right| \quad (2.13)$$

Consequently, if we have a maximum length sequence for ,  $N = 7$ ,  $\{1, 1, 0, 1, 0, 0, 0\}$ , reflection factors ( $R_n$ ) are  $\{1, 1, -1, 1, -1, -1, -1\}$ . However, if the incident wave has one octave higher frequency than the design frequency, therefore having half the wavelength, the phase is shifted  $2\pi$ , meaning that the surface behaves like a plane surface. As a result, maximum length sequence diffusers are useful over a limited bandwidth, which is over an octave (Cox & D'Antonio 2004; Schroeder 1997). Therefore the scattering pressure magnitude is given by Equation 2.14:

$$|P_m| = \begin{cases} A & m = 0, \pm N, \pm 2N \\ A\sqrt{N+1} & \text{otherwise} \end{cases} \quad (2.14)$$

To overcome this limited scattering properties of maximum length sequences, Cox, Avis and Xiao (2006) introduced active diffusers. They placed an active controller in the central well of a maximum length diffuser for  $N = 7$  as shown in Figure 2.6. The active controller has set to generate reflection factor ( $R_n$ ) of  $-1$ . The passive and active diffusers were built specifically for the design frequency of 500 Hz.

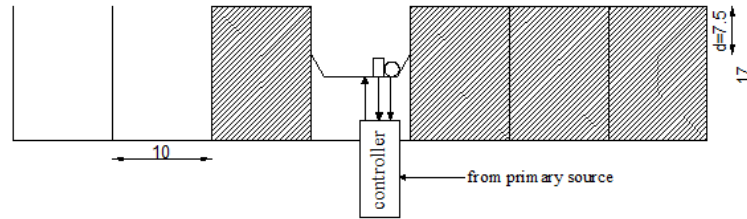


Figure 2.6. Cross section of a one period of an active maximum length sequence for  $N=7$ . The central well has active controller. (Source: Cox, Avis & Xiao 2006, page:808)

At the design frequency of 500 Hz., both active and passive diffusers produced similar scattering properties. However, at 1000 Hz, the passive diffuser behaved like a plane surface as the well depth is half a wavelength. Therefore, the waves reflecting from the surface were in phase. On the contrary, the active diffuser continued scattering, as the reflection factor of the central well was still  $-1$ . Figure 2.7 shows the measured polar responses from a plane surface, the passive and the active maximum length diffuser.

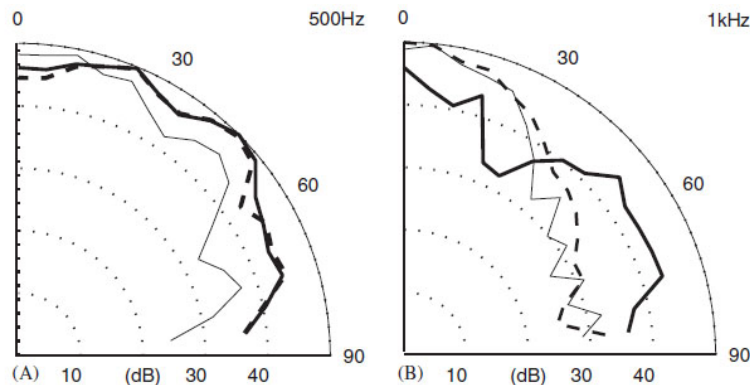


Figure 2.7. The scattering from three surfaces at 500 Hz. and 1000 Hz: Thin line: plane surface, bold line: active MLS diffuser, dotted line: passive MLS diffuser (Source: Cox, Avis & Xiao 2006, page:813)

### 2.2.2. Quadratic Residue Diffusers

Schroeder (1979) continued his research about number theoretic diffusers. Because of the limited diffusion properties of maximum length sequence diffusers, Schroeder (1979) searched for new sequences which should give excellent sound diffusion over more broadband frequency range. Thus, Schroeder (1979) proposed quadratic

residue sequences (also called Legendre sequences) first introduced by Adrien Marie Legendre and Johann Carl Friedrich Gauss. Quadratic residue sequences are given by Equation 2.15:

$$s_n = n^2 \text{ mod } N \quad (2.15)$$

where  $s_n$  is the sequence number for the  $n^{\text{th}}$  well, mod the indication of the least non-negative remainder,  $N$  an odd prime which is also the number of wells per period. For instance, for one period of an  $N = 7$ , quadratic residue diffuser has  $s_n = \{0, 1, 4, 2, 2, 4, 1\}$ . Quadratic residue sequences are symmetrical between  $n \equiv 0$  and  $n \equiv (N - 1)/2$ . Figure 2.8 and Figure 2.9 shows one dimensional quadratic residue diffusers.

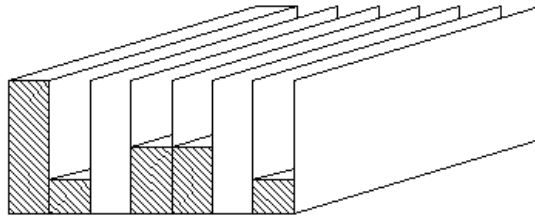


Figure 2.8. One dimensional quadratic residue diffuser (Source: Cox & D'Antonio 2000, page:121)

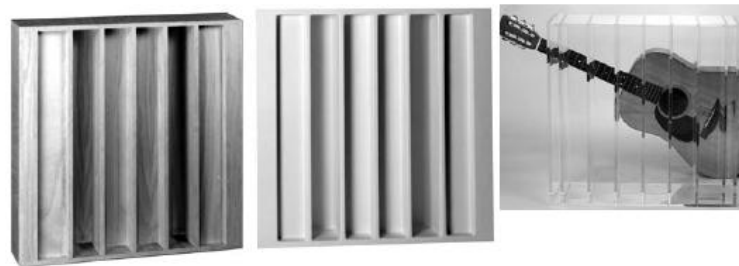


Figure 2.9. One dimensional quadratic residue diffusers made from different materials (Source: Cox & D'Antonio 2009, page:290)

The Fourier Transform of the surface reflection coefficients  $R(x)$  nearly equals to the scattered energy distribution as stated in Equation 2.2. The reflection coefficients of quadratic residue sequence is given by Equation 2.16 (Schroeder 1979):

$$R(n) = e^{2\pi j s_n / N} \quad (2.16)$$

where  $s_n$  is the sequence number for the  $n^{\text{th}}$  well and  $N$  is the number of wells. The auto-correlation of quadratic residue sequences shows the following property (Fan & Darnell

1996):

$$R_n(\tau) = \begin{cases} N & \text{for } \tau \equiv 0(\text{mod}N) \\ E & \text{otherwise} \end{cases} \quad (2.17)$$

If we apply Fourier Transform to the autocorrelation  $R_n(\tau)$ :

$$R_n(\tau) \leftrightarrow \sum_{\tau=0}^{N-1} R(\tau)e^{-2\pi jnk/N} = R(0)e^{-2\pi j0k/N} = |F(k)|^2 = N \quad (2.18)$$

and we can write:

$$|F(k)| = \sqrt{R(0)} = \sqrt{N} \quad (2.19)$$

The power spectrum, e.g. the Fourier transform of the autocorrelation function of the quadratic residue sequences have a constant magnitude. Therefore according to Fraunhofer model, we can say each scattered wave from the quadratic residue diffusers have a constant magnitude which shows us the optimum diffusion properties. Consequently the scattered energy distribution in terms of pressure magnitude is given by Equation 2.20 (Cox & D'Antonio 2009):

$$|P_m| = \sqrt{N}, m = 0, \pm 1, \pm 2, \dots \quad (2.20)$$

Even energy lobes at the scattering can also be seen in Figure 2.10 which shows the polar responses of a quadratic residue diffuser and a flat surface.

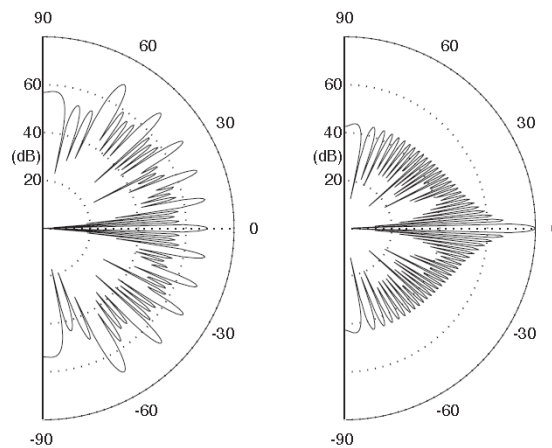


Figure 2.10. Scattering from a quadratic residue sequence and a flat surface (Source: Cox & D'Antonio 2009, page:291)



## *Design of Quadratic Residue Diffusers*

Quadratic residue diffusers shows optimum diffusion properties for certain bandwidths. At the beginning of the design stage of the quadratic residue diffuser, an upper frequency limit,  $f_{max}$  should be found. The chosen well width,  $W$  determines the lowest wavelength,  $\lambda_{min}$ , and is related to it by Equation 2.21 (Cox & D'Antonio 2004):

$$W = \lambda_{min}/2 \quad (2.21)$$

$W$  is the total well width of one well and is equal to (D'Antonio & Konnert 1983):

$$W = w + t \quad (2.22)$$

where  $w$  is the well width and  $t$  is the width of the fins separating the wells. Since we know the speed of sound is  $c = f \cdot \lambda$  in  $m/s$ , the Equation 2.21 becomes:

$$W = c/2f_{max} \quad (2.23)$$

Cox and D'Antonio (2009) states that the criterion for the well width is that the wells should be as narrow as possible to maximize the upper frequency but not so narrow to prevent absorption and difficulty of manufacturing. According to D'Antonio and Konnert (1992), manufacturing limits the lowest well width to 2.5 cm. Also, as the well width increases, the upper frequency limit decreases which may cause specular reflections at higher frequencies. Cox and D'Antonio (2009) states that the usual well widths are around 5 cm. The design frequency,  $f_0$  of the quadratic residue diffusers determines the lower frequency limit. For a given maximum depth,  $d_{max}$  that depends on the manufacturing and space limitation, the design frequency is given by Equation 2.24 (Cox & D'Antonio 2004):

$$f_0 = \frac{s_{max}}{N} \frac{c}{2d_{max}} \quad (2.24)$$

where  $s_{max}$  is the largest number in the given quadratic residue sequence. The quadratic residue diffusers show even scattering behavior at the integer multiples of the design fre-

quency as stated in Equation 2.20. We can see from Equation 2.24 that the choice of prime number  $N$  and the maximum number  $s_{max}$  in the quadratic residue sequence determines the lower frequency efficiency of the device (Cox & D'Antonio 2004). For instance for quadratic residue sequence based on prime number 7,  $s_n = \{0, 1, 4, 2, 2, 4, 1\}$  and the  $s_{max} = 4$ . In addition let's consider another sequence based on prime number 17,  $s_n = \{0, 1, 4, 9, 16, 8, 2, 15, 13, 13, 15, 2, 8, 16, 9, 4, 1\}$  and the  $s_{max} = 16$ . If we compare  $s_{max}/N$  for  $4/7$  and  $16/17$ , it is clear that the quadratic residue diffuser based on prime number 7 is more efficient in terms of lower frequency. Furthermore, in order to increase the bass response of the diffuser, Cox and D'Antonio (2004) suggests a constant phase shift which is given in Equation 2.25:

$$s_n = (n^2 + m) \bmod N \quad (2.25)$$

In addition, architectural requirements and manufacturing determines the lower frequency of the device in terms of allowable maximum depth,  $d_{max}$ . The allowable space changes from one architectural space to another. Therefore, before the design process, it is crucial to discuss the space requirements in order to construct the quadratic residue diffusers for a particular design frequency. However, D'Antonio and Konnert (1992) states that the allowable maximum depth cannot exceed 40 cm. in terms of absorption and manufacturing. After the lower and upper frequency limits are set based on previously mentioned criteria, well depths of each well are calculated for the given design frequency  $f_0$  based on Equation 2.26:

$$d_n = \frac{s_n c}{2N f_0} \quad (2.26)$$

where  $d_n$  is the depth of the  $n^{th}$  well in the quadratic residue diffuser,  $s_n$  is the sequence number for the  $n^{th}$  well, and  $N$  is the number of wells. Figure 2.11 shows the cross-section of a one dimensional quadratic residue diffuser based on prime number 7.

Critical frequencies at quadratic residue diffusers occur at  $mNf_0$  where  $m = 1, 2, 3, \dots$ . At these frequencies, diffuser behaves like a plane surface because of the wells radiating in phase. In order to avoid this, it is essential to place the first critical frequency above the maximum frequency,  $f_{max}$  of the device which is given by Equation 2.27 (Cox

& D'Antonio 2004):

$$N \gg \frac{c}{2\omega f_0} \quad (2.27)$$

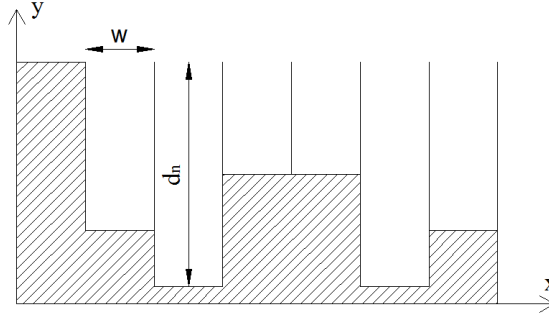


Figure 2.11. Cross-section of one dimensional quadratic residue diffuser based on prime number 7 (Source: Cox & D'Antonio 2009, page:290)

### 2.2.3. Primitive Root Diffusers

A primitive root sequence is given by Equation 2.28 (Cox & D'Antonio 2004; Schroeder 1997):

$$s_n = r^n \text{ mod } N \quad n = 1, 2, 3, \dots, N - 1 \quad (2.28)$$

where  $N$  is an odd prime and  $r$  the primitive root of  $N$ . The primitive root has  $N-1$  wells per period. In general, an integer  $r$  is said to be a primitive root of a prime  $N$  if and only if  $r^0, r^1, r^2, \dots, r^{N-1}$  are all different modulo  $N$  (Fan & Darnell 1996). Since  $\text{gcd}(r, N) = 1$ , it is clear that  $r^{N-1} = 1(\text{mod } N)$ . For instance, if  $r = 3$ , and  $N = 7$ , the  $s_n$  will be  $s_n = \{3, 2, 6, 4, 5, 1\}$  which are all distinct. Therefore 3 is a primitive root of 7.

The well depths  $d_n$  for the  $n^{\text{th}}$  element of the primitive root sequence is given by Equation 2.29 (Cox & D'Antonio 2000):

$$d_n = \frac{s_n c}{2N f_0} \quad (2.29)$$

where  $d_n$  is the depth of the  $n^{\text{th}}$  well in the quadratic residue diffuser,  $s_n$  is the sequence number for the  $n^{\text{th}}$  well,  $N$  is the prime number and  $f_0$  is the design frequency.

The primitive root diffusers reduce the energy in the specular direction and therefore produce a notch diffuser, meaning groovy at the scattering directions (Cox & D'Antonio 2000). Like quadratic residue diffusers, primitive root diffusers has increased diffusion at the integer multiples of the design frequency. However, Cox and D'Antonio states that a large of  $N$  is required to achieve minimum pressure at the specular reflection. For instance, their comparative study (2009) on the scattering of two primitive root diffusers based on prime numbers  $N = 7$  and  $N = 37$  and a flat surface indicates that scattering from primitive root diffuser for  $N = 7$  produces 3 lobes showing specular direction as in plane surface scattering. However when a large number of prime is selected,  $N = 37$ , a significant decrease occurs in the specular direction. The results of this study is shown in Figure 2.12. The requirement of large primes is disadvantageous for manufacturing and construction.

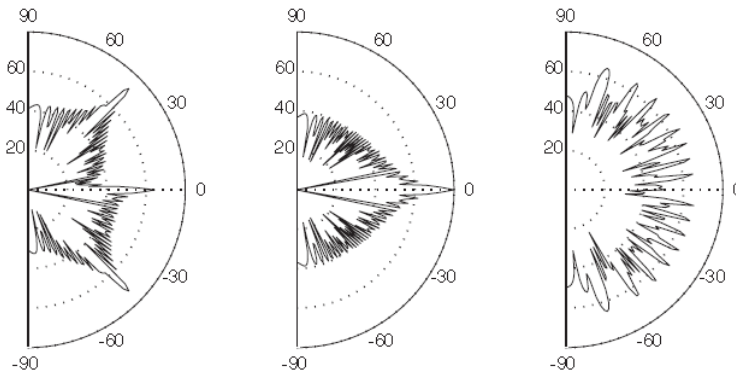


Figure 2.12. Scattering from PRD based on  $N = 7$ , a plane surface, and PRD based on  $N = 37$  and for normal incidence (Source: Cox & D'Antonio 2009, page:298)

In addition, the scattering in terms of pressure amplitudes of the lobes are given by Equation 2.30 (Cox & D'Antonio 2004):

$$|P_m| \begin{cases} A & m = 0, \pm N, \pm 2N \\ A\sqrt{N} & otherwise \end{cases} \quad (2.30)$$

We can say that a decrease will occur at the integer multiples of  $N$ . However, they will be above the upper frequency limit of the primitive root diffuser and can be ignored.

## 2.3. Two Dimensional Diffusers

One dimensional diffusers scatter into a hemi-disc and act like a plane surface at other directions as mentioned before. There is also a need for a diffuser that scatters into a hemisphere. This can be achieved by two dimensional diffusers. Currently, there are two known procedures for constructing two dimensional diffusers: Product Arrays Method and Folding Array Method (Cox & D'Antonio 2009). The main concept of constructing two dimensional diffusers is to transfer the scattering properties of one dimensional diffusers while forming multi-dimensional ones. Therefore, the autocorrelation properties of the sequences forming 1D diffusers should be preserved in 2D arrays. If we take two perfect sequences  $a_m$  and  $a_n$  which have autocorrelation properties as described in Equation 2.8, an array of  $a_{m,n}$  should have autocorrelation function properties such as in Equation 2.31 (Fan & Darnell 1996):

$$R(\tau, \rho) = \begin{cases} E & \text{for } (\tau, \rho) = (0, 0) \\ 0 & \text{for } (\tau, \rho) \neq (0, 0) \end{cases} \quad (2.31)$$

in order to be called a perfect array. Furthermore, the Fourier transform of autocorrelation function of perfect arrays are given by Equation 2.32 (Fan & Darnell 1996):

$$R(\tau) \leftrightarrow |F(u, v)|^2 = E \quad (2.32)$$

or we can write:

$$|F(u, v)| = \sqrt{E} \quad (2.33)$$

Therefore, the scattering magnitude of perfect arrays should have a frequency dependent constant,  $\sqrt{E}$  in order to provide the perfect array properties.

### 2.3.1. Product Array Method

Product Array Method is basically a vector product of a row and column sequence vector to produce a P by Q matrix (Schyndel et al. 2000). In other words, two sequences, one for the x direction, one for the z direction is considered and the amplitude of both

forms the two dimensional diffuser. For quadratic residue sequence the product array method is given by Equation 2.34 (Cox & D'Antonio 2009):

$$s_{n,m} = (n^2 + m^2) \text{mod} N \quad (2.34)$$

where n and m are integers and give the sequence for the  $n^{\text{th}}$  well in the x direction and  $m^{\text{th}}$  well in the z direction. The same method can be applied to primitive root diffusers and is given by Equation 2.35 (Cox & D'Antonio 2009):

$$s_{n,m} = (r^n + r^m) \text{mod} N \quad (2.35)$$

In addition, Cox and D'Antonio (2009) stated that it is also possible to use two different number sequences at x and z directions. But both residue sequences should be based on the same prime number modulo. A two dimensional (2D) quadratic residue sequence for  $N = 7$  based on Product Array Method is shown at Figure 2.13:

$s_m = \{0, 1, 4, 2, 2, 4, 1\} \text{ mod } 7$

$\xrightarrow{m}$   $s_n = \{0, 1, 4, 2, 2, 4, 1\} \text{ mod } 7$

n ↓	0	1	4	2	2	4	1
	1	2	5	3	3	5	2
	4	5	1	6	6	1	5
	2	3	6	4	4	6	3
	2	3	6	4	4	6	3
	4	5	1	6	6	1	5
	1	2	5	3	3	5	2

Figure 2.13. Two dimensional quadratic residue sequence for N=7 based on Product Array Method

After the array is constructed, one dimensional equations for  $f_{max}$ ,  $f_0$ , and the well depths  $d_n$  are calculated according to the equations in Section 2.2.2. In 1976, Schroeder also proposed 2D quadratic residue diffusers based on Product Array Method on a scaled model. But the polar response data of proposed structure shown in Figure 2.14 could not be found.

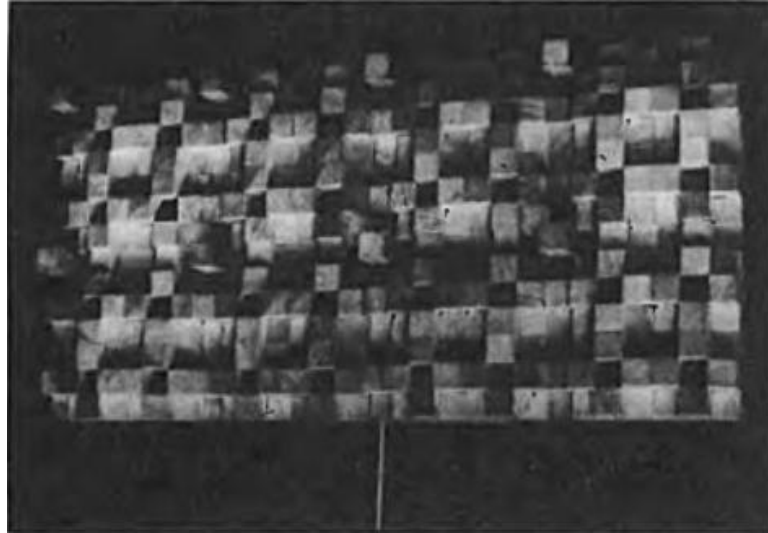


Figure 2.14. Scaled model of two dimensional quadratic residue sequence for  $N=7$  based on Product Array Method (Source: Schroeder 1979, page:962)

The two dimensional autocorrelation plot and power spectrum of 2D quadratic residue sequence based on Product Array Method is configured and calculated with MATLAB in Figure 2.15 and Figure 2.16 (see Appendix A: script 2.1).

We can see from Figure 2.15 that the two dimensional autocorrelation properties is not perfect, showing irregular formations for  $(\tau, \rho) \neq (0, 0)$ . The power spectrum is flat except at the DC. In addition, Cox and D'Antonio states that 2D diffusers based on Product Array Method have lower frequency efficiency than 1D diffusers as  $s_{max}/N$  is closer to 1. If we have a look at Figure 2.13,  $s_{max}/N = 6/7$  for 2D quadratic residue sequence. However,  $s_{max}/N = 4/7$  for 1D quadratic residue structures.

In addition, it is possible to adjust the original sequence,  $s_n = \{0, 1, 4, 2, 2, 4, 1\}$  such as in Figure 2.17. In order to place 0 in the middle of the diffuser,  $n$  and  $m$  are started from 4 so that on the diagonal the original sequence becomes  $s_n = \{4, 1, 2, 0, 2, 1, 4\}$ . Cox and D'Antonio (2009) states that it is suitable to start the  $n$  and  $m$  from any integer, because the surface is periodic.

At the same study, Cox and D'Antonio (2009) predicted the scattering from this modified 2D quadratic residue diffusers based on  $N = 7$ . Figure 2.14 shows the scattering in 3D polar responses. The autocorrelation and power spectrum for the modified 2D quadratic residue diffuser for  $N = 7$  is configured and calculated with MATLAB in Figure 2.19 and Figure 2.20 (see Appendix A: script 2.2).

When compared to Figure 2.15, Figure 2.19 shows more irregular formations for

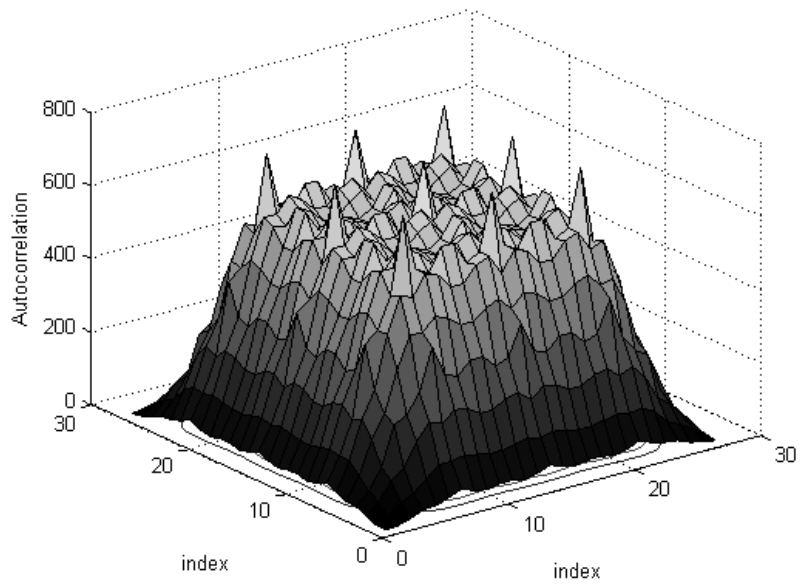


Figure 2.15. Autocorrelation plot of two dimensional quadratic residue sequence for N=7 based on Product Array Method

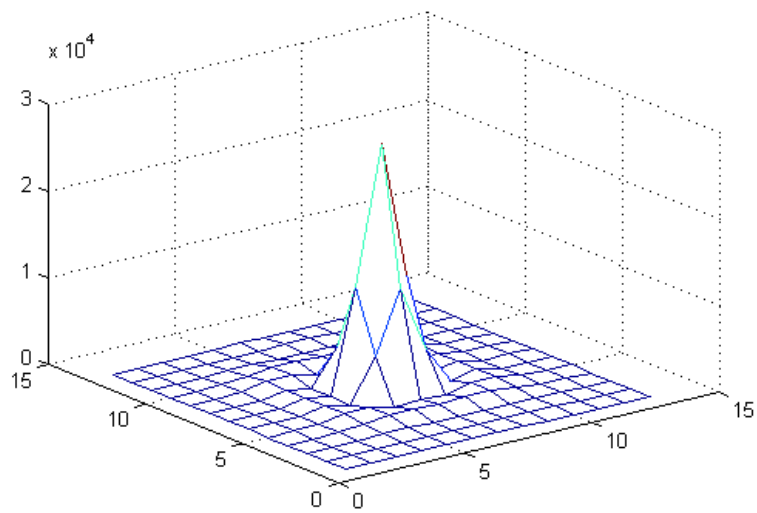


Figure 2.16. Power spectrum of two dimensional quadratic residue sequence for N=7 based on Product Array Method



4	6	3	2	3	6	4
6	1	5	4	5	1	6
3	5	2	1	2	5	3
2	4	1	0	1	4	2
3	5	2	1	2	5	3
6	1	5	4	5	1	6
4	6	3	2	3	6	4

Figure 2.17. A sequence array for two dimensional quadratic residue diffuser for  $N = 7$   
 (Source: Cox & D'Antonio 2004, page:316)

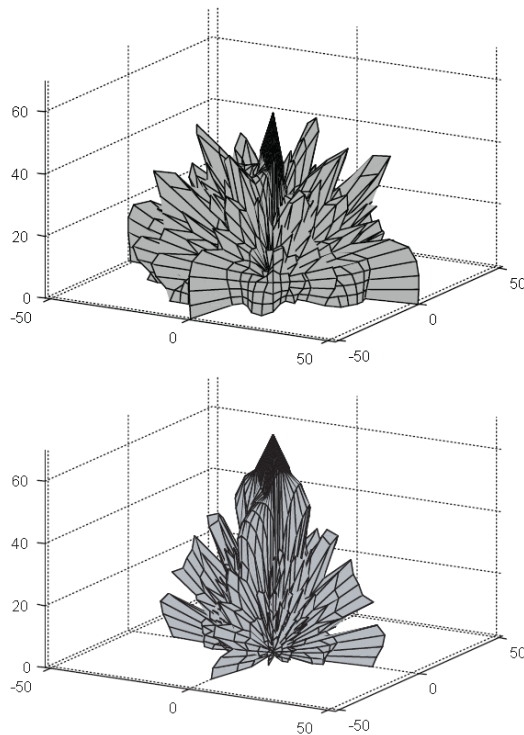


Figure 2.18. Scattering from two dimensional quadratic residue diffuser for  $N = 7, s_n = \{4, 1, 2, 0, 2, 1, 4\}$  (top), and a flat surface (below) at four times the design frequency (Source: Cox & D'Antonio 2009, page:318)

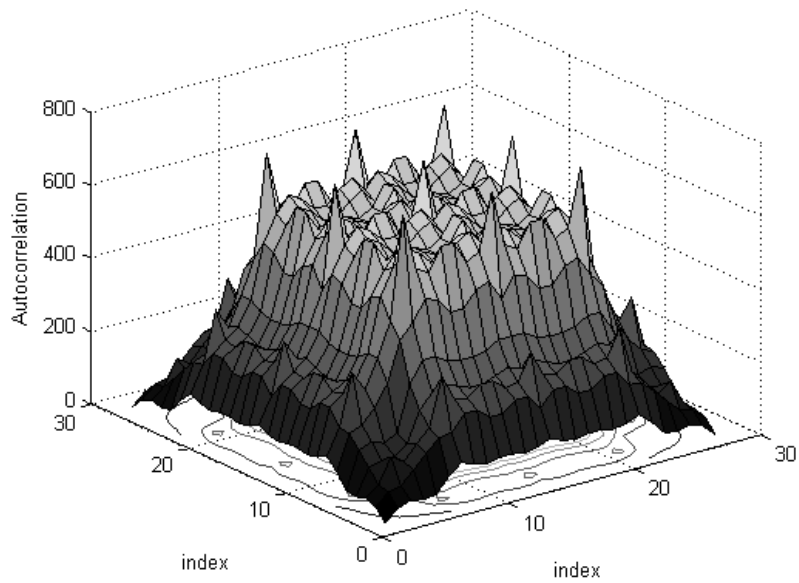


Figure 2.19. Autocorrelation plot of two dimensional quadratic residue sequence for  $N=7, s_n = \{4, 1, 2, 0, 2, 1, 4\}$  based on Product Array Method

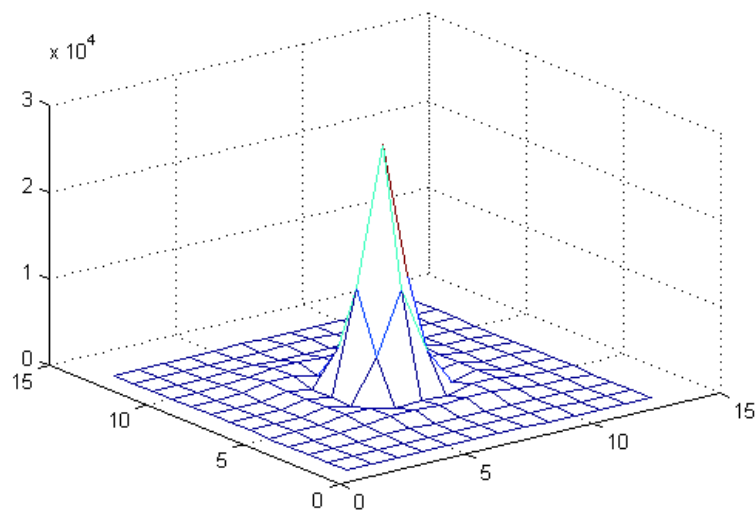


Figure 2.20. Power spectrum of two dimensional quadratic residue sequence for  $N=7, s_n = \{4, 1, 2, 0, 2, 1, 4\}$  based on Product Array Method

$(\tau, \rho) \neq (0, 0)$ . In addition, the power spectrum is less flat for  $(\tau, \rho) \neq (0, 0)$ . Therefore it is clear that the shifted version will not show scattering properties as the original 1D quadratic residue sequence.

As for the manufactured and patented products based on Product Array Method, D'Antonio and Konnert (1987) modified two dimensional quadratic residue diffusers under the registered trademark Omniffusor and FRG Omniffusor with a well-depth optimization technique over the Product Array Method which is shown in Figure 4.11. The diffusion coefficients are requested and obtained from D'Antonio (personal communication 2011) for further comparison. However, the optimization procedure is not stated in registered trademark Omniffusor, which is described in U.S. Pat. No. D306,764.

### **2.3.2. Folding Array Method**

The Folding Array Method is first introduced by MacWilliams and Sloane in 1976. It is based on Chinese Remainder Theorem which is mentioned in Section 1.1. MacWilliams and Sloane (1976) folded a pseudo-random sequence of composite length into a matrix diagonal and proved that the matrix has the same autocorrelation and the Fourier properties as the pseudo-random sequence. A sequence which has a composite length of  $pq$  can be folded into an array of length  $p$  and width  $q$ , where  $p$  and  $q$  are the co-prime. The construction of the arrays based on Folding Array Method is shown in Figure 2.21. For example, a sequence of length 21 can be folded into a  $3 \times 7$  array. The rule is to have two co-prime factors such as 3 and 7. Therefore, this method can not be applied to quadratic residue diffusers for the reason of having prime number of wells.

Cox and D'Antonio (2004) have studied the primitive root diffusers to form two dimensional diffusers based on folding array method. The prime number  $N = 43$  was generated and the sequence was 42 elements long. It was folded into a  $6 \times 7$  array. The predicted scattering of 2D primitive root diffuser is shown in Figure 2.22.

Another study based on the Folding Array Methods is the work of D'Antonio and Konnert (1993). They designed a two dimensional primitive root diffuser with Folding Arrays Method under the registered trademark Skyline which is shown in Figure 2.23. The scattering properties according to different multiples of design frequency is given in Figure 2.24 (D'Antonio & Konnert 1995). The 2D diffuser has no fins and due to

$$A = \{a_1, a_2, a_3, \dots, a_{13}, a_{14}, a_{15}\}$$

$$\text{Length}(A) = p \times q$$

$$p = 5$$

$$q = 3$$

a <sub>1</sub>				
	a <sub>2</sub>			
		a <sub>3</sub>		

a <sub>1</sub>			a <sub>4</sub>	
	a <sub>2</sub>			a <sub>5</sub>
a <sub>6</sub>		a <sub>3</sub>		

a <sub>1</sub>	a <sub>7</sub>	a <sub>13</sub>	a <sub>4</sub>	a <sub>10</sub>
a <sub>11</sub>	a <sub>2</sub>	a <sub>8</sub>	a <sub>14</sub>	a <sub>5</sub>
a <sub>6</sub>	a <sub>12</sub>	a <sub>3</sub>	a <sub>9</sub>	a <sub>15</sub>

Figure 2.21. Folding Array Construction Method

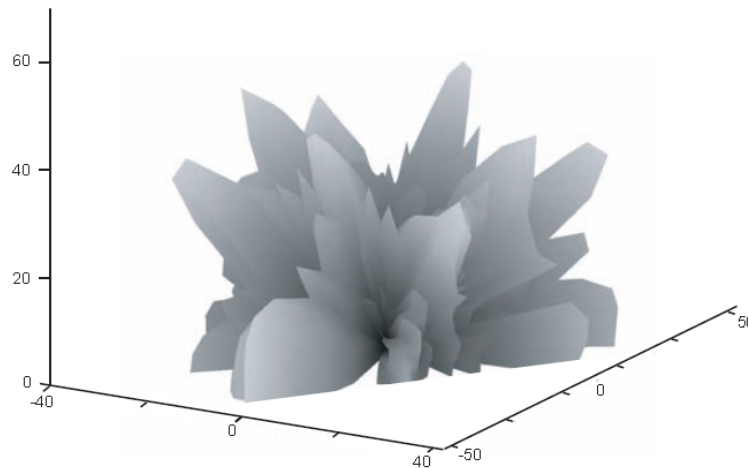


Figure 2.22. Scattering from 2D primitive root diffuser which is folded into a 6x7 array  
(Source: (Cox & D'Antonio 2009, page:320))

the nature of Folding Array Method, shows no symmetry. In addition, as it can be seen from Figure 2.24, the 2D primitive root diffuser's scattering becomes more even in the multiples of design frequency.

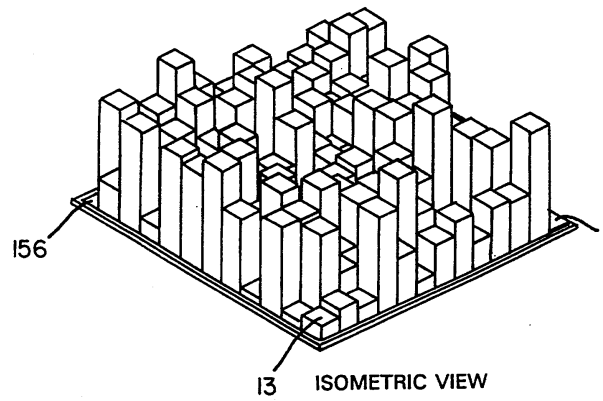


Figure 2.23. Skyline (Source: D'Antonio & Konnert 1993)

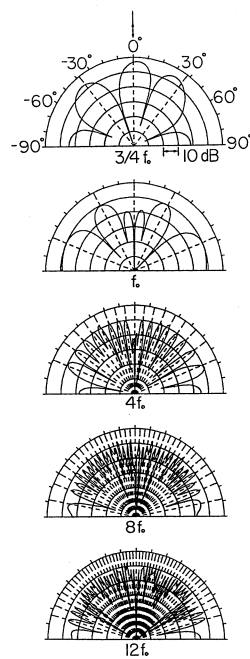


Figure 2.24. Scattering from registered trademark Skyline at 3/4, 1, 4, 8, 12 times design frequency,  $f_0$  (Source: D'Antonio & Konnert 1993)

## CHAPTER 3

# CONSTRUCTION OF TWO DIMENSIONAL QUADRATIC RESIDUE DIFFUSERS WITH DISTINCT SUMS PROPERTY METHOD

### 3.1. Distinct Sums Property Method

Schyndel et al. (1999; 2000) have introduced The Distinct Sums Property (DSP) method for folding a one dimensional sequence into a two dimensional array. The proposed method is used in digital watermarking and steganography for the reason of offering ideal two dimensional autocorrelation properties. The method is based on cyclic shifts on the rows or columns of the array. Schyndel et al. (2000) states that Distinct Sums Property (DSP) can only be applied to a sequence  $s_n = \{s_1, s_2, \dots, s_n\}$  based on prime  $N$  and if:

$s_1 + s_2, s_2 + s_3, \dots, s_{n-1} + s_n, s_n + s_1$  are all distinct, and also  $s_1 + s_2 + s_3, \dots, s_{n-1} + s_n + s_1, s_n + s_1 + s_2$ , and for  $k = 4, 5, \dots, N - 2$  consecutive sums.

To construct an array with Distinct Sums Property Method, first the seed sequence  $s_n = \{s_1, s_2, \dots, s_n\}$  is placed at each row. Second, seed sequence is shifted by  $m \times (\text{rownumber} - 1)$  depending on the previous row, where  $m = 1, 2, \dots, N - 1$ . Therefore the array is constructed by Distinct Sums Property and possesses the DSP property (Schyndel 1999; 2000). Schyndel (2000) states that duplicate rows can be removed or row of zeros can be added. In addition, Tirkel et al. (1998) mentions that the maximum duplicate of rows or columns cannot exceed 1. The method is basically shown at Figure 3.1.

### 3.2. Application of Distinct Sums Property Method to Quadratic Residue Sequence for $N = 7$ and Autocorrelation Properties

DSP Method is chosen for the applicable properties of both quadratic residue sequence and the method itself. Tirkel (1998) and Schyndel et al. (2000) states that the Legendre sequences shows a perfect response for the DSP Method. In addition, the phase shifting properties of the method offers many construction possibilities. Therefore DSP Method is applied for quadratic residue sequence based on prime number  $n = 7$ ,  $s_n = \{0, 1, 4, 2, 2, 4, 1\}$  for  $m = 1, 2, \dots, 6$  and arrays are formed in Figure 3.2.

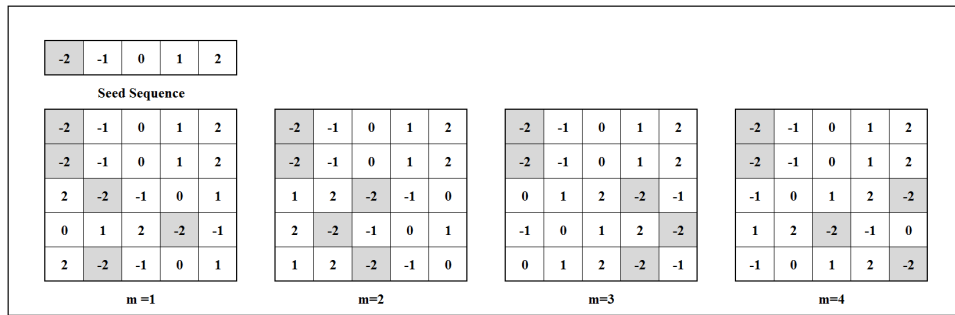


Figure 3.1. The Distinct Sums Property Array Method (Source: Schyndel et al. 1999)

It is stated that the autocorrelation properties of a sequence determines the even scattering from number theoretic diffusers. Therefore, two-dimensional autocorrelation plots of each  $m$  are calculated based on and plotted in Figure 3.3 and Figure 3.4. The evaluation of the autocorrelation properties of sequences are also determined by peak to largest sidelobe ratio. The ratio of the peak value magnitude for  $(\tau, \rho) = (0, 0)$  to the sidelobe magnitudes for  $(\tau, \rho) \neq (0, 0)$  should be highest in order to show the ideal autocorrelation property. For instance, a perfect array as shown in Equation 2.31 has a peak value of  $E$  for  $(\tau, \rho) = (0, 0)$ , and the sidelobes are 0 for  $(\tau, \rho) \neq (0, 0)$ . The ratio is  $E/0 = \infty$  for perfect arrays. Therefore for better comparison of the autocorrelation properties of arrays based on Product Array and Distinct Sums Property, Table 3.1 shows the peak to largest sidelobe ratios. As seen in Table 3.1, Distinct Sums Property method has higher ratios for all  $m$  than Product Array method. Therefore, the autocorrelation properties of quadratic residue sequence array based on DSP is better than the array based on Product Array method. In addition, power spectrum plots of each  $m$  are shown in

Table 3.1. Peak to Largest Sidelobe Ratios

P. A.	P.A. Shifted	DSP for $m = 1, 2, 3, 4, 5, 6$
1,26	1,03	1,5

Figure 3.5 and Figure 3.6 (see Appendix A:script 3.1:3.6). As seen in Figure 3.3 and Figure 3.4, the autocorrelation properties of 2D arrays based on DSP method shows perfect array properties as stated in Equation 2.31. In addition, the power spectrum is more flat for  $m = 1$  than for  $m = 2, 3, 4, 5, 6$  and shifted Product Array as shown in Figure 2.20. It resembles the power spectrum of quadratic residue sequence based on Product Array method. Therefore, based on design equations of quadratic residue sequences in Section 2.2.2, the diffuser for can be constructed and modeled for  $m = 1$ .

### 3.3. Construction of Two Dimensional Quadratic Residue Diffusers

Cox and D'Antonio (2009) stated that the lower frequency efficiency of two dimensional diffusers tend to be less than one dimensional diffusers for the reason of  $s_{max}/N$  is greater for Product Array Method. For quadratic residue diffuser based on Product Array Method  $s_{max}/N$  is equal to  $6/7$ . However, DSP Method uses the original seed sequence,  $s_n = \{0, 1, 4, 2, 2, 4, 1\}$  and  $s_{max}/N$  is equal to  $4/7$ .

Therefore the DSP Method is expected to have more bass efficiency than Product Array Method.

In order to specify the upper frequency,  $f_{max}$  limit, the total well width,  $W = w + t$  should be decided. For further comparison and manufacturing, the author of the research uses the same total widths which are suggested and manufactured by D'Antonio et al. (1990) like Omniffusor and FRG Omniffusor. In addition Cox and D'Antonio (2009) suggests similar dimensions for scattering comparison. Therefore the total well width for both vertical and horizontal directions:

$$W = w + t = 7.8 + 0.6 = 8.4cm. \quad (3.1)$$

where  $w$  is the well width and  $t$  is the width of the fins separating the wells. Since the proposed diffuser will be constructed from wood, min. 0.6 cm. fin width is a necessity.



Seed Sequence  $s_n = \{0, 1, 4, 2, 2, 4, 1\}$

0	1	4	2	2	4	1
0	1	4	2	2	4	1
1	0	1	4	2	2	4
2	4	1	0	1	4	2
1	4	2	2	4	1	0
2	4	1	0	1	4	2
1	0	1	4	2	2	4

m=1

0	1	4	2	2	4	1
0	1	4	2	2	4	1
4	1	0	1	4	2	2
1	4	2	2	4	1	0
4	2	2	4	1	0	1
1	4	2	2	4	1	0
4	1	0	1	4	2	2

m=2

0	1	4	2	2	4	1
0	1	4	2	2	4	1
2	4	1	0	1	4	2
4	1	0	1	4	2	2
2	2	4	1	0	1	4
4	1	0	1	4	2	2
2	4	1	0	1	4	2

m=3

0	1	4	2	2	4	1
0	1	4	2	2	4	1
2	2	4	1	0	1	4
4	2	2	4	1	0	1
2	4	1	0	1	4	2
4	2	2	4	1	0	1
2	2	4	1	0	1	4

m=4

0	1	4	2	2	4	1
0	1	4	2	2	4	1
4	2	2	4	1	0	1
1	0	1	4	2	2	4
4	1	0	1	4	2	2
1	0	1	4	2	2	4
4	2	2	4	1	0	1

m=5

0	1	4	2	2	4	1
0	1	4	2	2	4	1
1	4	2	2	4	1	0
2	2	4	1	0	1	4
1	0	1	4	2	2	4
2	2	4	1	0	1	4
1	4	2	2	4	1	0

m=6

Figure 3.2. The Application of DSP Method for One Dimensional Quadratic Residue Sequence for  $N = 7$

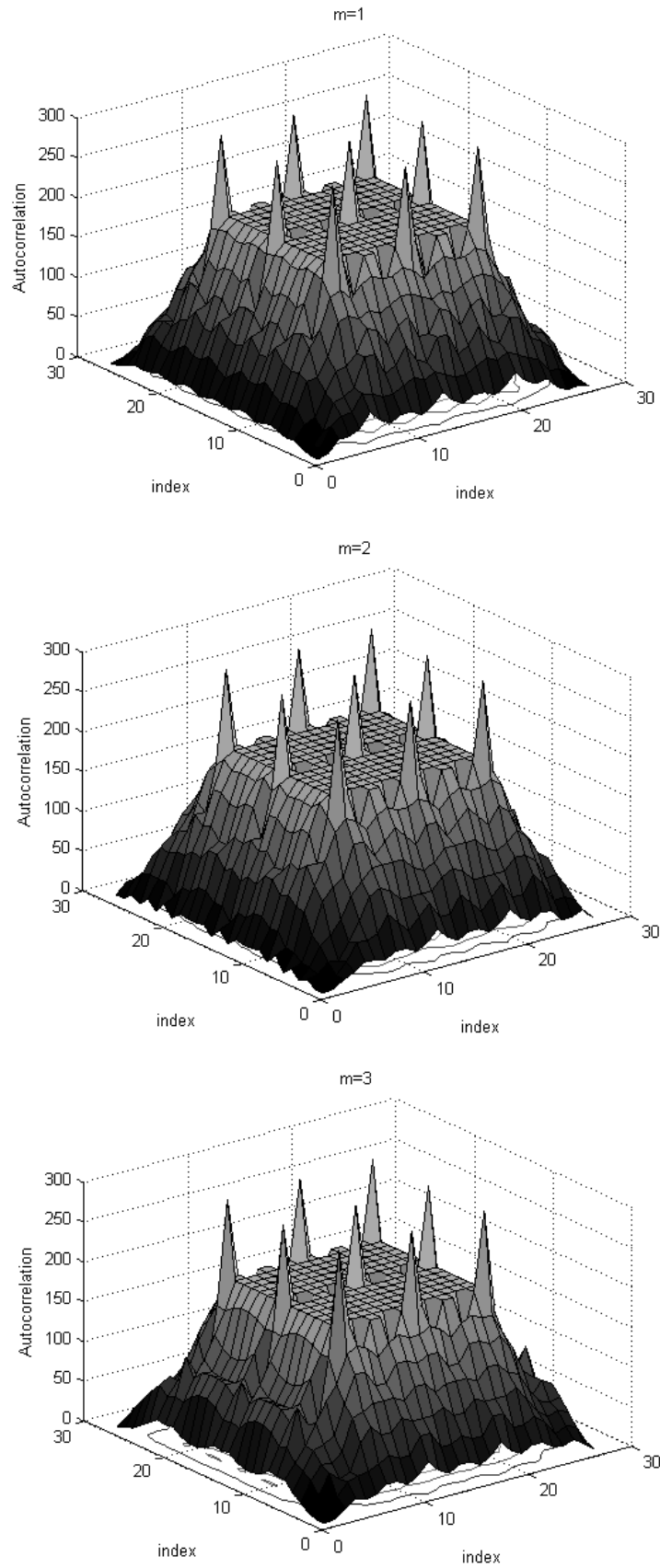


Figure 3.3. Autocorrelation Plot of 2D Quadratic Residue Sequences for  $N = 7$  based on DSP Method for  $m = 1, 2, 3$

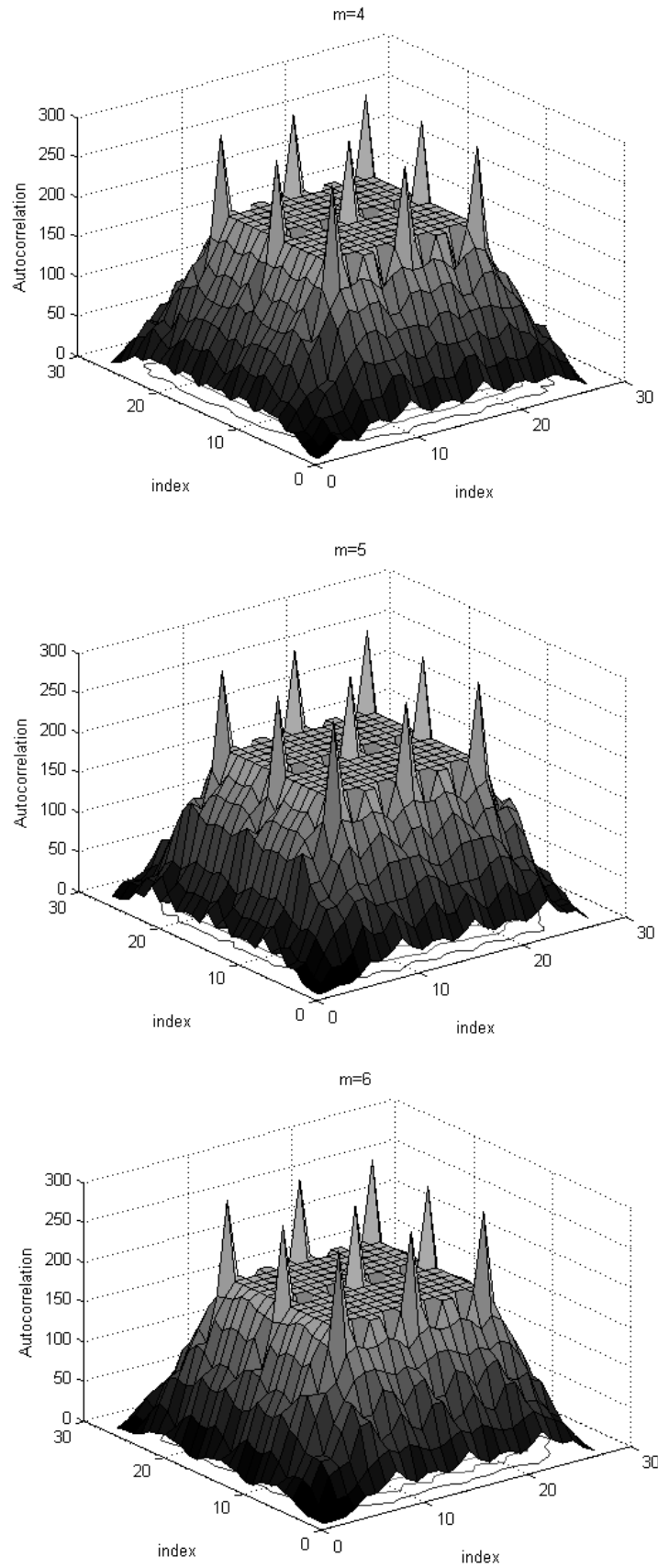


Figure 3.4. Autocorrelation Plot of 2D Quadratic Residue Sequences for  $N = 7$  based on DSP Method for  $m = 5, 6, 7$

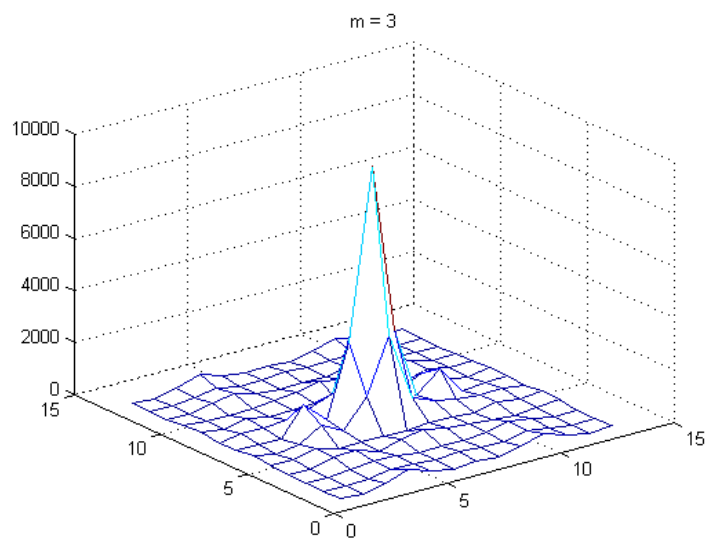
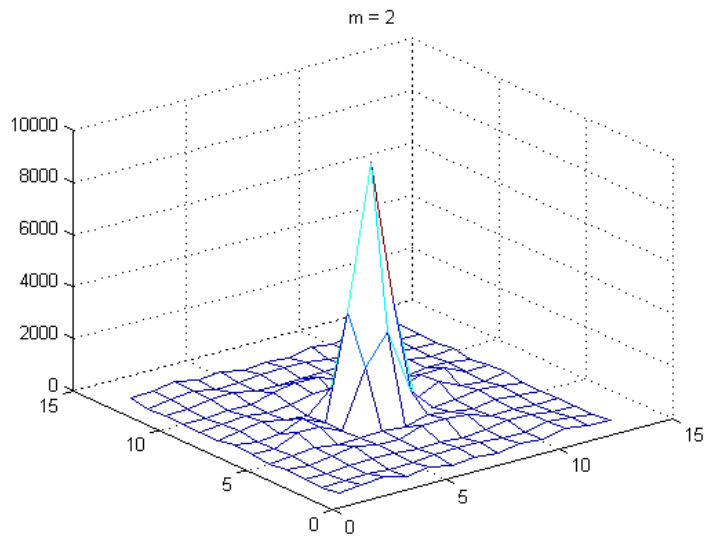
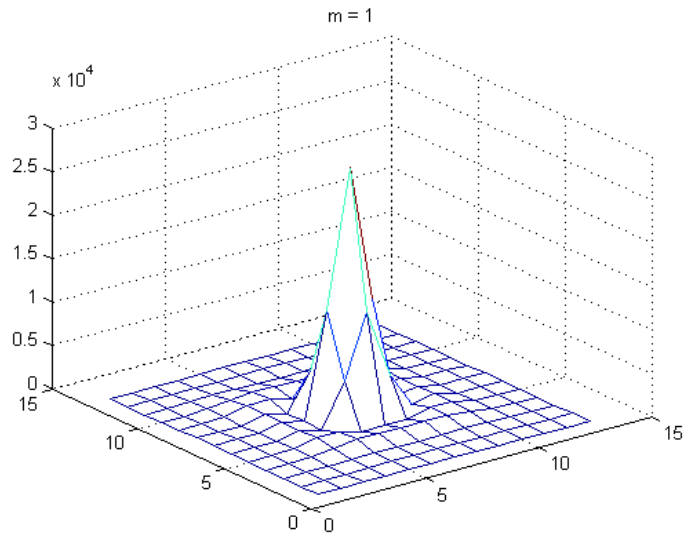


Figure 3.5. Power Spectrum of 2D Quadratic Residue Sequences for  $N = 7$  based on DSP Method for  $m = 1, 2, 3$

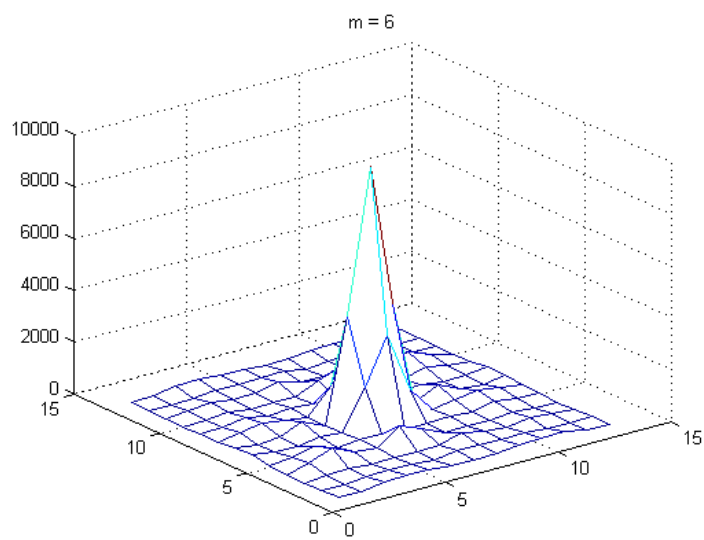
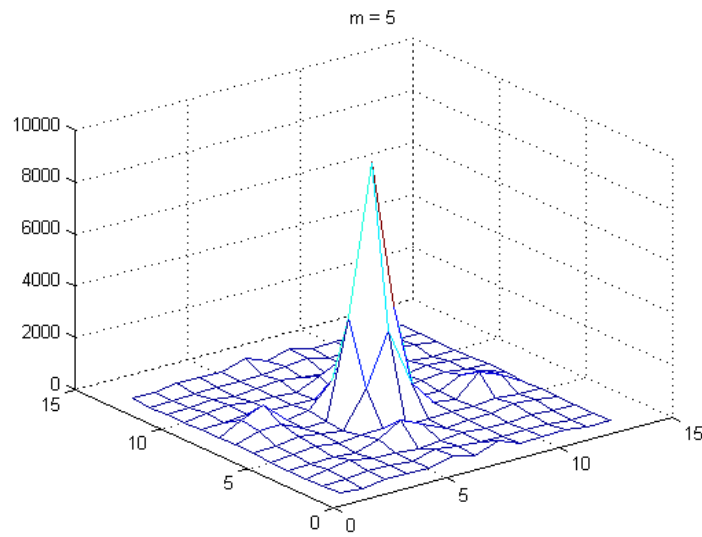
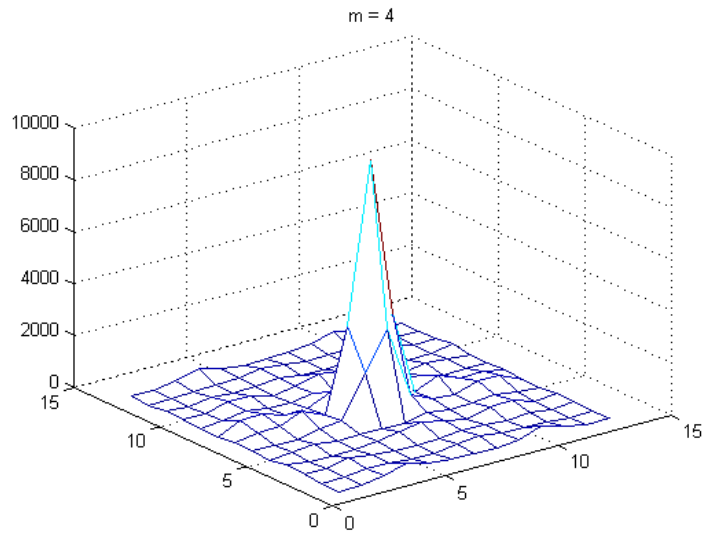


Figure 3.6. Power Spectrum of 2D Quadratic Residue Sequences for  $N = 7$  based on DSP Method for  $m = 4, 5, 6$

The total dimensions of the 2D diffuser is:

$$W_t = (w + t)N + t = (7.8 + 0.6)7 + 0.6 = 59.4cm. \quad (3.2)$$

The upper frequency limit is calculated according to Equation 3.3:

$$f_{max} = \frac{c}{2W} = 2041.667Hz. \quad (3.3)$$

The maximum well depth of the device determines the design frequency,  $f_0$  of the device, vice versa. For further bass efficiency, the maximum well depth is chosen around 20 cm. Correspondingly, the design frequency of the device should be around 500 Hz. for large bandwidth diffusion. For  $f_0 = 500Hz$ , the maximum well depth  $d_{max}$  is given by Equation 3.4:

$$d_{max} = \frac{s_{max}}{N} \frac{c}{2f_0} = 19.6cm. \quad (3.4)$$

Therefore both values satisfy the requirements. For construction and prediction the modulation based on  $m = 1$  is chosen. Consequently, for  $f_0 = 500Hz$ , well depths formed according to DSP Method are calculated according to Equation 3.5 and results are given in Table 3.2.

$$d_n = \frac{s_n c}{2N f_0} \quad (3.5)$$

Table 3.2. The Calculation of Well Depths for 2D Quadratic Residue Sequence for  $N = 7$

Well depths, $d_n$ in meters						
0	0,049	0,196	0,098	0,098	0,196	0,049
0	0,049	0,196	0,098	0,098	0,196	0,049
0,049	0	0,049	0,196	0,098	0,098	0,196
0,098	0,196	0,049	0	0,049	0,196	0,098
0,049	0,196	0,098	0,098	0,196	0,049	0
0,098	0,196	0,049	0	0,049	0,196	0,098
0,049	0	0,049	0,196	0,098	0,098	0,196

According to the calculated data, the proposed 2D diffuser is 3D modeled in CAD environment. The technical drawings are shown in Figure 3.7:

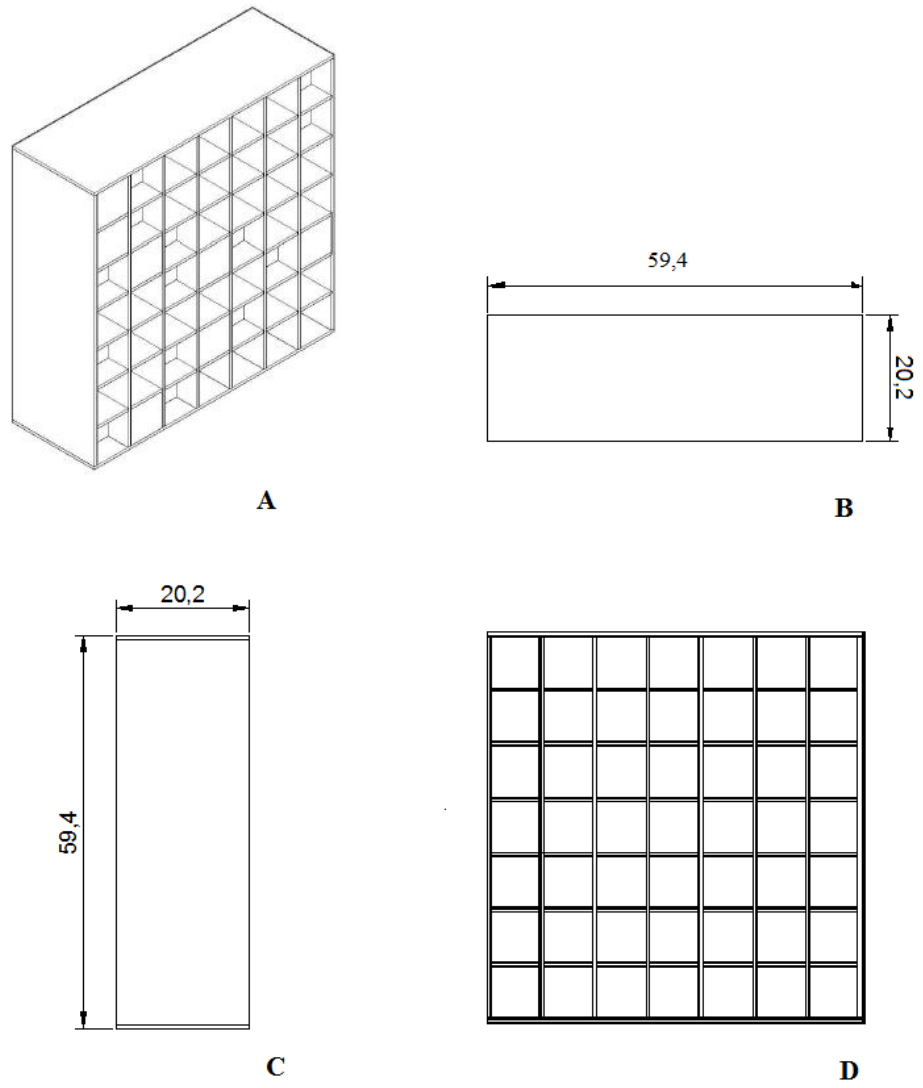


Figure 3.7. The technical drawings of 2D quadratic residue sequences for  $N = 7$  based on DSP Method for  $m = 1$  A: Isometric View B:Top View C:Left View D: Front View

## CHAPTER 4

# PREDICTION OF SCATTERING FROM TWO DIMENSIONAL DISTINCT SUMS PROPERTY APPLIED QUADRATIC RESIDUE DIFFUSERS WITH BOUNDARY ELEMENT METHOD

There are different methods to predict the scattering from acoustic diffusers in the literature such as Standard BEM, Thin Panel BEM, Kirchhoff boundary conditions, Fresnel and Fraunhofer Methods (Cox & D'Antonio 2009). The simplest and fastest method is the Fraunhofer Method described in Chapter 2. Although the Fraunhofer method is appropriate for understanding the physical process of scattering and good for the preliminary design stage, Cox (1992; 1994; 1995) Cox and Lam (1994) found it to be least accurate. They studied the scattering from acoustic diffusers with Fraunhofer Method and Boundary Element Method; then compared the predicted scattering with the measurements. The results clearly state that Fraunhofer method is especially problematic in the low frequencies and near-field conditions. A far-field near-field comparison of Cox (1992) is shown in Figure 4.1 and Figure 4.2. Although Cox and D'Antonio claims that a diffuser performing optimum scattering in far-field also performs well in the near-field, the author of the research also finds the results unrelated with the measurement results. On the contrary, Boundary Element Method (BEM) correlates high with the measurement results as a prediction method for the scattering properties of diffusers (Cox 1992, Cox & D'Antonio 2004, Cox & Lam 1994; D'Antonio 1995). The prediction method is essential to predict the reflected pressure from the surface to form acoustic diffusers based on a new method in acoustics. In addition, whole space prediction algorithms such as Finite Element Method require long computational times. Therefore the scattering of the acoustic diffusers is predicted in isolation of other objects and boundaries with BEM.



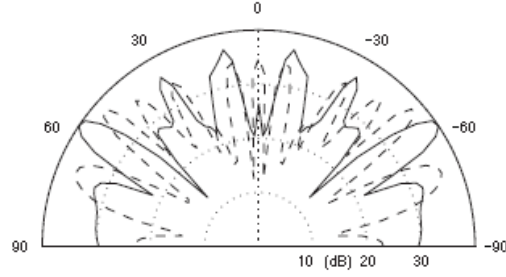


Figure 4.1. The prediction of scattering from a surface in far-field: Cont. line: BEM, Dotted line: Fraunhofer (Source: (Cox & D'Antonio 2009, page:276))

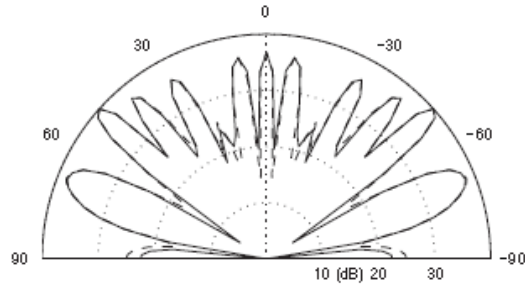


Figure 4.2. The prediction of scattering from a surface in near-field: Cont. line: BEM, Dotted line: Fraunhofer (Source: (Cox & D'Antonio 2009, page:276))

#### 4.1. The Theory and Formulation of Boundary Element Method

Models to predict scattering are based on Helmholtz-Kirchhoff integral equation. The wave equation reduces to Helmholtz equation under steady-state, constant frequency as in Equation 4.1 (Cox & D'Antonio 2009; Kirkup 2007):

$$\nabla^2 p(r) + kp(r) = 0 \quad (4.1)$$

where  $p$  is the sound pressure,  $r$  is a point in space and  $k$  is the wavenumber and equals to  $2\pi f/c$ . If we apply Green's functions ( $G$ ) for the transformation of integral equations on Equation 4.1, the pressure  $p(r)$  at point  $r$  for a single frequency is given by Equation 4.2 (Cox 1994; Cox & D'Antonio 2004; 2009):

$$p_i(r, r_0) + \int_s p(r_s) \frac{\partial G(r, r_s)}{\partial n(r_s)} - G(r, r_s) \frac{\partial p(r_s)}{\partial n(r_s)} ds \begin{cases} r \in E & p(r) \\ r \in s & \frac{1}{2}p(r) \\ r \in D & 0 \end{cases} \quad (4.2)$$

where  $r_0 = \{x_0, y_0, z_0\}$  is the vector describing the source location;  $r = \{x, y, z\}$  is the vector describing the receiver location;  $r_s = \{x_s, y_s, z_s\}$  is the vector describing a point on the surface,  $p_i(r, r_0)$  is the pressure radiated from source to the receiver  $r$ ,  $n$  is the normal to the surface,  $E$  the external region,  $s$  the surface, and  $D$  the interior of the surface. The Helmholtz-Kirchhoff integral equation is comprised of three parts: First part formulates the combination of pressures direct from sources, second part takes the surface integral of the pressure, and third part takes its derivative over the reflecting surfaces (Cox 1994; Cox & D'Antonio 2004; 2009). The geometry which is used in equations and for scattering is shown in Figure 4.3:

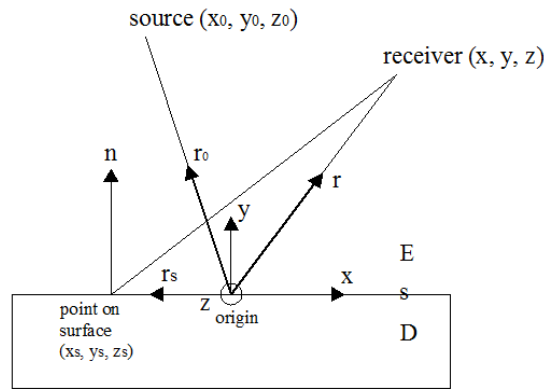


Figure 4.3. Geometry used for prediction with BEM (Source: Cox & D'Antonio 2009, page: 254)

Equation 4.2 determines the direct pressure from the source to the receiver point  $r$ . In addition, the integral is applied to determine the reflected energy from a point on the surface  $r_s$  to the receiver point  $r$ . In order to understand the propagation of the sound pressure and its derivative from one point to another, Green's function is used and for 3D case  $G$  is given by Equation 4.3 (Cox 1994; Cox & D'Antonio 2004; 2009; Kirkup 2007):

$$G(r) = \frac{e^{-jkr}}{4\pi r}, (k \in C) \quad (4.3)$$

where  $r = |r - r_0|$ ,  $k$  is the wavenumber and  $C$  is the complex set of numbers. There is also formulation for 2D case for two dimensional prediction with BEM. Cox (1994) formulated equations for 2D BEM for predicting scattering from 1D Schroeder diffusers. 1D Schroeder diffusers scatter sound into a hemi-disc meaning that the diffusion occurs along the width. However in case of 2D diffusers, diffusion occurs into a hemisphere;

both in width and height. Therefore 3D BEM is used throughout the study.

BEM is used to calculate the sound pressures at desired external points such as stated in Equation 4.2, depending on the receiver point  $r$ . The receiver point  $r$  can be on the external region,  $E$ , on the surface,  $s$ , or on the interior region  $D$  which is shown at Figure 4.3. The solution of the Equation 4.2 involves the surface pressure,  $p(r_s)$  and its derivative,  $\frac{\partial p(r_s)}{\partial n(r_s)}$ . If we assume a point source, locally reacting surface, the derivative of the surface pressure is related to the surface pressure by Equation 4.4 (Cox & D'Antonio 2009):

$$jkp(r_s) - \beta(r_s) = \frac{\partial p(r_s)}{\partial n(r_s)} \quad (4.4)$$

where  $\beta$  is the surface admittance. The surface admittance is related to the surface impedance,  $Z$  by Equation 4.5 (Cox & D'Antonio 2009; Iemma & Marchese 2011):

$$\beta = 1/Z \quad (4.5)$$

We know that the  $Z$  is related to the pressure reflection coefficient  $R$  in terms of Equation 4.6 (Cox & D'Antonio 2009; Iemma & Marchese 2011):

$$Z \cos(\psi) = \rho c \frac{1 + R}{1 - R} \quad (4.6)$$

where  $\psi$  is the angle of incidence,  $\rho$  is the density of the medium which air travels,  $c$  is the speed of sound. The reflection coefficient  $R$  is related to the incident and reflected sound pressure levels by Equation 4.7 and naturally contains information about the phase angle and the magnitude of the reflected sound.

$$R = \frac{p_r}{p_i} \quad (4.7)$$

After obtaining the necessary information about the solution of the integral contents in Equation 4.2, the BEM is applied to solve Equation 4.2 twice. First, the surface pressures,  $p(r_s)$  on the diffuser surfaces are found. Then to obtain the sound pressures at external receiver points, integral is carried out over the obtained surface pressures (Cox & D'Antonio 2004; 2009).

BEM involves the meshing process which is an obligatory application to calculate

the surface pressures. The surface is meshed into boundary elements. It is assumed that the pressure is constant. Cox and D'Antonio (2009) suggests to use elements which are smaller than  $\lambda/8$  for the largest frequency in order to prevent discrete values while presenting the continuous pressure variation. Figure 4.4 shows a meshed Schroeder diffuser.

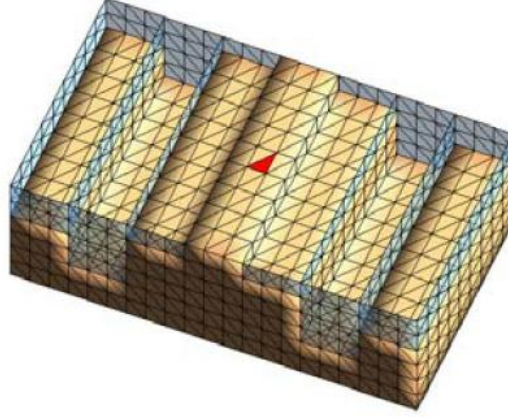


Figure 4.4. A meshed Schroeder diffuser (Source: Hargreaves & Cox 2005)

After the meshing procedure is completed, surface pressures are calculated separately for each of the element, involving a number of equations. Therefore, we can write Equation 4.2 in matrix form in terms of Equation 4.8, Equation 4.9 and Equation 4.10 (Cox & D'Antonio 2004; 2009):

$$\left(\frac{1}{2}\delta + A\right)P = P_i \quad (4.8)$$

$$\delta_{nm} = 1 \quad m = n \quad (4.9)$$

$$\delta_{nm} = 0 \quad m \neq n$$

$$A_{mn} = \int_{S_m} \frac{\partial G(r_n, r_s)}{\partial n_m(r_s)} - G(r_n, r_s)jk(-\beta)_m ds_m \quad (4.10)$$

where P is matrix form of surface pressures in  $(1 \times N)$ ,  $P_i$  is the direct incident pressures from the source to the surface in  $(1 \times N)$ , N is the number of elements which are shown in  $(m, n)$ , m and n are the elements of the matrix, and  $s_m$  is the surface of the  $m^{th}$  element. After the surface pressures are obtained, the external pressures at a desired point r is obtained by solving Equation 4.2.

## 4.2. The Formation of the Prediction Setup for the Boundary Element Method Software

The author of the research uses AcouSTO software package for the prediction of scattering from 2D quadratic residue diffusers based on DSP Method. The software is open-source and developed by Prof. Umberto Iemma and Vincenzo Marchese in University of Rome Tre. The selection of the correct software is a difficult process since there are many software for Boundary Element Method applications. The clear definition of the BEM equations used in the software is the most important criteria. Because there are numerous methods within the theory based on different equations. The author finds AcouSTO to be the most applicable one since the software uses 3D BEM method based on Helmholtz-Kirchoff integral equations and all related equations are clearly defined in the user manual. The author applied AcouSTO under the inspection of Prof. Iemma in order to prevent errors.

The prediction process simulates the measurement procedures. Therefore, we carefully applied the prediction criteria suggested by the Audio Engineering Society Standard AES-4id-2001(r2007):"AES information document for room acoustics and sound reinforcement systems - Characterization and measurement of surface scattering uniformity" to the software input. For the measurement of scattering, AES (2001:r2007) recommends a point source and an arc of receivers around the surface which is measured. The point source (loudspeaker) should be 10 meters away from the center of the surface while the receivers (microphones) should be on an arc of 5 meter radius,  $5^\circ$  apart. Hence the total number of receivers are 37. The arc of receivers should be centered with the middle of the width of the surface. Figure 4.5 shows the measurement procedure.

For the prediction, AES suggests source position of 100 meters and receiver arc radius of 50 meters to ensure the far-field. For further comparison and accordance, we take the receiver coordinates in  $(x, y)$  from Prof. Cox's database (See Appendix B). The point source is a pure tone and normal to the diffuser for the normal incidence of sound. After the coordinates are set, we transfer the modeled 2D quadratic residue diffuser based on DSP Method into Blender, a meshing software. For the transformation, we construct the model again with surface elements for easy meshing. Since the predictions are run for

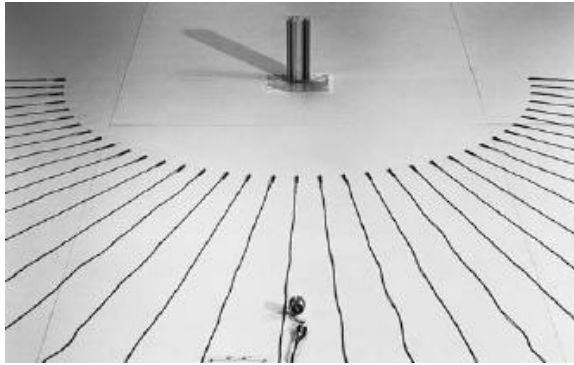


Figure 4.5. The measurement procedure of AES (Source: Cox & D'Antonio 2009, page: 112)

each octave band frequency, 125 Hz., 250 Hz., 500 Hz., 1000 Hz., 2000 Hz., and 4000 Hz., the highest frequency 4000 Hz. determines the number of elements in the meshed diffuser. For  $\lambda/8 = c/8f$ , the element sizes are approximately 0.0107 meters. After the meshing is complete, we import the model into the AcouSTO. The geometry of the prediction is in Figure 4.6. In order to define the geometry in the study, note that the source and the receivers are closer to the diffuser. Otherwise, both the source and the receivers are too far away that it is impossible to take a screen shot of the geometry.

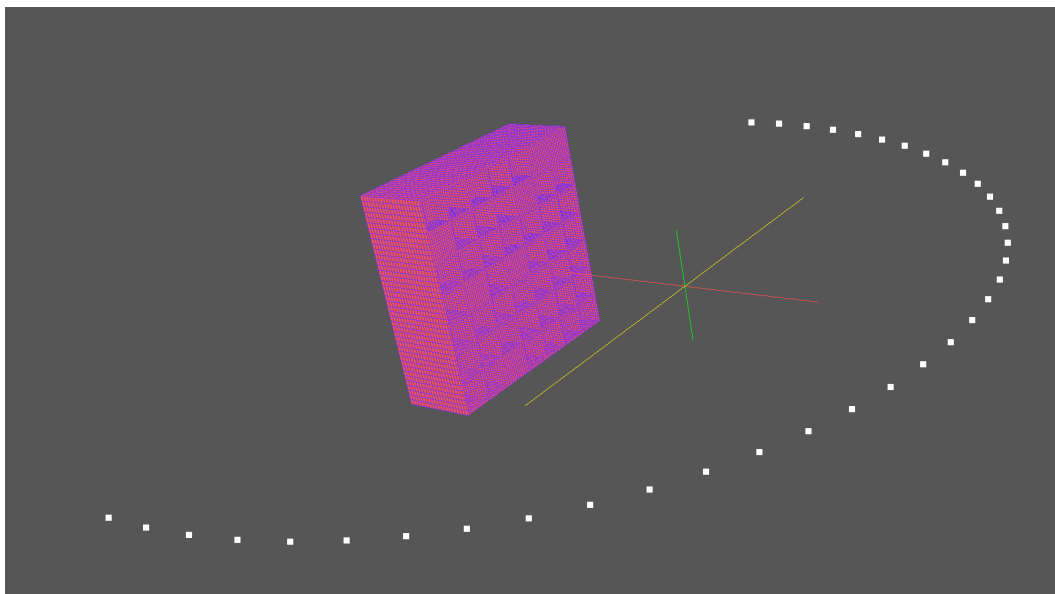


Figure 4.6. The geometry of the prediction of 2D quadratic residue diffuser based on DSP Method

The results obtained in each receiver are in pressure magnitudes, Pascal. In order

to calculate the sound pressure level (SPL) in dB, the following Equation 4.11 is applied:

$$SPL = 20 \log \frac{P(r)}{P_0} \quad (4.11)$$

where  $P(r)$  is the pressure at the receiver and  $P_0$  is the reference atmospheric pressure which is equal to  $20 \times 10^{-6}$  Pa. After obtaining the sound pressure levels at each receiver, the data is plotted as polar responses for each octave band frequency.

In addition, in the literature and database, diffusion coefficients are used to measure the uniformity of the scattering (AES 2001:r2007; Cox & D'Antonio 2009; Farina 2006). Diffusion coefficients are different from scattering coefficients and it is crucial to state the difference. Cox and D'Antonio (2009) define both in the following terms:

“A diffusion coefficient measures the quality of reflections produced by a surface, in the case of the AES coefficient, by measuring the similarity between the scattered polar response and a uniform distribution. A scattering coefficient is a measure of the amount of sound scattered away from a particular direction or distribution. This has the greatest similarity to the coefficients required as inputs to current geometric room acoustic models” (Cox and D'Antonio 2009, page:228).

In order to compare the results of this study to the previous studies, the author of the research uses diffusion coefficients since all related research are in diffusion coefficient form. Furthermore, evaluation of the uniformity of scattering is important for the application of DSP on two dimensional diffusers. AES (2001:r2007) gives the calculation of diffusion coefficient in terms of Equation 4.12:

$$d_\psi = \frac{\left( \sum_{i=1}^n 10^{\frac{L_i}{10}} \right)^2 - \sum_{i=1}^n \left( 10^{\frac{L_i}{10}} \right)^2}{(n-1) \sum_{i=1}^n \left( 10^{\frac{L_i}{10}} \right)^2} \quad (4.12)$$

where  $d_\psi$  is the diffusion coefficient of the surface,  $L_i$  is the sound pressure levels in dB at the receivers,  $n$  is the number of receivers and  $\psi$  is the angle of incidence. In order to see the actual performance of the diffuser in regard to a reference flat surface with the same dimensions, the diffusion coefficients are normalized according to the flat surface's

diffusion coefficients with Equation 4.13 (Cox & D'Antonio 2009):

$$d_{\psi,n} = \frac{d_{\psi} - d_{\psi,r}}{1 - d_{\psi,r}} \quad (4.13)$$

where  $d_{\psi,n}$  is the normalized diffusion coefficient,  $d_{\psi}$  is the diffusion coefficient of the diffuser and  $d_{\psi,r}$  is the diffusion coefficient of the reference flat panel.

### 4.3. The Results

After the test setup, BEM is applied to obtain pressures at each receiver according to the equations stated in Section 4.1. The results are total field pressures and scattered field pressures. In order to evaluate the data in terms of scattering, the scattered field pressures are used. Equation 4.11 is applied to calculate the sound pressure levels in each receiver.

Therefore, the scattering of 2D quadratic residue diffusers based on DSP Method for  $m = 1$  modulation are given in terms of pressure magnitude  $P(r)$  and in Sound Pressure Levels (SPL) in decibels. Since 2D diffusers scatter sound into both x and y directions, pressure magnitudes are predicted in both coordinates and converted to sound pressure levels. Table 4.1 and Table 4.2 gives the results for each octave band frequency at x-coordinate. In order to evaluate the scattering in terms of angles for each octave band frequency, scattered sound pressure levels from each receiver are plotted as polar responses as shown in Figure 4.7.  $0^\circ$  direction is plotted at  $90^\circ$  in order to refer to the normal incident sound. The dots refer to the receiver points in degrees and the sound pressure levels in dB.

The design frequency,  $f_0$  of the 2D diffuser is 500 Hz. and the upper frequency,  $f_{max}$  limit is 2041.667 Hz. We should expect optimum diffusion between those frequencies. For 500 Hz., we see incident sound is dispersed into all angles, meaning that the spatial response is achieved. No grating lobes are present even though lobes with the same energy was expected due to the nature of Schroeder diffusers' gratings. At the upper frequency limit which is around 2000 Hz., lobes begin to appear however spatial diffusion in all angles is still present. Pressure variation is constant at overall distribution and around 60 dB. Between those frequencies, at 1000 Hz. we examine grating lobes



between  $270^\circ$  ( $-90^\circ$ ) and  $330^\circ$  ( $-60^\circ$ ) but the energy of the lobes are the same. The unsymmetrical distribution of pressure is due to the unsymmetrical design of the 2D diffuser and is expected at some frequencies. At 4000 Hz., scattering becomes more specular. The sound pressure level increases at the specular direction meaning that the diffuser reflects the incident sound. In addition, grating lobes should have the same energy at Schroeder diffusers but what we examine is the variable lobes with uneven energy. However, 4000 Hz. is beyond the upper frequency limit.

In lower frequencies, the spatial response is achieved. However, sound absorption occurs. The sound pressure level highly decreases because of sound absorption. This may have advantages and disadvantages due to the acoustical requirements of the architectural space. If the space requires sound absorption in low frequencies, this situation is an important advantage. Absorbing nearly half low-frequency content and dispersing the other half optimally is still an achievement. Because diffusion is surprisingly symmetrical between  $-90^\circ$  and  $90^\circ$ . However, if we want diffusion at lower frequencies, we should increase the maximum well-depth  $d_{max}$  according to Equation 2.24. This depends on the spatial requirements of the architectural space and is achievable. As a result, for x-coordinate, 2D quadratic residue diffuser based on DSP Method scatters sound optimally between proposed frequency limits.

Table 4.3 and Table 4.4 give results for each octave band frequency at y-coordinate. In order to evaluate the scattering in terms of angles for each octave band frequency, scattered sound pressure levels from each receiver are plotted as polar responses as shown in Figure 4.8.  $0^\circ$  direction is plotted at its place in order to refer to the normal incident sound coming from the y direction of the diffuser. The dots refer to the receiver points in degrees and the sound pressure levels in dB.

The scattering in the horizontal direction is also important in case of 2D diffusers. At design frequency,  $f_0 = 500$  Hz., the diffuser also shows optimal diffusion qualities. At the upper frequency limit, around 2000 Hz., the scattering is better than the scattering at x direction. Grating lobes are more even in both  $-90^\circ$  and  $90^\circ$ . However, there is specular reflection at  $0^\circ$ . At 1000 Hz., we examine suppressed reflection at  $0^\circ$  proving that the lateral reflections are present. The lobe energies are more even. Therefore between designed bandwidths, 2D diffuser scatters sound in both directions. At 4000 Hz which is 8 times the design frequency, scattering is achieved although there are pressure variations.

Table 4.1. Predicted Pressures  $P_r$  in Pa. and Sound Pressure Levels in dB. from 2D Quadratic Residue Diffusers based on DSP Method for  $m = 1$  at x-coordinate for 125 Hz., 250 Hz., and 500 Hz.

RC No	Frequency (Hz.)					
	125( $f_0/4$ )		250( $f_0/2$ )		500 ( $f_0$ )	
	$P_{rx}$ (Pa)	SPL (dB)	$P_{rx}$ (Pa)	SPL (dB)	$P_{rx}$ (Pa)	SPL (dB)
1	0,0001508	17,549835	0,00092695	33,320542	0,00525672	48,393701
2	0,0002197	20,814958	0,00146324	37,285739	0,00552734	48,829719
3	0,0002881	23,171454	0,00200117	40,005061	0,00591420	49,417327
4	0,0003559	25,004809	0,00254001	42,076118	0,00640927	50,11557
5	0,0004224	26,494023	0,00307830	43,745605	0,00699525	50,875459
6	0,0004874	27,736796	0,00361479	45,141065	0,00763695	51,637796
7	0,0005503	28,792129	0,00414636	46,332738	0,00831291	52,37446
8	0,0006108	29,698075	0,00466886	47,363622	0,00899566	53,060056
9	0,0006684	30,480423	0,00517865	48,263736	0,00964408	53,664613
10	0,0007226	31,157247	0,00566924	49,049899	0,01023493	54,181102
11	0,0007729	31,741594	0,00613641	49,737694	0,01072676	54,58877
12	0,0008188	32,242986	0,00657169	50,332938	0,01110784	54,891991
13	0,0008599	32,668485	0,00696971	50,84369	0,01135214	55,080951
14	0,0008958	33,023335	0,00732205	51,27206	0,01145716	55,16094
15	0,0009260	33,311453	0,00762298	51,621898	0,01141642	55,130002
16	0,0009502	33,535741	0,00786859	51,897334	0,01122779	54,985286
17	0,0009681	33,698242	0,00805151	52,096947	0,01091070	54,736451
18	0,0009796	33,80036	0,00816864	52,222393	0,01047730	54,384388
19	0,0009844	33,842965	0,00821994	52,276775	0,00993780	53,925209
20	0,0009825	33,826367	0,00820201	52,257809	0,00931814	53,365981
21	0,0009740	33,750447	0,00811848	52,168894	0,00862765	52,697249
22	0,0009589	33,614541	0,00796952	52,008041	0,00788997	51,920908
23	0,0009374	33,417471	0,00775832	51,774749	0,00712399	51,033869
24	0,0009097	33,157432	0,00749240	51,471817	0,00633792	50,018329
25	0,0008762	32,831832	0,00717554	51,096498	0,00555584	48,874401
26	0,0008373	32,437141	0,00681330	50,646545	0,00479980	47,60387
27	0,0007933	31,968568	0,00641397	50,121936	0,00408323	46,199468
28	0,0007448	31,419726	0,00598244	49,516971	0,00343358	44,694336
29	0,0006920	30,781912	0,00552703	48,829234	0,00286307	43,116044
30	0,0006356	30,043404	0,00505125	48,047369	0,00240085	41,586709
31	0,0005760	29,187944	0,00456123	47,161036	0,00206026	40,257831
32	0,0005136	28,192711	0,00405994	46,1498	0,00186182	39,378173
33	0,0004490	27,024387	0,00355107	44,986579	0,00181565	39,160051
34	0,0003825	25,632184	0,00303734	43,629263	0,00192813	39,682119
35	0,0003146	23,934558	0,00251932	42,005082	0,00220701	40,855501
36	0,0002457	21,787601	0,00199813	39,99186	0,00265033	42,445395
37	0,0001762	18,90032	0,00147414	37,350188	0,00325194	44,222264

Table 4.2. Predicted Pressures  $P_r$  in Pa. and Sound Pressure Levels in dB. from 2D Quadratic Residue Diffusers based on DSP Method for  $m = 1$  at x-coordinate for 1000 Hz., 2000 Hz., and 4000 Hz.

RC No	Frequency (Hz.)					
	1000 ( $2f_0$ )		2000( $4f_0$ )		4000( $8f_0$ )	
	$P_{rx}$ (Pa)	SPL (dB)	$P_{rx}$ (Pa)	SPL (dB)	$P_{rx}$ (Pa)	SPL (dB)
1	0,01885295	59,486985	0,01766013	58,919276	0,05421599	68,661948
2	0,01896939	59,540466	0,02440609	61,729364	0,02698797	62,602805
3	0,01793035	59,051174	0,02999825	63,521319	0,02328432	61,32067
4	0,01571263	57,904376	0,03440867	64,712758	0,08329831	72,392124
5	0,01238892	55,840068	0,03761254	65,486053	0,12936614	76,215813
6	0,00820924	52,265462	0,03953015	65,91797	0,13797921	76,775673
7	0,00347263	44,792567	0,04068814	66,168756	0,10491384	74,396056
8	0,00131501	36,357997	0,04186342	66,416095	0,05386230	68,605098
9	0,00541940	48,658418	0,04366589	66,782246	0,01704959	58,613679
10	0,00805531	52,101042	0,04640865	67,311379	0,01466352	57,304163
11	0,00837606	52,440192	0,04927147	67,831311	0,06013810	69,562394
12	0,00577189	49,205764	0,04997177	67,953894	0,04484874	67,014404
13	0,00005433	8,680724	0,04518304	67,07891	0,14629566	77,284029
14	0,00886989	52,937767	0,03220368	64,13751	0,35158026	84,89989
15	0,01989009	59,952137	0,01082398	54,667136	0,20529596	80,227008
16	0,03183692	64,038021	0,01482129	57,39712	0,15194311	77,61302
17	0,04314485	66,67798	0,03670019	65,272766	0,01239539	55,844606
18	0,05226842	68,344188	0,04636479	67,303165	0,85128630	92,580913
19	0,05799599	69,247359	0,03825620	65,633436	1,37900981	96,770747
20	0,05970270	69,499279	0,01570012	57,897462	0,84074951	92,472733
21	0,05745215	69,165525	0,01319465	56,38736	0,07971717	72,010437
22	0,05196980	68,294422	0,03648172	65,220906	0,30991436	83,804234
23	0,04443500	66,933903	0,04703377	67,427595	0,02836680	63,035608
24	0,03613720	65,13849	0,04494944	67,033887	0,13743599	76,741409
25	0,02830138	63,015554	0,03574396	65,043453	0,05010074	67,976282
26	0,02180826	60,751819	0,02641099	62,415093	0,08175502	72,229689
27	0,01703733	58,607429	0,02096895	60,410934	0,04777334	67,563112
28	0,01402943	56,9202	0,01911916	59,608774	0,05036219	68,021492
29	0,01242723	55,866889	0,01833115	59,243196	0,05194120	68,28964
30	0,01182244	55,433542	0,01614563	58,140501	0,04290202	66,628955
31	0,01171259	55,352456	0,01233663	55,803332	0,08619033	72,68857
32	0,01172342	55,360487	0,00846574	52,5327	0,17501896	78,841102
33	0,01157429	55,249285	0,00682084	50,656155	0,13810411	76,783532
34	0,01112167	54,902804	0,00900607	53,07011	0,03008368	63,54602
35	0,01030466	54,240071	0,01531637	57,682519	0,05004224	67,966135
36	0,00910037	53,160585	0,02459031	61,79468	0,05042101	68,031631
37	0,00751685	51,500122	0,03439009	64,708067	0,02179414	60,746196

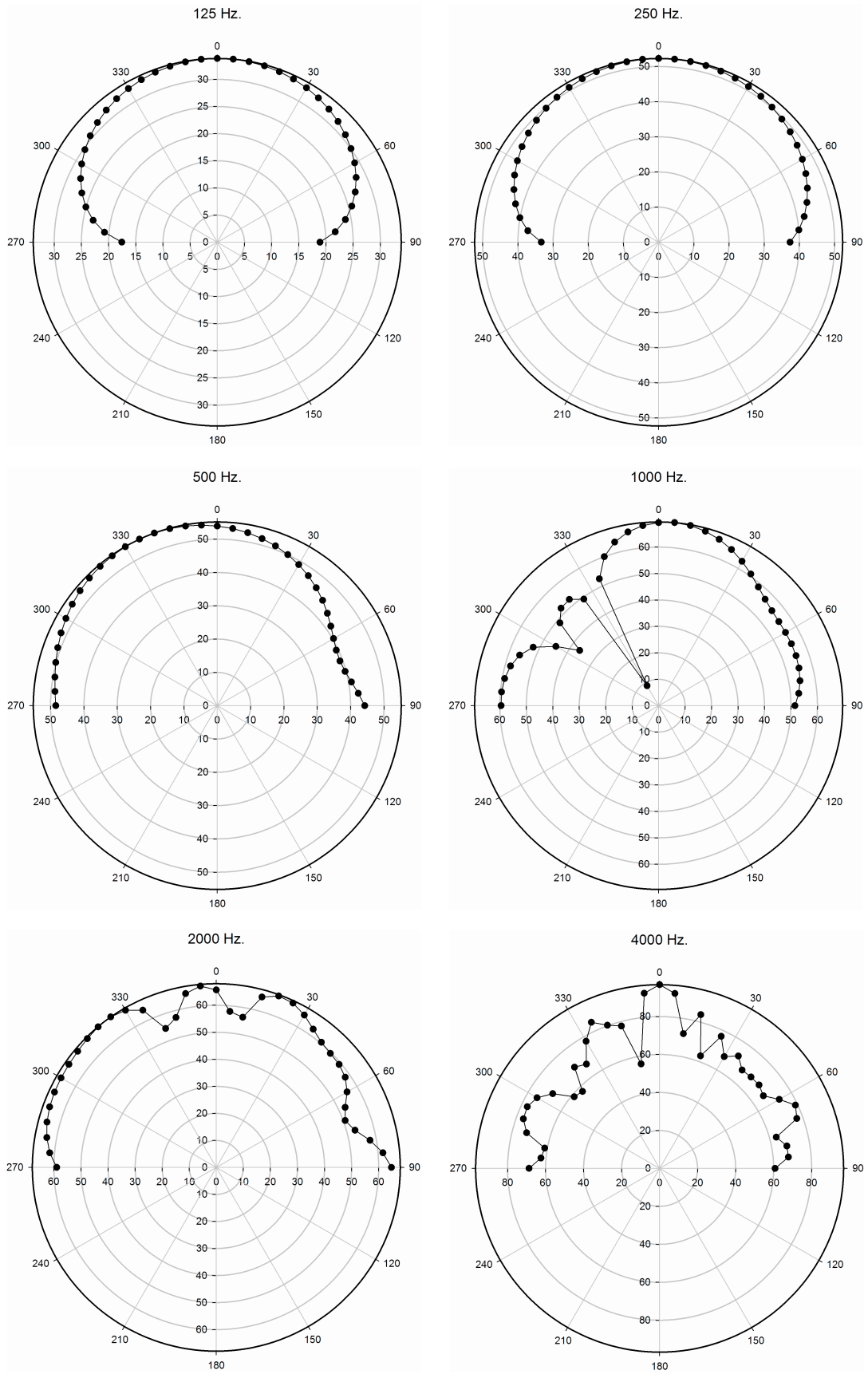


Figure 4.7. Scattered sound pressure levels in dB for normal sound incident on 2D quadratic residue diffuser based on DSP Method for  $m = 1$  modulation at x-coordinate

Table 4.3. Predicted Pressures  $P_r$  in Pa. and Sound Pressure Levels in dB. from 2D Quadratic Residue Diffusers based on DSP Method for  $m = 1$  at y-coordinate for 125 Hz., 250 Hz., and 500 Hz.

RC No	Frequency (Hz.)					
	125( $f_0/4$ )		250( $f_0/2$ )		500 ( $f_0$ )	
	$P_{ry}$ (Pa)	SPL (dB)	$P_{ry}$ (Pa)	SPL (dB)	$P_{ry}$ (Pa)	SPL (dB)
1	0,0000215	32,432458	0,00278697	42,882038	0,00557394	48,902638
2	0,0000172	30,482177	0,00312473	43,875637	0,00624945	49,896237
3	0,0000131	28,113649	0,00342146	44,663641	0,00684293	50,684241
4	0,0000092	25,024181	0,00367547	45,285654	0,00735094	51,306254
5	0,0000054	20,44005	0,00388466	45,766457	0,00776932	51,787057
6	0,00000196	11,636617	0,00405121	46,131091	0,00810242	52,151691
7	0,0000012	7,7022773	0,00416863	46,379267	0,00833726	52,399867
8	0,0000043	18,421901	0,00423159	46,509481	0,00846319	52,530081
9	0,0000070	22,671837	0,00424256	46,531955	0,00848512	52,552555
10	0,0000095	25,353212	0,00419735	46,43891	0,00839471	52,45951
11	0,0000116	27,060389	0,00410757	46,25109	0,00821513	52,27169
12	0,0000134	28,362045	0,00397363	45,963156	0,00794727	51,983756
13	0,0000149	29,258438	0,00381307	45,604905	0,00762615	51,625505
14	0,0000162	29,965025	0,00363541	45,190459	0,00727081	51,211058
15	0,0000171	30,468563	0,00346014	44,761276	0,00692028	50,781876
16	0,0000176	30,68404	0,00330942	44,374447	0,00661885	50,395047
17	0,0000178	30,789979	0,00318972	44,054452	0,00637944	50,075052
18	0,0000177	30,757916	0,00311232	43,841091	0,00622464	49,86169
19	0,0000171	30,452644	0,00308594	43,767159	0,00617189	49,787759
20	0,0000163	30,020722	0,00310009	43,806899	0,00620019	49,827499
21	0,0000149	29,248044	0,00315066	43,947432	0,00630132	49,968032
22	0,0000132	28,20639	0,00321695	44,128276	0,00643389	50,148876
23	0,0000113	26,842654	0,00327918	44,294705	0,00655836	50,315305
24	0,0000088	24,684445	0,00332250	44,408706	0,00664500	50,429306
25	0,0000060	21,343866	0,00332537	44,416204	0,00665074	50,436804
26	0,0000030	15,210106	0,00327297	44,278245	0,00654594	50,298845
27	0,0000005	0	0,00315963	43,972113	0,00631925	49,992713
28	0,0000042	18,239617	0,00298086	43,466225	0,00596172	49,486825
29	0,0000083	24,216193	0,00274282	42,743346	0,00548564	48,763946
30	0,0000126	27,836695	0,00245136	41,767534	0,00490272	47,788134
31	0,0000173	30,541011	0,00211953	40,504178	0,00423905	46,524778
32	0,0000220	32,647685	0,00175946	38,886974	0,00351891	44,907574
33	0,0000269	34,394437	0,00138484	36,807397	0,00276968	42,827997
34	0,0000320	35,908749	0,00100817	34,050097	0,00201635	40,070697
35	0,0000372	37,204942	0,00063722	30,065229	0,00127445	36,085829
36	0,0000424	38,339618	0,00027776	22,852664	0,00055551	28,873264
37	0,0000476	7,5364807	0,00006699	10,498997	0,00013397	16,519597

Table 4.4. Predicted Pressures  $P_r$  in Pa. and Sound Pressure Levels in dB. from 2D Quadratic Residue Diffusers based on DSP Method for  $m = 1$  at y-coordinate for 1000 Hz., 2000 Hz., and 4000 Hz.

RC No	Frequency (Hz.)					
	1000 ( $2f_0$ )		2000( $4f_0$ )		4000( $8f_0$ )	
	$P_{ry}$ (Pa)	SPL (dB)	$P_{ry}$ (Pa)	SPL (dB)	$P_{ry}$ (Pa)	SPL (dB)
1	0,01839534	59,273555	0,01234426	55,8087	0,00040186	26,060913
2	0,01988987	59,95204	0,00323530	44,177701	0,00573031	49,142968
3	0,02095468	60,405019	0,00793370	51,968916	0,02239516	60,982485
4	0,02152245	60,637236	0,02038087	60,163853	0,03257709	64,237645
5	0,02147591	60,618432	0,03148857	63,942459	0,00187520	39,440332
6	0,02067914	60,290048	0,03760680	65,484727	0,08606587	72,676019
7	0,01911927	59,608824	0,03519415	64,908809	0,16234944	78,188416
8	0,01684328	58,507936	0,02374533	61,490965	0,16975942	78,576078
9	0,01400975	56,908006	0,00790113	51,933186	0,14920918	77,455311
10	0,01088012	54,712071	0,00383433	45,653186	0,18976765	79,543844
11	0,00781350	51,836314	0,00274341	42,745209	0,22909385	81,179669
12	0,00512660	48,175994	0,01250051	55,917955	0,11275983	75,022488
13	0,00309279	43,786418	0,03259865	64,243391	0,07204590	71,131586
14	0,00181701	39,166531	0,03947006	65,904756	0,07844018	71,870172
15	0,00122532	35,74441	0,01694807	58,561807	0,01395275	56,872599
16	0,00098754	33,870493	0,03808980	65,595574	0,06777894	70,601296
17	0,00075502	31,538521	0,11072735	74,864498	0,21175316	80,495998
18	0,00010230	14,177028	0,17406268	78,793513	0,14870034	77,42564
19	0,00141579	36,999353	0,20354398	80,152565	0,02515543	61,992034
20	0,00379092	45,554282	0,18928727	79,521828	0,06019779	69,57101
21	0,00705868	50,953866	0,14102942	76,965594	0,12696933	76,053376
22	0,01074401	54,60273	0,08115313	72,165506	0,08394316	72,459106
23	0,01433015	57,104413	0,03256059	64,233245	0,06592029	70,359782
24	0,01741140	58,796075	0,00728296	51,225556	0,11520582	75,208889
25	0,01945111	59,75829	0,00407234	46,176289	0,10926777	74,749241
26	0,02016917	60,07316	0,01255639	55,956697	0,06637708	70,419762
27	0,01956227	59,807785	0,02132297	60,556354	0,09303411	73,352244
28	0,01772519	58,951216	0,02422129	61,663345	0,15191880	77,611631
29	0,01496816	57,482769	0,02087116	60,370332	0,15568801	77,824503
30	0,01157302	55,248338	0,01440491	57,149612	0,12812800	76,132281
31	0,00787624	51,905779	0,00776833	51,785949	0,13171085	76,371831
32	0,00410590	46,247569	0,00235799	41,430243	0,16006618	78,065392
33	0,00044916	27,027452	0,00197964	39,91111	0,17278477	78,729509
34	0,00296344	43,415325	0,00576942	49,202049	0,16011682	78,068139
35	0,00609864	49,684066	0,00893784	53,004055	0,13701427	76,714716
36	0,00889795	52,965202	0,01057812	54,467567	0,11383863	75,105193
37	0,01127923	55,024992	0,00925004	53,302272	0,08046531	72,091573

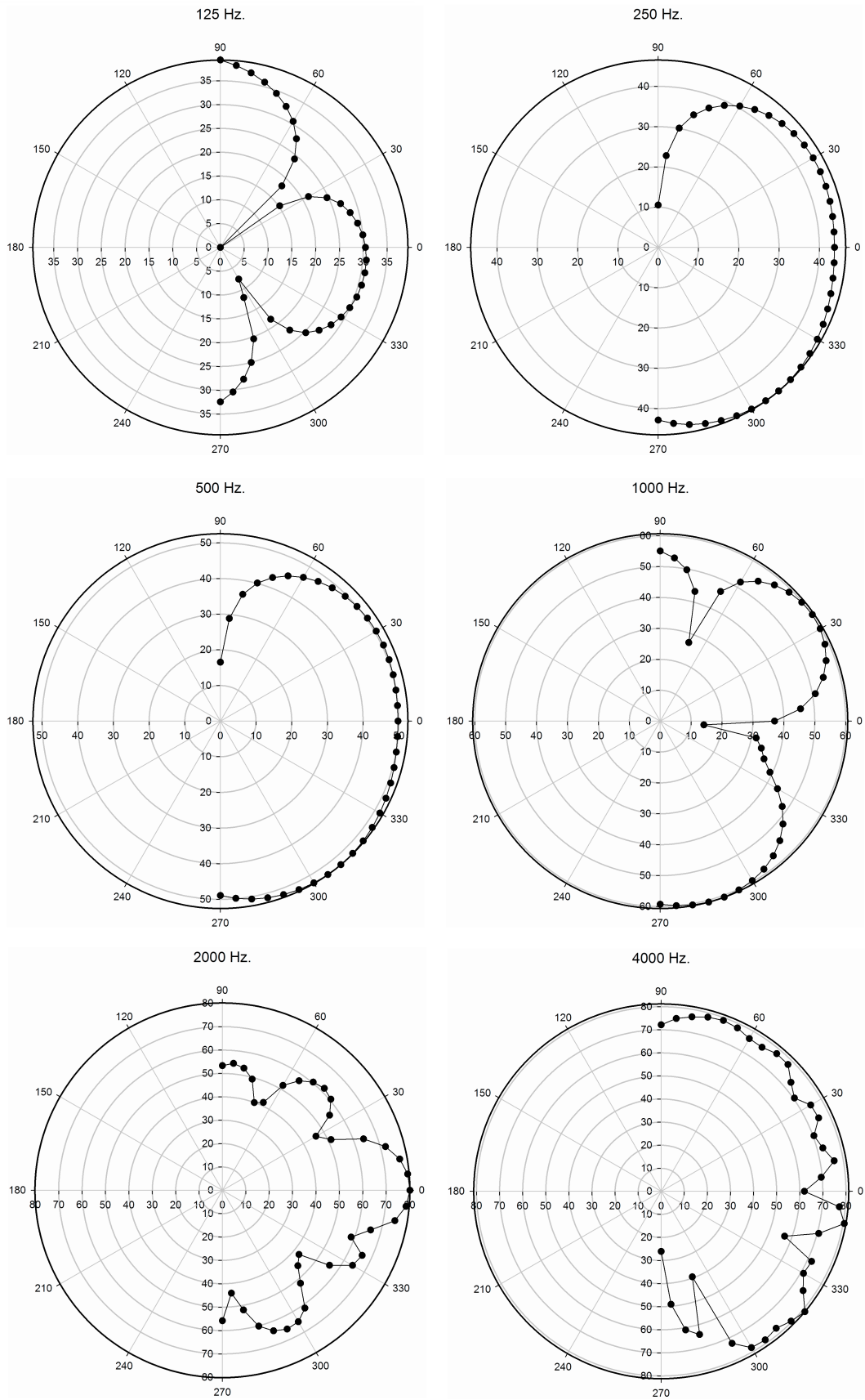


Figure 4.8. Scattered sound pressure levels in dB for normal sound incident on 2D quadratic residue diffuser based on DSP Method for  $m = 1$  modulation at y-coordinate

If we compare the results with x-coordinate, it is clear that the scattering is more even at y-coordinate in terms of lobe energies and the specular reflection does not occur at y.

At 125 Hz. and 250 Hz., the diffuser continues to absorb sound. We examine symmetrical lobes due to the nature of grating lobes at 125 Hz. The scattering looks optimal. However at 250 Hz, the diffuser almost does not scatter sound at 90° and extreme absorption occurs. Further studies are required for increasing the maximum well-depth  $d_{max}$  and examine the scattering in lower frequencies.

Furthermore, in real applications to architectural spaces, we use series of diffusers on the walls or on the ceilings. Therefore, Cox and D'Antonio (2009) suggests using at least 5 periods of diffusers for additional prediction in order to see the performance of series of diffusers. Hence, in future studies, this will be taken into account. In addition, the maximum well-depth  $d_{max}$  should be adjusted to decrease or increase the design frequency  $f_0$  with paying careful attention to the suggested upper limit of 40 cm. by D'Antonio and Konnert (1992).

In order to evaluate the diffusion by a single merit, the diffusion coefficients of the reference flat panel and 2D quadratic residue diffuser are calculated according to Equation 4.12. The pressure magnitudes for both x and y coordinates are also given as a scalar product at the software. In order to calculate the overall pressure, these values are converted to sound pressure levels. The diffusion coefficients of the reference flat panel are taken from the study of Farina et. al (2006) since the panel has the same dimensions, 60 m. x 60 m. The formulation is set in MS Excel and for each octave band frequency, the diffusion coefficients are found and shown at Figure 4.9. By using Equation 4.13, the diffusion coefficients of the diffuser are normalized according to flat panel and shown at Figure 4.10.

As seen from Figure 4.9 and Figure 4.10, the 2D diffuser scatters sound optimally between 250 Hz. and 1500 Hz. However, after 2000 Hz., the diffusion quality decreases significantly. We examined the same results at the polar responses. At 125 Hz., both the diffuser and the reflector has almost the same diffusion coefficient. But, we must remember that the diffusion coefficient does not evaluate the polar responses. Therefore, the achievement of spatial response at 125 Hz. is still valid.

It is important to compare the results with other 2D quadratic residue diffusers. The registered trademarks FRG Omniffusor and Omniffusor developed by D'Antonio et



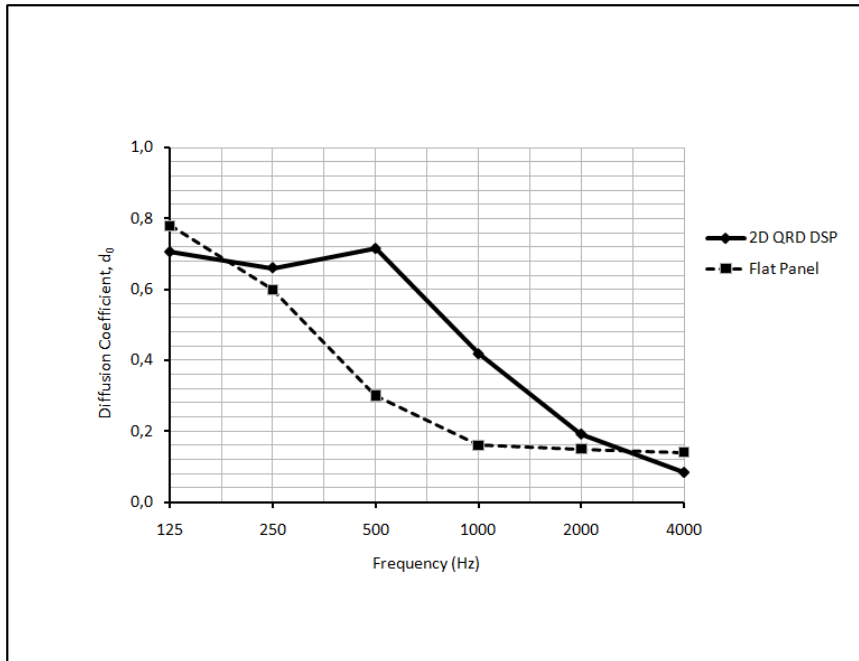


Figure 4.9. Diffusion coefficients of 2D quadratic residue diffuser based on DSP Method for  $m = 1$  and reference flat panel at octave band frequencies

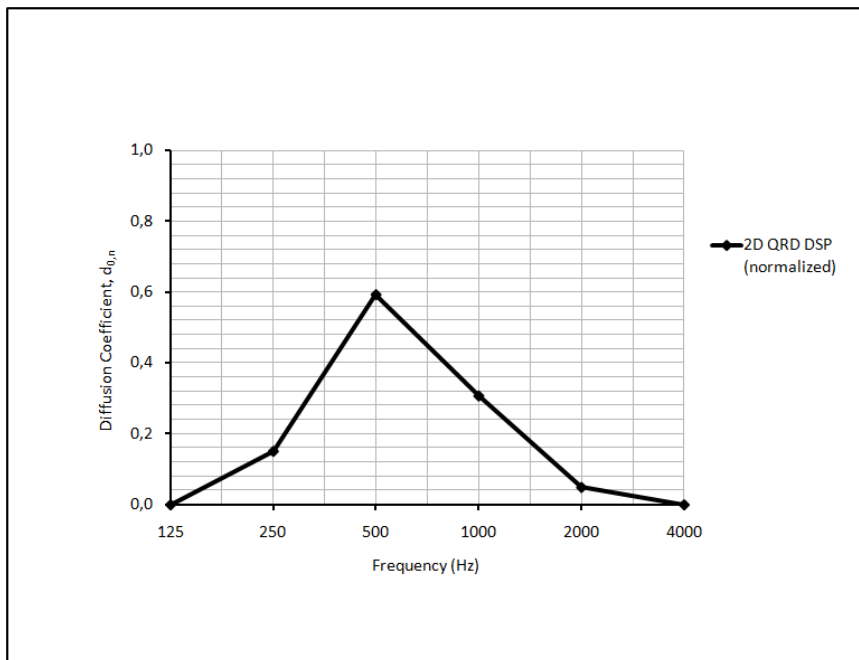


Figure 4.10. Normalized diffusion coefficients of 2D quadratic residue diffuser based on DSP Method for  $m = 1$  at octave band frequencies

al. (1990) are both based on prime number 7 and developed according to well-depth optimization technique applied on Product Array Method. FRG Omniffusor consist of 7 x 7 wells while Omniffusor consist of 8 x 8 wells. In order to achieve symmetrical design, Omniffusor has additional wells. Both have the same dimensions with the proposed diffuser (approx. 60 centimeters x 60 centimeters) and shown at Figure 4.9. The diffusion coefficients for normal incident sound are given by D'Antonio (pers. comm. 2011). The comparison of diffusion coefficients with 2D quadratic residue diffuser based on DSP Method are given in Figure 4.12 and Figure 4.13.



Figure 4.11. Left: FRG Omniffusor, Right: Omniffusor (Source: RPG Diffusor Systems)

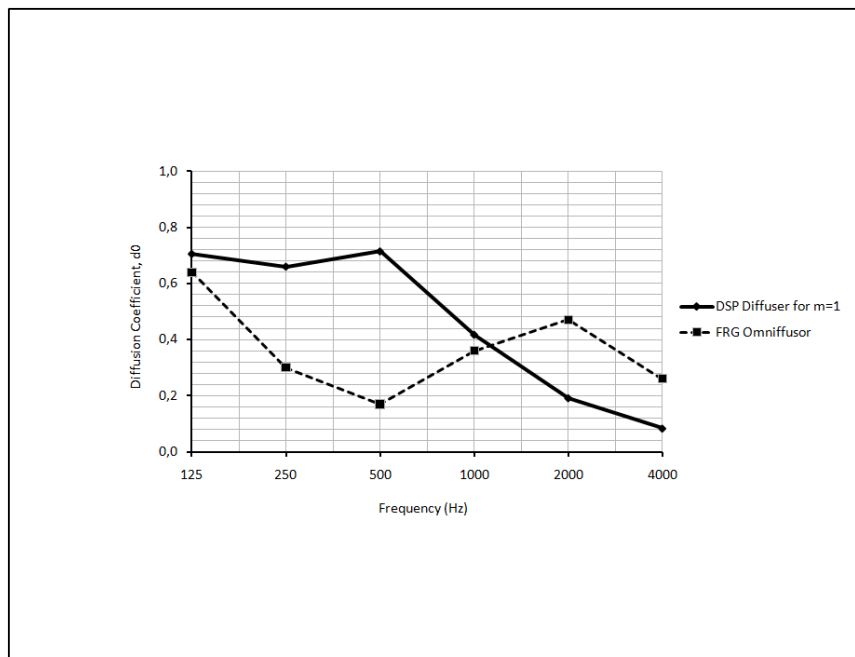


Figure 4.12. Diffusion coefficients of 2D quadratic residue diffuser based on DSP Method for  $m = 1$  and FRG Omniffusor at octave band frequencies

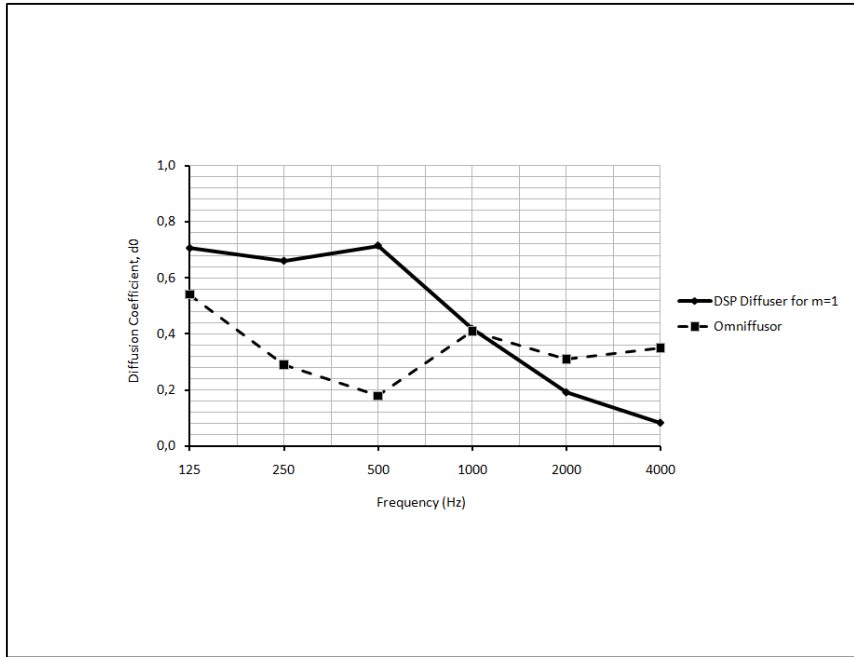


Figure 4.13. Diffusion coefficients of 2D quadratic residue diffuser based on DSP Method for  $m = 1$  and Omniffusor at octave band frequencies

The results for FRG Omniffusor and the proposed diffuser indicate that between 125 Hz. and 1000 Hz. the diffusion coefficients of the proposed diffuser is higher than FRG Omniffusor. After 1000 Hz. FRG Omniffusor behaves better in terms of overall diffusion. This may be due to the fact of design frequencies. We know from the related product documents that the design frequency,  $f_0$  of FRG Omniffusor and Omniffusor is around 1500 Hz. while the DSP based 2D diffuser has a design frequency of 500 Hz. But the overall comparison shows the validation of the relevant data in terms of design parameters. Both diffusers behave according to the proposed frequency bandwidths. If we compare the diffusion coefficients of Omniffusor and the proposed diffuser, we examine the parallel results with above as shown at Figure 4.13. However, at 2000 Hz. the diffusion coefficient of Omniffusor slightly drops.

In conclusion, all the results predicted with Boundary Element Method indicate that the application of Distinct Sums Property Method on the construction of two dimensional quadratic residue diffusers is successful. The proposed diffuser scatters sound spatially between desired bandwidths. However, for higher frequencies the scattering should be determined by adjusting well-widths or by applying a well-depth optimization technique. In addition, a series of diffusers should be tested in order to predict diffusion in more realistic manner.

## CHAPTER 5

### CONCLUSIONS

This dissertation introduces Distinct Sums Property Method, which has been used in digital watermarking, to construct two dimensional quadratic residue diffusers in the field of acoustics. The current methods for the construction of two dimensional diffusers does not offer variable design solutions both for the architects and the acousticians in terms of visual options and diffusion bandwidth. In addition, current literature on the subject of two dimensional acoustic diffusers is limited to the works of Peter D'Antonio and Trevor Cox who made pioneering studies on the field of acoustic diffusers. The lack of scientific data on the prediction of scattering from two dimensional diffusers with BEM is another area of problem.

Therefore, the study firstly concentrates on the construction of two dimensional quadratic residue diffusers with a new method in acoustics. Quadratic residue sequences are chosen for their optimum diffusion properties validated by studies of Late Manfred Schroeder. On the other hand, Distinct Sums Property Methods is chosen for the successful applications of constructing two dimensional arrays from one dimensional sequences in the field of digital watermarking. In addition, the method offers many construction possibilities since it is based on different cyclic shifts ranging from  $m = 1, 2, \dots, N - 1$ . The pre-prediction method based on Fraunhofer Theory shows that the autocorrelation properties of two dimensional quadratic residue diffusers based on Distinct Sums Property Method are producing nearly perfect arrays when compared to Product Array method which is used currently. Furthermore, the peak to largest sidelobe ratios of the autocorrelation function indicate that Distinct Sums Property Method has larger magnitudes when compared to Product Array Method which result in better diffusion.

Secondly, the study focuses on the Boundary Element Method for the prediction of scattering from two dimensional diffusers. Since the current literature is based on one dimensional diffusers, the study is an additional reference on the subject. The results of the prediction validates the current methodology and assures that Distinct Sums Property Method is applicable at constructing two dimensional acoustic diffusers. The predicted diffusion coefficients are higher than the diffusion coefficients based on Prod-

uct Array Method from 250 Hz to 1000 Hz. In addition, the proposed diffuser scatters sound optimally at the desired frequency range. However, this study will be a starting point. More prediction schemes must be developed for different design frequencies. Because the results also indicate sound absorption at low frequencies while indicating less diffusion at higher frequencies. However, the proposed diffuser behaves ideally at mid-frequency range. These data should be used for the construction of other modulations for the quadratic residue sequence.

The application of the Distinct Sums Property is not complex when compared to Product Array Method. The architect will be able to use an interface to select the desired design which ranges from  $m = 1$  to  $m = 6$ . In addition, the cyclic shifts can be applied at the rows or columns of the two dimensional array. Therefore, there are visual options for the architect to choose from. There are also different options depending on the space requirements of the architectural space. The available maximum well depth determines the design frequency where the well width determines the upper frequency limit. Therefore, depending on the architectural space limits, the acoustician will choose the most appropriate design for the aimed architectural space.

In conclusion, this dissertation achieves to apply a new method for the construction of two dimensional acoustic diffusers with the validated results predicted with Boundary Element Method.

## **5.1. Future Work**

Future studies could concentrate on constructing other modulations for quadratic residue sequence as a starting point. Using different modulations at the same row or column should be studied in order to see the variable options. A joint study for the measurement of proposed diffusers is also planned to compare the predicted results with measurement results. In addition, application of DSP on other sequences such as primitive root and Huffman codes are planned for near future.

There are various methods currently used in other fields such as Chaotic Maps and Costas Arrays to form two dimensional arrays from sequences. Therefore, future studies also include application of different methods for constructing two dimensional acoustic diffusers.

## BIBLIOGRAPHY

- AES-4id-2001(r2007), 'AES Information Document for Room Acoustics and Sound Reinforcement Systems - Characterization and Measurement of Surface Scattering Uniformity', *Journal of Audio Engineering Society*, Vol. 49, pp.149-165.
- Angus, J. A. S. 1992, 'Alternative Diffuser Sequences', *Proceedings of the Institute of Acoustics*, Vol. 14, Part 5, pp. 193-202.
- Angus, J. A. S. 1995, 'Sound Diffusers Using Reactive Absorption Gratings', *Audio Engineering Society 98th Convention*, preprint no. 3953, Paris, France.
- Angus, J. A. S. 1999, 'Non-Integer-Based Diffusers', *Audio Engineering Society 107th Convention*, preprint no. 5064, New York, USA.
- Angus, J. A. S. 2001, 'Phase Reflection Diffusers Design Using Huffman Sequences', *Journal of the Acoustical Society of America*, Vol. 109, Iss. 5, pp. 2418.
- Angus, J. A. S., D'Antonio P. 1999, 'Two Dimensional Binary Amplitude Diffusers', *Proceedings of the Audio Engineering Society*, paper no:3953.
- Angus, J. A. S. & Simpson, A. 1997, 'Wideband Two Dimensional Diffusers Using Orthogonal Modulated Sequences', *Audio Engineering Society 103rd Convention*, preprint no. 4640, New York, USA.
- Barron, M. 1971, 'The Subjective Effects of First Reflections in Concert Halls – The Need for Lateral Reflections', *Journal of Sound and Vibration*, Vol. 15, pp. 475-494.
- Barron, M. & Marshall, A. H. 1981, 'Spatial Impression due to Early Lateral Reflections in Concert Halls', *Journal of Sound and Vibration*, Vol. 77, pp. 211-232.
- Beranek, L. L. 1992, 'Concert Hall Acoustics', *Journal of the Acoustical Society of America*, Vol. 92, No. 1, pp. 1 – 40.
- Beranek, L. L. 2003, *Concert Halls and Opera Houses: Music, Acoustics, and Architecture*, Springer Verlag, 2nd ed., New York.
- Bracewell, R. N. 2000, *The Fourier Transform and Its Applications*, McGraw-Hill, 3<sup>rd</sup> ed.
- Brooker, G. 2003, *Modern Classical Optics*, Oxford University Press.
- Commins, D. E., Auletta, N. & Suner, B. 1988, "Diffusion and Absorption of Quadratic Residue Diffusers," *Proceedings of the Institute of Acoustics*, Vol. 10, No. 2, pp. 223-232.
- Cox, T. J. 1994, 'Predicting the Scattering from Reflectors and Diffusers Using Two – Dimensional Boundary Element Method', *Journal of the Acoustical Society of America*, Vol. 96, No. 2, pp. 874 – 878.

- Cox, T. J. 1995, 'The Optimization of Profiled Diffusers', *Journal of the Acoustical Society of America*, Vol. 97, No. 5, pp. 2928 – 2936.
- Cox, T. J. 1998, 'Practical Prediction Techniques for Sound Diffusers', *Journal of the Acoustical Society of America, 136th Meeting: Acoustical Society of America*, Vol. 104, No. 3, Pt. 2, p. 1857.
- Cox, T. J., Angus, J. A. S. & D'Antonio, P. 2006, 'Ternary and Quadriphase Sequence Diffusers', *Journal of the Acoustical Society of America*, Vol. 119, No. 1, pp. 310 – 319.
- Cox, T. J., Avis, M. R. & Xiao, L. 2002, 'The Potential for Room Acoustic Active Diffusers', Forum Sevilla.
- Cox, T. J. & D'Antonio P. 1999, 'Optimized Planar and Curved Diffusers', *Proceedings of the 107th Convention of the Audio Engineering Society*, Paper no. 5062, New York.
- Cox, T. J. & D'Antonio P. 2000, 'Acoustic Phase Gratings for Reduced Specular Reflection', *Applied Acoustics*, Vol. 60, pp. 167-186.
- Cox, T. J. & D'Antonio P. 2003, 'Engineering Art: The Science of Concert Hall Acoustics', *Interdisciplinary Science Reviews*, Vol. 28, No. 2, pp. 119-129.
- Cox, T. J. & D'Antonio P. 2004, *Acoustic Absorbers and Diffusers: Theory, Design, and Application*, Spon Press, 1st ed., USA.
- Cox, T. J. & D'Antonio P. 2009, *Acoustic Absorbers and Diffusers: Theory, Design, and Application*, Taylor & Francis, 2nd ed., USA.
- Cox, T. J. & Lam, Y. W. 1994, 'Prediction and Evaluation of the Scattering from Quadratic Residue Diffusers', *Journal of the Acoustical Society of America*, Vol. 95, No. 1, pp. 297 – 305.
- D'Antonio, P. 1989, 'The Reflection Phase Grating Diffusor: A Five Year Progress Report', *Journal of the Acoustical Society of America Suppl. 1, 117th Meeting: Acoustical Society of America* Vol. 85, p.S16.
- D'Antonio, P. 1990, 'The QRD® Diffractal™: A New 1 - or 2- Dimensional Fractal Sound Diffusor', *Journal of the Acoustical Society of America Suppl. 1, 119th Meeting: Acoustical Society of America*, Vol. 87, p.S10.
- D'Antonio, P. 1995, 'Performance Evaluation of Optimized Diffusers', *Journal of the Acoustical Society of America*, Vol. 97, No. 5, pp. 2937 – 2941.
- D'Antonio, P. 1998, 'Planar Binary Amplitude Diffusor', U.S. Patent No. 5,817,992.
- D'Antonio, P. & Cox, T. J. 1998a, 'Two Decades of Sound Diffusor Design and Development. Part 1: Applications and Design', *Journal of Audio Engineering Society*, Vol. 46, Iss. 11, pp. 955 – 976.

- D'Antonio, P. & Cox, T. J. 1998b, 'Two Decades of Sound Diffusor Design and Development. Part 2: Prediction, Measurement and Characterization', *Journal of Audio Engineering Society*, Vol. 46, Iss. 12, pp. 1075 – 1091.
- D'Antonio, P. & Cox, T. J. 1998c, 'A review of diffusor design over the past two decades', *Journal of the Acoustical Society of America, 136th Meeting: Acoustical Society of America*, Vol. 104, No. 3, Pt. 2, p. 1857.
- D'Antonio, P. & Cox, T. J. 2001, 'Application of Number Theory Sequences in Architectural Acoustics', *Journal of the Acoustical Society of America, 141st Meeting: Acoustical Society of America*, Vol. 109, No. 5, Pt. 2, p. 2417.
- D'Antonio, P., Cox, T. J., Hargreaves, T. & Lam, Y. W. 1998, 'Experimental Measurement and Characterization of Scattering Surfaces', *Journal of the Acoustical Society of America, 136th Meeting: Acoustical Society of America*, Vol. 104, No. 3, Pt. 2, p. 1857.
- D'Antonio, P. & Cox, T. J. 2000, 'Diffusor Application in Rooms', *Applied Acoustics*, Vol. 60, pp. 113 – 142.
- D'Antonio, P. & Konnert, J. H. 1983, 'The Schroeder Quadratic – Residue Diffusor: Design Theory and Application, *Audio Engineering Society 74th Convention*, preprint no. 74, New York, USA.
- D'Antonio, P. & Konnert, J. H. 1987, 'Acoustical Baffle', U.S. Patent No. 306,764.
- D'Antonio, P. & Konnert, J. H. 1992, 'The QRD Diffractal™: A New 1 - or 2-Dimensional Fractal Sound Diffusor', *Journal of Audio Engineering Society*, Vol. 40, No.3, pp. 117 – 129.
- D'Antonio, P. & Konnert, J. H. 1993, 'Two Dimensional Primitive Root Diffusor', U.S. Patent No. 5,401,921.
- Embrechts, J. J., Archambeau, D. & Stan, G. B. 2001, 'Determination of the Scattering Coefficient of Random Rough Diffusing Surfaces for Room Acoustics Applications', *Acta Acustica united with Acustica*, Vol.87, pp. 482–494.
- Fan, P. & Darnell, M. 1996, *Sequence Design for Communication Applications*, John Wiley & Sons.
- Farina, A., Galaverna, P., Martignon, P., Conti, L. & Rosati, A. 2006, 'Surface Scattering Uniformity Measurements in Reflection Free Environments', *Audio Engineering Society 121th Convention*, preprint no. 6922, San Francisco, USA.
- Fedorov, G. A. & Tereshchenko, S. A. 1999, 'Use of Generalized One Dimensional Sequences for Constructing Two Dimensional Codes and Encoding Devices in Integrated Encoding Measuring Systems', *Measurement Techniques*, Vol. 42, pp. 181 – 191.
- Fujiwara, K. & Miyajima, T. 1992, 'Absorption Characteristics of a Practically



- Constructed Schroeder Diffuser of Quadratic-Residue Type', *Applied Acoustic*, Vol. 35, pp. 149–152.
- Fujiwara, K. & Miyajima, T. 1995, 'A Study of the Sound Absorption of a Quadratic-Residue Type Diffuser', *Acustica*, Vol. 81, pp. 370–378.
- Girod, B. 2001, *Signals and Systems*, John Wiley & Sons.
- Guicking, D., Karcher K. & Rollwage, M. 1985, 'Coherent Active Methods for Applications in Room Acoustics', *Journal of the Acoustical Society of America*, Vol.78, pp.1426–1434.
- Haan, C. & Fricke, F. R. 1997, 'An Evaluation of Importance of Surface Diffusivity in Concert Halls', *Applied Acoustics*, Vol. 51, No.1, pp. 53 – 69.
- Hargreaves, T., Cox, T. J. & Lam, Y. W. 1998, 'Diffusion Coefficients', *Journal of the Acoustical Society of America*, 136th Meeting: *Acoustical Society of America*, Vol. 104, No. 3, Pt. 2, p. 1858.
- Hargreaves, T., Cox, T. J. 2005, 'A Stable Transient Boundary Element Method (BEM) for Diffuser Scattering', *Journal of the Acoustical Society of America*, Joint 150<sup>th</sup> ASA Meeting/NOISE-CON 2005, Vol. 118, No. 3, Pt. 2, p. 1999.
- Hidaka, T. & Beranek, L. L. 2000, 'Objective and Subjective Evaluations of Twenty-three Opera Houses in Europe, Japan, and the Americas', *Journal of the Acoustical Society of America*, Vol. 107, No. 1, pp. 368 – 383.
- International Standards Organization, ISO 17497-1: 2004, 'Acoustics - Sound-scattering properties of surfaces - Part 1: Measurement of the random-incidence scattering coefficient in a reverberation room'.
- Jarvinen, A. & Savioja, L. 1999, 'Absorption and Scattering Characteristics of a Modified Schroeder Diffuser', *Journal of the Acoustical Society of America*, Joint Meeting: ASA/EAA/DEGA, Vol. 105, No. 2, Pt. 2, p. 1317.
- Jeon, C., Lee, S. C. & Vorländer, M. 2004, 'Development of Scattering Surfaces for Concert Halls', *Applied Acoustics*, Vol. 65, pp. 341 – 355.
- Kate, W. R. T. 1995, 'On the Bandwidth of Diffusers Based Upon the Quadratic Residue Sequence', *Journal of the Acoustical Society of America*, Vol. 98, No. 5, pp. 2575 – 2579.
- Kawai, Y. & Terai, T. 1990, 'A Numerical Method for the Calculation of Transient Acoustic Scattering from Thin Rigid Plates', *Journal of Sound and Vibration*, Vol. 1, Iss. 1, pp. 83 – 96.
- Kirkup, S. 2007, *The Boundary Element Method in Acoustics*, published in electronic format, <http://www.boundary-element-method.com>.
- Kosaka, Y. & Sakuma, T. 2005, 'Numerical Examination on the Scattering Coefficients

- of Architectural Surfaces Using the Boundary Element Method', *Acoustical Science and Technology*, Vol. 26, pp. 136 – 144.
- Kuttruff, H. 1994, 'Sound Absorption by Pseudostochastic Diffusers (Schroeder Diffusers)', *Applied Acoustics*, Vol. 42, Iss. 3, pp. 215-231.
- Lam Y. W. 1999, 'A Boundary Integral Formulation for the Prediction of Acoustic Scattering from Periodic Structures', *Journal of the Acoustical Society of America*, Vol. 105, Iss. 2, pp.762-769.
- Long, M. 2006, *Architectural Acoustics*, Elsevier Academic Press.
- MacWilliams, F. J. & Sloane, N. J.A. 1976, 'Pseudo-Random Sequences and Arrays', *Proceedings of the IEEE*, Vol 64, No.12, pp. 1715-1729.
- Manolakis, D. 2005, *Statistical and Adaptive Signal Processing: Spectral Estimation, Signal Modeling, Adaptive Filtering and Array Processing*, Artech House, Incorporated, Norwood, MA, USA.
- Marshall, A. H. 1967, 'A Note on the Importance of Room Cross-Section in Concert Halls', *Journal of Sound and Vibration*, Vol. 5, pp. 100 – 112.
- Marshall, A. H. 1978, 'Evolution of a Concert Hall: Lateral Reflections and the Acoustical Design for Wellington Town Hall', *Journal of the Acoustical Society of America*, Vol. 63, Suppl. No. 1, p. S36.
- Mommertz, E. 2000, 'Determination of Scattering Coefficients from the Reflection Directivity of Architectural Surfaces', *Applied Acoustics*, Vol. 60, pp. 201–203.
- Nelson, P. A. & Elliot, S. J. 1992, *Active Control of Sound*, Academic Press, London.
- Schroeder, M. 1974, 'Comparative Study of European Concert Halls: Correlation of Subjective Preference with Geometric and Acoustic Parameters', *Journal of the Acoustical Society of America*, Vol. 56, No. 4, pp. 1195 – 1201.
- Schroeder, M. 1975, 'Diffuse Sound Reflection by Maximum-Length Sequences', *Journal of the Acoustical Society of America*, Vol. 57, No. 1, pp. 149 – 150.
- Schroeder, M. 1979, 'Binaural Dissimilarity and Optimum Ceilings for Concert Halls: More Lateral Sound Diffusion', *Journal of the Acoustical Society of America*, Vol. 65, No. 4, pp. 958 – 963.
- Schroeder, M. 1997, *Number Theory in Science and Communication: With Applications in Cryptography, Physics, Digital Information, Computing, and Self – Similarity*, Springer.
- Schroeder, M. R. 2005, 'From Philharmonic Hall to number theory: The way to more diffusion', *Journal of the Acoustical Society of America, Joint 150th Meeting/NOISE-CON*, Vol. 118, No. 3, Pt. 2, p. 2015.

- Schyndel, R. van, Tirkel, A. Z., Svalbe, I. D., Hall, T. E. & Osborne, C. F. 1999, 'Algebraic Construction of a New Class of Quasi -Orthogonal Arrays in Steganography', *SPIE Electronic Imaging 1999*, San Jose, USA, pp. 354-364.
- Schyndel, R. van, Tirkel, A. Z., Svalbe, I. D., Hall, T. E. & Osborne, C. F. 2000, 'Spread Spectrum Digital Watermark Concepts and Higher Dimensional Array Constructions', *First International Online Symposium on Electronics Engineering*, July 2000, at <http://www.techonline.com/osee>.
- Tirkel, A. Z., Hall, T. E. & Osborne, C. F. 1998a, 'A New Class of Spreading Sequences', *ISSSTA'98*, Sun City, South Africa, September 1998, Vol. 1, pp. 46-50.
- Tirkel, A. Z., Schyndel, R. van, Hall, T. E. & Osborne, C. F. 1998b, 'Secure Arrays for Digital Watermarking', *IEEE International Conference on Pattern Recognition*, Brisbane, Australia, pp. 1643-1645.
- Wu, T., Cox, T. J. & Lam, Y. W. 2000, 'From a Profiled Diffuser to an Optimized Absorber', *Journal of the Acoustical Society of America*, Vol. 108, No. 2, pp. 643-650.
- Wu, T., Cox, T. J. & Lam, Y. W. 2001, 'A Profiled Structure with Improved Low Frequency Absorption', *Journal of the Acoustical Society of America*, Vol. 110, No. 6, pp. 3064 – 3070.
- Xiao, L., Cox, T. J. & Avis, M. R. 2005, 'Active Diffusers: Some Prototypes and 2D Measurements', *Journal of Sound and Vibration*, Vol. 285, pp. 321 – 339.
- Xiao, L., Cox, T. J. & Avis, M. R. 2006, 'Maximum Length Sequence and Bessel Diffusers Using Active Technologies', *Journal of Sound and Vibration*, Vol. 289, pp. 807 – 829.

# APPENDIX A

## MATLAB SCRIPTS

### Chapter 2

#### script 2.1

```
%Autocorrelation Plot of 2D Quadratic Residue Diffuser for N = 7
%Based on Product Array Method
%not shifted
%for s_n = {0, 1, 4, 2, 2, 4, 1}
x = [0 1 2 4 4 2 1;
     1 2 3 5 5 3 2;
     2 3 4 6 6 4 3;
     4 5 6 1 1 6 5;
     4 5 6 1 1 6 5;
     2 3 4 6 6 4 3;
     1 2 3 5 5 3 1];
y = [x x x;
     x x x;
     x x x];
r = xcorr2 (x,y);
surfc (r);
colormap gray
%Power Spectrum of 2D Quadratic Residue Diffuser for N = 7
%Based on Product Array Method
%not shifted
%for s_n = {0, 1, 4, 2, 2, 4, 1}
x = [0 1 2 4 4 2 1;
     1 2 3 5 5 3 2;
     2 3 4 6 6 4 3;
     4 5 6 1 1 6 5;
```

```

    4 5 6 1 1 6 5;
    2 3 4 6 6 4 3;
    1 2 3 5 5 3 1];
r = xcorr2 (x);
y = fft2 (r);
yshifted = fftshift (y);
mesh(abs(yshifted))

```

## script 2.2

```

%Autocorrelation Plot of 2D Quadratic Residue Diffuser for N = 7
%Based on Product Array Method
%shifted for n,m = 4
%for s_n = {4, 1, 2, 0, 2, 1, 4}
x = [4 6 3 2 3 6 4;
     6 1 5 4 5 1 6;
     3 5 2 1 2 5 3;
     2 4 1 0 1 4 2;
     3 5 2 1 2 5 3;
     6 1 5 4 5 1 6;
     4 6 3 2 3 6 4];
y = [x x x;
     x x x;
     x x x];
r = xcorr2(x,y);
surfc(r);
colormap gray
%Power Spectrum of 2D Quadratic Residue Diffuser for N = 7
%Based on Product Array Method
%shifted for n,m = 4
%for s_n = {4, 1, 2, 0, 2, 1, 4}
x = [4 6 3 2 3 6 4;
     6 1 5 4 5 1 6;
     3 5 2 1 2 5 3;
     2 4 1 0 1 4 2;

```

```

    3 5 2 1 2 5 3;
    6 1 5 4 5 1 6;
    4 6 3 2 3 6 4];
r = xcorr2(x);
y = fft2 (r);
yshifted = fftshift (y);
mesh(abs(yshifted))

```

## Chapter 3

### script 3.1

```

%Autocorrelation Plot of 2D Quadratic Residue Diffuser for N = 7
%Based on Distinct Sums Property Method
%for m = 1
%for s_n = {0, 1, 4, 2, 2, 4, 1}
x = [0 1 4 2 2 4 1;
     0 1 4 2 2 4 1;
     1 0 1 4 2 2 4;
     2 4 1 0 1 4 2;
     1 4 2 2 4 1 0;
     2 4 1 0 1 4 2;
     1 0 1 4 2 2 4];
y = [x x x;
     x x x;
     x x x];
r = xcorr2 (x,y);
surfc (r);
colormap gray
%Power Spectrum of 2D Quadratic Residue Diffuser for N = 7
%Based on Distinct Sums Property Method
%for m = 1
%for s_n = {0, 1, 4, 2, 2, 4, 1}
x = [0 1 4 2 2 4 1;
     0 1 4 2 2 4 1;

```

```

    1 0 1 4 2 2 4;
    2 4 1 0 1 4 2;
    1 4 2 2 4 1 0;
    2 4 1 0 1 4 2;
    1 0 1 4 2 2 4];
r = xcorr2 (x);
y = fft2 (r);
zshifted = fftshift (y);
mesh(abs(yshifted))

```

### script 3.2

```

%Autocorrelation Plot of 2D Quadratic Residue Diffuser for N = 7
%Based on Distinct Sums Property Method
%for m = 2
%for s_n = {0, 1, 4, 2, 2, 4, 1}
x = [0 1 4 2 2 4 1;
     0 1 4 2 2 4 1;
     4 1 0 1 4 2 2;
     1 4 2 2 4 1 0;
     4 2 2 4 1 0 1;
     1 4 2 2 4 1 0;
     4 1 0 1 4 2 2];
y = [x x x;
     x x x;
     x x x];
r = xcorr2 (x,y);
surfc (r);
colormap gray
%Power Spectrum of 2D Quadratic Residue Diffuser for N = 7
%Based on Distinct Sums Property Method
%for m = 2
%for s_n = {0, 1, 4, 2, 2, 4, 1}
x = [0 1 4 2 2 4 1;
     0 1 4 2 2 4 1;

```

```

    4 1 0 1 4 2 2;
    1 4 2 2 4 1 0;
    4 2 2 4 1 0 1;
    1 4 2 2 4 1 0;
    4 1 0 1 4 2 2];
r = xcorr2 (x);
y = fft2 (r);
yshifted = fftshift (y);
mesh(abs(yshifted))

```

### script 3.3

```

%Autocorrelation Plot of 2D Quadratic Residue Diffuser for N = 7
%Based on Distinct Sums Property Method
%for m = 3
%for s_n = {0, 1, 4, 2, 2, 4, 1}
x = [0 1 4 2 2 4 1;
     0 1 4 2 2 4 1;
     2 4 1 0 1 4 2;
     4 1 0 1 4 2 2;
     2 2 4 1 0 1 4;
     4 1 0 1 4 2 2;
     2 4 1 0 1 4 2];
y = [x x x;
     x x x;
     x x x];
r = xcorr2 (x,y);
surfc (r);
colormap gray
%Power Spectrum of 2D Quadratic Residue Diffuser for N = 7
%Based on Distinct Sums Property Method
%for m = 3
%for s_n = {0, 1, 4, 2, 2, 4, 1}
x = [0 1 4 2 2 4 1;
     0 1 4 2 2 4 1;

```



```

    2 4 1 0 1 4 2;
    4 1 0 1 4 2 2;
    2 2 4 1 0 1 4;
    4 1 0 1 4 2 2;
    2 4 1 0 1 4 2];
r = xcorr2 (x);
y = fft2 (r);
yshifted = fftshift (y);
mesh(abs(yshifted))

```

### script 3.4

```

%Autocorrelation Plot of 2D Quadratic Residue Diffuser for N = 7
%Based on Distinct Sums Property Method
%for m = 4
%for s_n = {0, 1, 4, 2, 2, 4, 1}
x = [0 1 4 2 2 4 1;
     0 1 4 2 2 4 1;
     2 2 4 1 0 1 4;
     4 2 2 4 1 0 1;
     2 4 1 0 1 4 2;
     4 2 2 4 1 0 1;
     2 2 4 1 0 1 4];
y = [x x x;
     x x x;
     x x x];
r = xcorr2 (x,y);
surfc (r);
colormap gray
%Power Spectrum of 2D Quadratic Residue Diffuser for N = 7
%Based on Distinct Sums Property Method
%for m = 4
%for s_n = {0, 1, 4, 2, 2, 4, 1}
x = [0 1 4 2 2 4 1;
     0 1 4 2 2 4 1;

```

```

    2 2 4 1 0 1 4;
    4 2 2 4 1 0 1;
    2 4 1 0 1 4 2;
    4 2 2 4 1 0 1;
    2 2 4 1 0 1 4];
r = xcorr2 (x);
y = fft2 (r);
yshifted = fftshift (y);
mesh(abs(yshifted))

```

### script 3.5

```

%Autocorrelation Plot of 2D Quadratic Residue Diffuser for N = 7
%Based on Distinct Sums Property Method
%for m = 5
%for s_n = {0, 1, 4, 2, 2, 4, 1}
x = [0 1 4 2 2 4 1;
     0 1 4 2 2 4 1;
     4 2 2 4 1 0 1;
     1 0 1 4 2 2 4;
     4 1 0 1 4 2 2;
     1 0 1 4 2 2 4;
     4 2 2 4 1 0 1];
y = [x x x;
     x x x;
     x x x];
r = xcorr2 (x,y);
surfc (r);
colormap gray
%Power Spectrum of 2D Quadratic Residue Diffuser for N = 7
%Based on Distinct Sums Property Method
%for m = 5
%for s_n = {0, 1, 4, 2, 2, 4, 1}
x = [0 1 4 2 2 4 1;
     0 1 4 2 2 4 1;

```

```

    4 2 2 4 1 0 1;
    1 0 1 4 2 2 4;
    4 1 0 1 4 2 2;
    1 0 1 4 2 2 4;
    4 2 2 4 1 0 1];
r = xcorr2 (x);
y = fft2 (r);
yshifted = fftshift (y);
mesh(abs(yshifted))

```

### script 3.6

```

%Autocorrelation Plot of 2D Quadratic Residue Diffuser for N = 7
%Based on Distinct Sums Property Method
%for m = 6
%for s_n = {0, 1, 4, 2, 2, 4, 1}
x = [0 1 4 2 2 4 1;
     0 1 4 2 2 4 1;
     1 4 2 2 4 1 0;
     2 2 4 1 0 1 4;
     1 0 1 4 2 2 4;
     2 2 4 1 0 1 4;
     1 4 2 2 4 1 0];
y = [x x x;
     x x x;
     x x x];
r = xcorr2 (x,y);
surfc (r);
colormap gray
%Power Spectrum of 2D Quadratic Residue Diffuser for N = 7
%Based on Distinct Sums Property Method
%for m = 6
%for s_n = {0, 1, 4, 2, 2, 4, 1}
x = [0 1 4 2 2 4 1;
     0 1 4 2 2 4 1;

```

```
1 4 2 2 4 1 0;  
2 2 4 1 0 1 4;  
1 0 1 4 2 2 4;  
2 2 4 1 0 1 4;  
1 4 2 2 4 1 0];  
r = xcorr2 (x);  
y = fft2 (r);  
yshifted = fftshift (y);  
mesh(abs(yshifted))
```

# APPENDIX B

## LIST OF RECEIVER POINTS

Scattering data courtesy of T. J. Cox, University of Salford and P.D'Antonio, RPG Diffusor Systems Inc., database at: [www.acoustics.salford.ac.uk](http://www.acoustics.salford.ac.uk)

(x, y)

0 -50  
4.3578 -49.8097  
8.6824 -49.2404  
12.941 -48.2963  
17.101 -46.9846  
21.1309 -45.3154  
25 - 43.3013  
28.6788 -40.9576  
32.1394 -38.3022  
35.3553 -35.3553  
38.3022 -32.1394  
40.9576 -28.6788  
43.3013 -25  
45.3154 -21.1309  
46.9846 -17.101  
48.2963 -12.941  
49.2404 -8.6824  
49.8097 -4.3578  
50 0  
49.8097 4.3578  
49.2404 8.6824  
48.2963 12.941  
46.9846 17.101  
45.3154 21.1309  
43.3013 25  
40.9576 28.6788

38.3022 32.1394  
35.3553 35.3553  
32.1394 38.3022  
28.6788 40.9576  
25 43.3013  
21.1309 45.3154  
17.101 46.9846  
12.941 48.2963  
8.6824 49.2404  
4.3578 49.8097  
0 50

## APPENDIX C

### INPUT AND OUTPUT FILES OF BEM SOFTWARE

#### Input File for 125 Hz, 250 Hz., 500 Hz., 1000 Hz., 2000 Hz., 4000 Hz.

```
runinfo={
  active = 1;
  title = "Ayce.coarse";
  owner = "Acousto";
  ksymmi=0;
  krow  =-1;
  vsound =343.0;
# nprows=1;
# npcpls=1;
};
modgeom={
  active = 1;
  geoms = ["diffuser"];
  chief_file = "acousto.chief.mesh";
  nchief = 0;
  mics_file = "acousto.mics.mesh";
  nmics = 160;
# mics_file = "mics.acousto";
# nmics = 9511;
};
diffuser={
  type="nodes";
  filename="ayce.final.coarse.scaled.in";
  nnodb=12557;
  nelmb=11556;
  ncnttr=11556;
translation={x=0.0; y=0.0; z=0.0;};
rotation={x=0.0; y=0.0; z=0.0;};
```

```

    scale={x=0.02136; y=0.02136; z=0.02136;};
};
modcoefac={
    active=1;
};
modcoemic={
    active=1;
};
modsol={
    active=1;
    sources_file="acousto.sources.mesh";
    nsourc=1;
    imped_file="acousto.imped.mesh";
    nimped=0;
    radiants_file="acousto.radiants.mesh";
    nradian=0;
    radiant_real=0.0;
    radiant_imag=0.0;
    planw_file="acousto.planw.mesh";
    nplanw=0;
    knw=1;
    rho=1.225;
    minsig=0.0;
    maxsig=0.0;
    nsig=1;
    % each frequency input are in different files
    % plotted under same file
    minfreq=125.00;250.00;500.00;1000.00;2000.00;4000.00
    maxfreq=125.01;250.01;500.01;1000.01;2000.01;4000.01
    nome=1;
    printvtk=1;

    pre_calculate_coefs=1;

```



```
solver="PSEUDOINV";
tolerance=1E-6;

maxiterations=1000;
restart=2000;
};
mysql={
  active=1;
  host="localhost";
  user="acousto";
  password="acousto";
  db="acoustorun";
  port=0;
};
```

## **Output Files for 125 Hz, 250 Hz., 500 Hz., 1000 Hz., 2000 Hz., 4000 Hz.**

### **125 Hz.**

```
SCALARS Re(Scat_Solution) float
LOOKUP_TABLE default
1.56861362E-07
2.28439997E-07
2.99638058E-07
3.70053647E-07
4.39263779E-07
5.06831999E-07
5.72309167E-07
6.35225583E-07
6.95096961E-07
7.51426698E-07
8.03718469E-07
8.51478272E-07
8.94228485E-07
```

9.31517420E-07  
9.62934798E-07  
9.88123680E-07  
1.00678407E-06  
1.01869048E-06  
1.02369952E-06  
1.02174521E-06  
1.01285340E-06  
9.97128881E-07  
9.74760266E-07  
9.46010222E-07  
9.11204440E-07  
8.70725544E-07  
8.24997577E-07  
7.74480655E-07  
7.19647556E-07  
6.60989363E-07  
5.98992570E-07  
5.34145804E-07  
4.66921220E-07  
3.97771314E-07  
3.27153920E-07  
2.55507893E-07  
1.83248421E-07  
SCALARS Im(Scat\_Solution) float  
LOOKUP\_TABLE default  
2.23269881E-08  
1.78367647E-08  
1.35796854E-08  
9.51516471E-09  
5.61319030E-09  
2.03722079E-09  
1.29515311E-09  
4.44940888E-09

7.25770170E-09  
9.88252337E-09  
1.20289215E-08  
1.39736391E-08  
1.54927733E-08  
1.68057728E-08  
1.78088298E-08  
1.82561515E-08  
1.84801810E-08  
1.84120873E-08  
1.77762213E-08  
1.69138838E-08  
1.54742440E-08  
1.37254548E-08  
1.17311332E-08  
9.15017742E-09  
6.22874483E-09  
3.07406161E-09  
5.33589174E-10  
4.35700526E-09  
8.66995580E-09  
1.31535203E-08  
1.79579933E-08  
2.28871399E-08  
2.79852450E-08  
3.33153738E-08  
3.86771401E-08  
4.40745742E-08  
4.95277142E-08  
SCALARS Abs(Scat\_Solution) float  
LOOKUP\_TABLE default  
1.58442360E-07  
2.29135293E-07  
2.99945618E-07

3.70175958E-07  
4.39299642E-07  
5.06836093E-07  
5.72310632E-07  
6.35241165E-07  
6.95134849E-07  
7.51491681E-07  
8.03808480E-07  
8.51592925E-07  
8.94362683E-07  
9.31669007E-07  
9.63099465E-07  
9.88292312E-07  
1.00695367E-06  
1.01885686E-06  
1.02385385E-06  
1.02188520E-06  
1.01297160E-06  
9.97223342E-07  
9.74830855E-07  
9.46054473E-07  
9.11225729E-07  
8.70730970E-07  
8.24997750E-07  
7.74492910E-07  
7.19699780E-07  
6.61120226E-07  
5.99261703E-07  
5.34635914E-07  
4.67759125E-07  
3.99164042E-07  
3.29432252E-07  
2.59281414E-07  
1.89823545E-07

## 250 Hz.

SCALARS Re(Scat\_Solution) float

LOOKUP\_TABLE default

4.81971517E-07

7.60818713E-07

1.04051253E-06

1.32068781E-06

1.60056946E-06

1.87952244E-06

2.15591269E-06

2.42758998E-06

2.69265709E-06

2.94774011E-06

3.19064836E-06

3.41696999E-06

3.62392140E-06

3.80712588E-06

3.96359383E-06

4.09129654E-06

4.18640860E-06

4.24730947E-06

4.27398512E-06

4.26466278E-06

4.22122931E-06

4.14377627E-06

4.03396124E-06

3.89569638E-06

3.73094743E-06

3.54259500E-06

3.33496328E-06

3.11059012E-06

2.87379611E-06

2.62641121E-06

2.37162528E-06

2.11098075E-06  
1.84638897E-06  
1.57927376E-06  
1.30993082E-06  
1.03893237E-06  
7.66484978E-07  
SCALARS Im(Scat\_Solution) float  
LOOKUP\_TABLE default  
8.36820347E-08  
7.31786936E-08  
2.30476039E-07  
3.88705872E-07  
5.48148990E-07  
7.07464463E-07  
8.66749266E-07  
1.02568666E-06  
1.18187894E-06  
1.33505967E-06  
1.48117881E-06  
1.62033104E-06  
1.74856657E-06  
1.86535436E-06  
1.96765478E-06  
2.05140258E-06  
2.11746109E-06  
2.16381291E-06  
2.18717125E-06  
2.18976438E-06  
2.16867474E-06  
2.12653757E-066  
2.06476865E-06  
1.98190248E-06  
1.88155322E-06  
1.76640366E-06

1.63664001E-06  
1.49610298E-06  
1.34450919E-06  
1.18607158E-06  
1.02110540E-06  
8.52357289E-07  
6.80431683E-07  
5.05517914E-07  
3.29599132E-07  
1.52891312E-07  
2.46819251E-08  
SCALARS Abs(Scat\_Solution) float  
LOOKUP\_TABLE default  
4.89182201E-07  
7.64329925E-07  
1.06573239E-06  
1.37670205E-06  
1.69183034E-06  
2.00826059E-06  
2.32362084E-06  
2.63537972E-06  
2.94061899E-06  
3.23597838E-06  
3.51768782E-06  
3.78168700E-06  
4.02371612E-06  
4.23954648E-06  
4.42512614E-06  
4.57678489E-06  
4.69144524E-06  
4.76673096E-06  
4.80111100E-06  
4.79399799E-06  
4.74572724E-06

4.65757918E-06  
4.53167881E-06  
4.37085663E-06  
4.17854176E-06  
3.95855544E-06  
3.71491192E-06  
3.45168003E-06  
3.17276048E-06  
2.88180527E-06  
2.58210432E-06  
2.27656598E-06  
1.96777527E-06  
1.65820806E-06  
1.35076065E-06  
1.05012201E-06  
7.66882272E-07

## **500 Hz.**

SCALARS Re(Scat\_Solution) float

LOOKUP\_TABLE default

1.36662476E-06  
1.43697827E-06  
1.53755485E-06  
1.66626004E-06  
1.81860014E-06  
1.98542755E-06  
2.16116173E-06  
2.33865991E-06  
2.50723428E-06  
2.66084358E-06  
2.78870616E-06  
2.88777788E-06  
2.95128961E-06  
2.97859379E-06



2.96800332E-06  
2.91896264E-06  
2.83652630E-06  
2.72385307E-06  
2.58359648E-06  
2.42249725E-06  
2.24298666E-06  
2.05120781E-06  
1.85207124E-06  
1.64770974E-06  
1.44438949E-06  
1.24783668E-06  
1.06154313E-06  
8.92649650E-07  
7.44331627E-07  
6.24165433E-07  
5.35618811E-07  
4.84030718E-07  
4.72026946E-07  
5.01268239E-07  
5.73771939E-07  
6.89023463E-07  
8.45429582E-07  
SCALARS Im(Scat\_Solution) float  
LOOKUP\_TABLE default  
1.44909270E-06  
1.62471096E-06  
1.77900144E-06  
1.91107153E-06  
2.01984067E-06  
2.10643850E-06  
2.16749256E-06  
2.20023124E-06  
2.20593148E-06

2.18242711E-06  
2.13574189E-06  
2.06610337E-06  
1.98262015E-06  
1.89024102E-06  
1.79911144E-06  
1.72074533E-06  
1.65850522E-06  
1.61826179E-06  
1.60454607E-06  
1.61190414E-06  
1.63819600E-06  
1.67266153E-06  
1.70502012E-06  
1.72754580E-06  
1.72903761E-06  
1.70179217E-06  
1.64285758E-06  
1.54990649E-06  
1.42613807E-06  
1.27459135E-06  
1.10205474E-06  
9.14835435E-07  
7.20052381E-07  
5.24202523E-07  
3.31326134E-07  
1.44420032E-07  
3.48292471E-08  
SCALARS Abs(Scat\_Solution) float  
LOOKUP\_TABLE default  
1.99186669E-06  
2.16900720E-06  
2.35136578E-06  
2.53547173E-06

2.71791515E-06  
2.89465123E-06  
3.06082408E-06  
3.21097302E-06  
3.33951455E-06  
3.44137714E-06  
3.51258815E-06  
3.55078079E-06  
3.55540336E-06  
3.52775171E-06  
3.47071256E-06  
3.38840780E-06  
3.28580599E-06  
3.16830345E-06  
3.04130545E-06  
2.90976423E-06  
2.77753043E-06  
2.64674330E-06  
2.51739181E-06  
2.38733363E-06  
2.25296073E-06  
2.11025898E-06  
1.95597925E-06  
1.78858423E-06  
1.60869493E-06  
1.41921302E-06  
1.22532125E-06  
1.03499257E-06  
8.60979017E-07  
7.25298650E-07  
6.62564144E-07  
7.03996078E-07  
8.46146710E-07

## 1000 Hz.

SCALARS Re(Scat\_Solution) float

LOOKUP\_TABLE default

2.45066245E-06

2.46579834E-06

2.33073530E-06

2.04245772E-06

1.61041439E-06

1.06710553E-06

4.51401122E-07

1.70936218E-07

7.04458120E-07

1.04709562E-06

1.08878936E-06

7.50278469E-07

7.06269521E-09

1.15298223E-06

2.58547948E-06

4.13842732E-06

5.60832637E-06

6.79428328E-06

7.53879962E-06

7.76065251E-06

7.46810686E-06

6.75546654E-06

5.77602993E-06

4.69741305E-06

3.67884888E-06

2.83481809E-06

2.21465314E-06

1.82366157E-06

1.61539494E-06

1.53677883E-06

1.52249908E-06

1.52390746E-06  
1.50452198E-06  
1.44568763E-06  
1.33948485E-06  
1.18294212E-06  
9.77103038E-07  
SCALARS Im(Scat\_Solution) float  
LOOKUP\_TABLE default  
2.39117872E-06  
2.58545058E-06  
2.72386267E-06  
2.79766720E-06  
2.79161734E-06  
2.68804571E-06  
2.48528089E-06  
2.18942989E-06  
1.82110322E-06  
1.41428787E-06  
1.01566381E-06  
6.66398429E-07  
4.02026925E-07  
2.36189615E-07  
1.59277619E-07  
1.28368633E-07  
9.81432244E-08  
1.32979789E-08  
1.84035625E-07  
4.92774644E-07  
9.17545377E-07  
1.39659595E-06  
1.86275143E-06  
2.26327871E-06  
2.52841739E-06  
2.62175600E-06

2.54286612E-06  
2.30406672E-06  
1.94568577E-06  
1.50435779E-06  
1.02381908E-06  
5.33719041E-07  
5.83857500E-08  
3.85212613E-07  
7.92752430E-07  
1.15662981E-06  
1.46616847E-06  
SCALARS Abs(Scat\_Solution) float  
LOOKUP\_TABLE default  
3.42395708E-06  
3.57277429E-06  
3.58493443E-06  
3.46389597E-06  
3.22281893E-06  
2.89211064E-06  
2.52594222E-06  
2.19609254E-06  
1.95260805E-06  
1.75972141E-06  
1.48897121E-06  
1.00349621E-06  
4.02088958E-07  
1.17692547E-06  
2.59038095E-06  
4.14041775E-06  
5.60918503E-06  
6.79429629E-06  
7.54104561E-06  
7.77628152E-06  
7.52426140E-06

6.89831924E-06  
6.06896734E-06  
5.21422284E-06  
4.46394708E-06  
3.86132078E-06  
3.37207008E-06  
2.93844601E-06  
2.52887207E-06  
2.15053053E-06  
1.83472313E-06  
1.61466714E-06  
1.50565443E-06  
1.49612883E-06  
1.55649481E-06  
1.65443180E-06  
1.76192518E-06

## **2000 Hz.**

SCALARS Re(Scat\_Solution) float  
LOOKUP\_TABLE default  
1.14780490E-06  
1.58625295E-06  
1.94971091E-06  
2.23636230E-06  
2.44459496E-06  
2.56922868E-06  
2.64449084E-06  
2.72087770E-06  
2.83802742E-06  
3.01629070E-06  
3.20235753E-06  
3.24787245E-06  
2.93663347E-06  
2.09305074E-06

7.03495124E-07  
9.63297167E-07  
2.38529769E-06  
3.01343989E-06  
2.48642908E-06  
1.02041622E-06  
8.57575333E-07  
2.37109825E-06  
3.05691977E-06  
2.92145092E-06  
2.32314812E-06  
1.71655971E-06  
1.36285908E-06  
1.24263328E-06  
1.19141778E-06  
1.04937167E-06  
8.01808857E-07  
5.50223683E-07  
4.43314593E-07  
5.85342113E-07  
9.95474672E-07  
1.59822620E-06  
2.23515490E-06  
SCALARS Im(Scat\_Solution) float  
LOOKUP\_TABLE default  
8.02304602E-07  
2.10275811E-07  
5.15644093E-07  
1.32463709E-06  
2.04657287E-06  
2.44422182E-06  
2.28741358E-06  
1.54330771E-06  
5.13527318E-07



2.49208908E-07  
1.78305497E-07  
8.12460051E-07  
2.11872130E-06  
2.56532321E-06  
1.10152568E-06  
2.47561421E-06  
7.19663020E-06  
1.13130559E-05  
1.32291678E-05  
1.23025650E-05  
9.16608711E-06  
5.27447878E-06  
2.11624778E-06  
4.73349676E-07  
2.64678539E-07  
8.16091949E-07  
1.38586835E-06  
1.57424216E-06  
1.35650339E-06  
9.36234965E-07  
5.04895769E-07  
1.53255617E-07  
1.28664801E-07  
3.74978817E-07  
5.80907533E-07  
6.87515696E-07  
6.01198463E-07  
SCALARS Abs(Scat\_Solution) float  
LOOKUP\_TABLE default  
1.40041021E-06  
1.60012948E-06  
2.01674526E-06  
2.59922676E-06

3.18818208E-06  
3.54614669E-06  
3.49651150E-06  
3.12809433E-06  
2.88411337E-06  
3.02656813E-06  
3.20731767E-06  
3.34794964E-06  
3.62115949E-06  
3.31085255E-06  
1.30700582E-06  
2.65642752E-06  
7.58163118E-06  
1.17075212E-05  
1.34608028E-05  
1.23448108E-05  
9.20611690E-06  
5.78292601E-06  
3.71796492E-06  
2.95954987E-06  
2.33817705E-06  
1.90067970E-06  
1.94371190E-06  
2.00558616E-06  
1.80543008E-06  
1.40631320E-06  
9.47532153E-07  
5.71168439E-07  
4.61608557E-07  
6.95150704E-07  
1.15257251E-06  
1.73982897E-06  
2.31459651E-06

## 4000 Hz.

SCALARS Re(Scat\_Solution) float

LOOKUP\_TABLE default

1.76186116E-06

8.77030159E-07

7.56672163E-07

2.70695159E-06

4.20402130E-06

4.48392079E-06

3.40939289E-06

1.75036719E-06

5.54061820E-07

4.76521411E-07

1.95431227E-06

1.45745278E-06

4.75418115E-06

1.14253303E-05

6.67151829E-06

4.93770668E-06

4.02813998E-07

2.76643151E-05

4.48137857E-05

2.73219002E-05

2.59057480E-06

1.00713102E-05

9.21838122E-07

4.46626761E-06

1.62812740E-06

2.65679904E-06

1.55249382E-06

1.63662391E-06

1.68793707E-06

1.39419021E-06

2.80093349E-06

5.68760428E-06  
4.48797973E-06  
9.77631670E-07  
1.62622645E-06  
1.63853541E-06  
7.08245942E-07  
SCALARS Im(Scat\_Solution) float  
LOOKUP\_TABLE default  
1.30593005E-08  
1.86218432E-07  
7.27777352E-07  
1.05866005E-06  
6.09383762E-08  
2.79688906E-06  
5.27588186E-06  
5.51668470E-06  
4.84886184E-06  
6.16689361E-06  
7.44487999E-06  
3.66436462E-06  
2.34128111E-06  
2.54907653E-06  
4.53423696E-07  
2.20261731E-06  
6.88135845E-06  
4.83232630E-06  
8.17477820E-07  
1.95625195E-06  
4.12613178E-06  
2.72790722E-06  
2.14221666E-06  
3.74385222E-06  
3.55088280E-06  
2.15706083E-06

3.02333632E-06  
4.93691671E-06  
5.05940488E-06  
4.16378512E-06  
4.28021729E-06  
5.20168273E-06  
5.61499952E-06  
5.20332835E-06  
4.45256290E-06  
3.69942247E-06  
2.61488711E-06  
SCALARS Abs(Scat\_Solution) float  
LOOKUP\_TABLE default  
1.76190956E-06  
8.96581956E-07  
1.04986315E-06  
2.90660421E-06  
4.20446294E-06  
5.28470757E-06  
6.28163110E-06  
5.78771072E-06  
4.88041450E-06  
6.18527683E-06  
7.69711469E-06  
3.94356902E-06  
5.29941842E-06  
1.17062361E-05  
6.68690880E-06  
5.40670604E-06  
6.89313813E-06  
2.80831927E-05  
4.48212411E-05  
2.73918446E-05  
4.87196483E-06

1.04342114E-05  
2.33214016E-06  
5.82786203E-06  
3.90634964E-06  
3.42220580E-06  
3.39864672E-06  
5.20112338E-06  
5.33354566E-06  
4.39099908E-06  
5.11522125E-06  
7.70755121E-06  
7.18819738E-06  
5.29437339E-06  
4.74024565E-06  
4.04605053E-06  
2.70910445E-06

# VITA

## Ayçe DÖŞEMECİLER

### EDUCATION

- 2003-2011**      **Ph.D. in Architecture**, Izmir Institute of Technology, Department of Architecture, Turkey  
**Thesis:** “A Study on Number Theoretic Construction and Prediction of Two Dimensional Acoustic Diffusers for Architectural Applications”
- 1999-2002**      **M.Sc. in Architecture**, Istanbul Technical University, Faculty of Architecture, Department of Architecture, Turkey  
**Thesis:** “Evaluation of the Sound Insulation of Building Façades: A Sample of Taksim – Beşiktaş; Istanbul”
- 1996-2000**      **Bachelor of Architecture**  
Istanbul Technical University, Faculty of Architecture, Department of Architecture, Turkey

### TEACHING EXPERIENCE

- 2009-2011**      **Part-time Instructor**, Izmir University of Economics, Faculty of Fine Arts and Design, Department of Interior Architecture and Environmental Design, Turkey
- 2004-2009**      **Research Assistant**, Izmir Institute of Technology, Department of Architecture, Turkey
- 2002-2003**      **Research Assistant**, Bahçeşehir University, Faculty of Architecture, Department of Architecture, Turkey

### PROFESSIONAL EXPERIENCE

- 1999-2000**      **Project Coordinator**, Kale Group, Turkey